

SEISMIC REFRACTION MEASUREMENTS
IN THE WESTERN MEDITERRANEAN SEA

by

DAVIS ARMSTRONG FAHLQUIST
B. S., Brown University
(1950)

SUBMITTED IN PARTIAL FULFILLMENT
OF THE REQUIREMENTS FOR THE
DEGREE OF DOCTOR OF
PHILOSOPHY

at the

MASSACHUSETTS INSTITUTE OF
TECHNOLOGY
June, 1963

Signature of Author

Department of Geology and Geophysics

Certified by

Thesis Supervisor

Accepted by

Chairman, Departmental Committee
on Graduate Students

ABSTRACT

SEISMIC REFRACTION MEASUREMENTS IN THE
WESTERN MEDITERRANEAN SEA

by

Davis Armstrong Fahlquist

Submitted to the Department of Geology and Geophysics on 4 February, 1963, in partial fulfillment of requirements for the degree of Doctor of Philosophy.

Results of seismic refraction studies conducted from the research vessels ATLANTIS and CHAIN (Woods Hole Oceanographic Institution), WINNARETTA SINGER (Musée Océanographique de Monaco), and VEMA (Lamont Geological Observatory) are presented. Depths to the Mohorovičić discontinuity vary from 11 to 14 km. at four refraction stations located in the deep water area bounded by the Balearic Islands, Corsica, and southern France; the mantle velocities measured at these stations vary from 7.7 to 8.0 km/sec. Overlying the high velocity material at three of these stations is a layer of material having a velocity of 6.5 to 6.8 km/sec and varying in thickness from 2 to 3 km. A significantly lower velocity, 6.0 km/sec, was measured for the layer directly overlying the mantle on the profile extending from near Cape Antibes to Corsica. All profiles in the northern part of the western Mediterranean Basin show the presence of a 4 to 6 km. thick section of material having intermediate velocities in the range 2 to 6 km/sec. Unconsolidated sediments (velocity less than 2.0 km/sec) are less than 0.5 km. thick. Seismic evidence of a major horizontal change in geologic structure is found on the eastern end of the profile extending from near Cape Corse to the basin margin south of Nice.

The single profile in the southern portion of the basin southwest of Sardinia also shows a thick intermediate velocity layer overlying material having a velocity of 7.2 km/sec. A velocity of 6.8 km/sec is measured at a depth of 7 to 8 km. on a single profile south of the Balearic Islands. Another single profile located west of Oran near

the extreme southwestern margin of the basin shows a velocity of 7.7 km/sec at 8 km. depth; this velocity measurement is however unreversed.

The seismic results are presented as a crustal structure section extending from north of the Balearic Islands across the western Mediterranean Basin to Genoa. The section emphasizes the relatively thin section of crustal rocks underlying the western Mediterranean Sea and the associated shallow depths to the Mohorovicic discontinuity. If the intermediate velocity material were absent and the water deeper, then the structure section would closely resemble that of a typical ocean basin. Depth to the Mohorovicic discontinuity is a minimum in the central part of the basin and increases toward the basin margin in the direction of both Corsica and the Balearic Islands.

The published free air gravity anomalies, after addition of a Bouguer correction, show excellent general agreement with the seismic results. The deduced crustal section is discussed with respect to various tectonic hypotheses which have been suggested for the origin of the western Mediterranean Sea, and a comparison is made with the crustal structure underlying the neighboring European continent and Alpine mountain chains.

Thesis Supervisor: Prof. J. B. Hersey
Geophysicist
Woods Hole Oceanographic Institution
Woods Hole, Massachusetts

TABLE OF CONTENTS

	<u>Page</u>
ABSTRACT	2
LIST OF FIGURES AND TABLES	6
INTRODUCTION	8
Scope of Investigation	8
Geography and Physiography	9
Tectonics	15
Previous Geophysical Studies	17
Seismic Refraction	17
Seismic Reflection	18
Surface Waves	18
Gravity Measurements	19
LOCATION OF GEOPHYSICAL OBSERVATIONS	21
Location of Seismic Refraction Stations	21
Location of Seismic Reflection Profiles	23
Navigational Accuracy	24
METHODS AND TECHNIQUES	28
General Procedure	28
Measurements	30
GEOPHYSICAL RESULTS	38
Notation	38
Results	41
Profile 193 - Tyrrhenian Sea	41
Profile 194 - Western Mediterranean Basin (S)	43
Profile 195 - Western Mediterranean Basin (N)	46
Profiles 196, 197 - Balearic Platform	48
Profile 198 - Western Mediterranean Basin (SW)	53
Profile 199 - Western Mediterranean Basin (SW)	54
Profile 2 - Western Mediterranean Basin (N)	58
Topography	58
Sections 2. 1, 2. 2, 2. 3	59
Sections 2. 4, 2. 5, 2. 6	60
Sections 2. 7, 2. 8	65
Profile 3 - Continental Shelf and Slope	67
Topography	67

	<u>Page</u>
Sections 3.1 to 3.6	68
Sections 3.7, 3.8	70
Structure along the profile	71
Profile 4 - Western Mediterranean Basin (N)	73
Sections 4.1 to 4.8	73
Results of Leenhardt (1962)	76
Profile 5 - Western Mediterranean Basin (N)	79
Sections 5.1 to 5.8	79
 DISCUSSION OF RESULTS	 93
Structure Cross Section	93
Mantle, High Velocity and Intermediate Velocity	
Crust	93
Significance of 5.7 - 6.0 km/sec Material	97
Continental Margin	99
Unconsolidated and Semiconsolidated Sediments	100
Significant Features: Summary	102
Comparison with European Crustal Structure	103
Comparison of Oceanic, Intermediate and Continental	
Crust	109
Gravity Field	117
Theories of Tectonic Origin	125
Unresolved Problems	131
 APPENDIX I - Profile Evaluations	 133
 APPENDIX II - Computations of Crustal Mass	 157
 ACKNOWLEDGEMENTS	 159
 BIBLIOGRAPHY	 163
 BIOGRAPHY	 171

LIST OF FIGURES AND TABLES

	<u>Page</u>
Figure 1. Location Chart - Refraction Profiles	10
Figure 2. Alpine Orogenies of the Western Mediterranean	14
Figure 3. Diagram of Procedure (Profiles 2, 3, 4, 5)	29
Figure 4. Seismograms - Profile 195	33
Figure 5. Seismograms - Profiles 195, 2. 5	34
Figure 6. Seismograms - Profile 2. 5	35
Figure 7. Seismograms - Profiles 4. 8, 5. 7	36
Figure 8. Seismograms - Profile 5. 7	37
Travel Time Graph and Velocity-Depth Section	
Figure 9. Profile 193	45
Figure 10. Profile 194	45
Figure 11. Profile 195	47
Figure 12. Profile 196	47
Figure 13. Profile 197	52
Figure 14. Profile 198	52
Figure 15. Profile 199	55
Figure 16. Travel Time Graph - Profile 2	84
Figure 17. " " " Profile 3	85
Figure 18. " " " Profile 4	86
Figure 19. " " " Profile 5	87
Figure 20. Velocity-Depth Structure - Profile 2	88
Figure 21. " " " Profile 3	89
Figure 22. " " " Profile 4	90
Figure 23. " " " Profile 5	91
Figure 24. CSP Reflection Record	92
Figure 25. Explosive Reflection Record	101
Figure 26. Velocity-Depth Structure - Western Mediter- ranean Sea	112
Figure 27. " " " - Venezuelan Basin	113
Figure 28. " " " - Western Atlantic Basin	114
Figure 29. " " " - Continental Europe and Asia	115
Figure 30. Comparison of Velocity-Depth Structure	116
Figure 31. Depth to Mohorovičić Discontinuity as a Function of Bouguer Gravity Anomaly and Surface Elevation	119
Figure 32. Gravity Field of Western Mediterranean Sea - Bouguer Anomaly	121
Table 1. Geographic Location - Profiles 193 to 199	25
Table 2. " " Profiles 2 to 5	26

	<u>Page</u>
Seismic Velocities, Layer Thicknesses and Depth	
Table 3. Profiles 193 to 199	56
Table 4. Profile 2	65
Table 5. Profile 3	72
Table 6. Profile 4	77
Table 7. Profile of Leenhardt (1962)	78
Table 8. Profile 5	81
Table 9. Values of C_0 and $\overline{C_V}$	83
Table 10. Heligoland Results	105
Table 11. Haslach Experiment	105
Table 12. Crustal Thickness (after Caloi, 1958)	107
Table 13. Comparison of Europe and Western Mediterranean Crustal Thickness	108
Table 14. Crustal Mass.	124
Plate 1. Bathymetric Chart of Mediterranean Sea	174
Plate 2. Seismic Crustal Section	175

INTRODUCTION

Scope of Investigation

The western Mediterranean Sea and the folded and thrust mountain ranges which encircle it have attracted the attention of earth scientists for more than a hundred years. The tectonic and structural relationship between the two continental blocks of Europe and Africa are effectively concealed from view by the intervening Mediterranean seaway. The relatively recent adaptation of geophysical methods for marine use now make possible direct physical measurements in water covered areas.

Several seas on the earth's surface are known to have water depths significantly shallower than that measured in the deep ocean; examples are the Gulf of Mexico, the Caribbean, and the Mediterranean. The crustal structure beneath these seas is significantly different from that beneath the oceans and also that associated with the continents. Studies of these intermediate regions are of interest to geologists and geophysicists because they contribute to an understanding of the transition between continental and oceanic crustal structure and because they are valuable in synthesizing the tectonic and geologic history of the region in question.

The seismic refraction and reflection experiments reported in this paper were made to determine the crustal structure underlying the western Mediterranean Basin. Specifically, measurements at each refraction station were designed to detail the velocity-depth layering within the crust and to determine the depth to mantle wherever possible.

The geophysical data include results of eleven seismic refraction stations and two short seismic reflection profiles made using explosive sources. These data were obtained during two cruises to the Mediterranean Sea in the summers of 1958 and 1959. Results obtained from continuous reflection profiles made in 1961 have been used to extend and supplement the results of the seismic refraction study; however, the detailed analysis of these seismic reflection records has not been attempted. The locations of the seismic refraction stations are shown in Figure 1 and Plate 1; the locations of the seismic reflection stations and continuous reflection profiles are shown in Plate 1.

Geography and Physiography

The Mediterranean Sea, land-locked except for the narrow strait leading to the Atlantic Ocean at Gibraltar, extends in an east-west direction for 2500 miles and is bounded to the north by the European continent and to the south by the African continent. The maximum

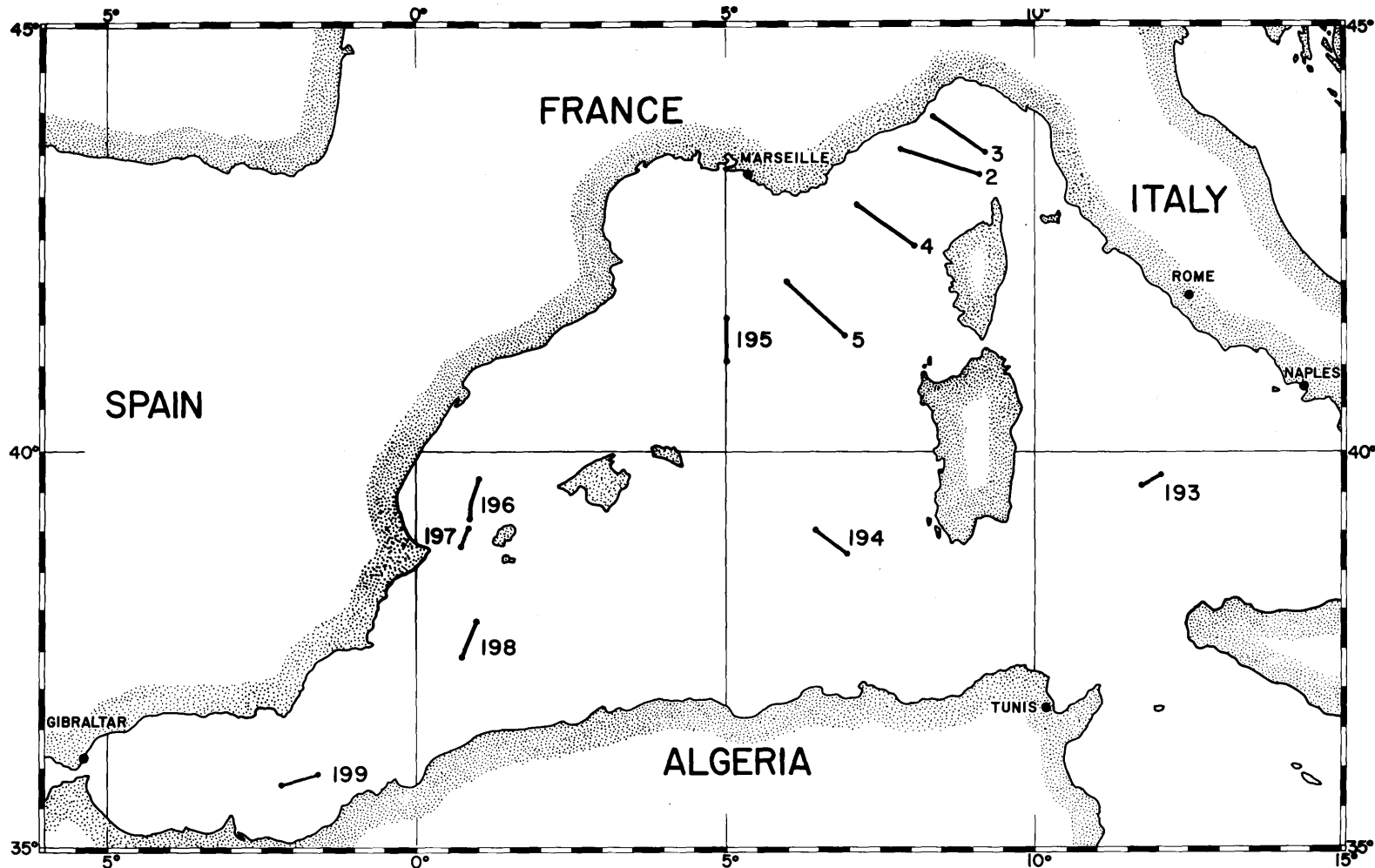


Figure 1. Location Chart - Refraction Profiles

water depth encountered in the western Mediterranean is slightly greater than 2800 meters (1530 fathoms); the boundary of the abyssal plain is approximately delineated by the 2500 meter (1370 fathoms) depth contour. The Mediterranean Sea is clearly not oceanic in depth (5000 to 5500 meters) nor is it a shallow epicontinental sea.

The geographic term, western Mediterranean Sea, as used here, will refer to that portion of the Mediterranean Sea delimited by the land masses of France, Spain, Corsica, Sardinia, and North Africa. The Tyrrhenian Sea, for purposes of this discussion, has not been included with the western Mediterranean Sea. Further subdivisions of the western Mediterranean Sea are in common usage. That portion of the Mediterranean located to the north of Corsica is frequently termed the Ligurian Sea. The shallow water embayment located south of France between Toulon and Pt. Vendres is the Gulf of Lyon. The oval shaped sea located just to the east of the Strait of Gibraltar is known as the Alboran Sea. South of the Balearic Islands, the deep water area has frequently been referred to as the Balearic Sea. The deep water area of the western Mediterranean Sea (more than 2500 meters), exclusive of the Alboran Sea, will be referred to in physiographic terms as the western Mediterranean Basin.

Bathymetric studies in the western Mediterranean Sea, including several detailed surveys in coastal areas, have been published by the Musée Océanographique de Monaco under the supervision of Bourcart, (1959a, 1960). A detailed chart of the northern Tyrrhenian Sea and a portion of the Ligurian Sea has been published by the Italian Hydrographic Office (Debrazzi and Segre, 1960). R. M. Pratt (personal communication) has analyzed all bathymetric data in the area taken by Woods Hole Oceanographic Institution vessels since 1946 and has made these results available to the author. The bathymetric studies have clearly defined the physiographic provinces of the western Mediterranean and established the extent and limits of the western Basin. Bourcart (1960) has noted the approximately right triangular shape of the western Basin; the two right sides of this triangle are bounded by Corsica - Sardinia on the east and the north African coast on the south; the hypotenuse of the triangle is formed by the coasts of France and Spain (Plate 1). Water depth in the basin generally exceeds 2500 meters (1370 fathoms) and reaches depths greater than 2700 meters (1480 fathoms) in its southwestern portion; the basin floor is an abyssal plain. The continental shelves bounding the basin are extremely narrow, seldom wider than 20-25 kilometers, except

in the region of the Gulf of Lyon, where the shelf attains a width of 90-100 kilometers. The continental slope, except along the east coast of Spain, is extremely steep, incised by numerous canyons, and has extremely rugged relief (Bourcart, et al, 1948; 1950; 1952; Bourcart, 1955; 1957; 1958; 1959b).

The Balearic Platform, a direct continuation of the Betic Cordillera of southern Spain, extends northeasterly into the western Mediterranean from the southeast coast of Spain. It is bounded by steep northeast-southwest trending slopes, probably of fault origin, and is separated from the Spanish coast to the northwest by a northeast-southwest trending trough which connects to the northeast with the main basin.

The western Mediterranean and Tyrrhenian Seas are bordered by chains of mountains formed by folding and faulting (Figure 2); tectonic activity in some of these ranges has continued from Cretaceous time up to the Pliocene. In North Africa the Rif of Spanish Morocco and the Tellian Atlas of Algeria form the southern border of the western Mediterranean Basin. The Betic range of southern Spain extends in a northeasterly direction toward the Balearic Islands. The Pyrenees of Southern France strike east-west and appear to end abruptly at the margin of the western Basin.

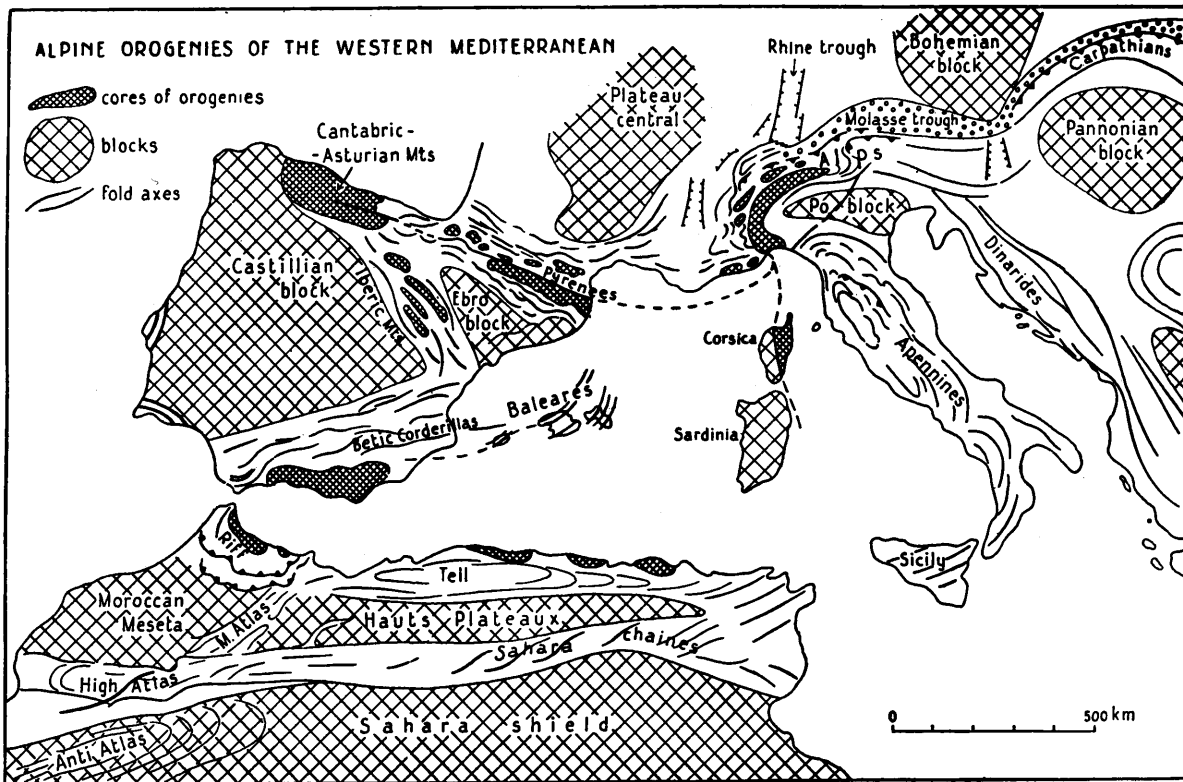


Figure 2. Alpine Orogenies of the Western Mediterranean (from "Structural Geology" by L. V. DeSitter, 1956)

The eastern margin of the Tyrrhenian Sea is bounded by the coast of Italy; the Appennines extend the entire length of Italy and into Sicily. The Maritime Alps of southern France and northwestern Italy strike into the western Basin in the region of the Ligurian Sea.

Tectonics

Regions of extensive Tertiary tectonic activity adjoin the shoreline of the modern Mediterranean Sea throughout much of its length. The Alpine mountain chains of Europe and the Atlas and Rif chains of North Africa either closely parallel the present shoreline or abut against it. Studies in these regions by geologists such as Suess, Staub, Stille and Termier, and more recently by L. Glangeaud and his students have contributed to the development of our understanding of earth tectonics. These geologists and others early attempted to establish the connecting links between the orogenic belts surrounding the Mediterranean; frequently the connecting links were postulated to lie beneath the present sea floor. Examples of this concept are the connecting link across the Strait of Gibraltar of the Betic-Rif system first proposed by Suess; the linking of the Atlas of North Africa through Sicily with the Southern Appennines; the extension of the Betic ranges into the Balearic Islands; and attempts to connect the Pyrenees with the Maritime Alps.

Several hypotheses have been proposed to explain the present structural configuration of the western Mediterranean Sea. Similarities between the stratigraphy along portions of the North African and southern European coast have led some geologists to suggest that the land masses of Europe and Africa were once continuous at some time in the geologic past. The depressed basin occupied by the present Mediterranean Sea might be accounted for by either one of three different mechanisms: (1) the pulling apart of Europe and Africa with subsequent thinning of the crust and attendant collapse of the central basin, (2) compression from the north and south forcing Europe and Africa together with eventual fracturing near the present continental margins and subsequent overriding and depressing of the basin by the European and African blocks and (3) the breaking apart of the European-African crust and subsequent drift to the present position. Gravity measurements do not support the second hypothesis.

The Mediterranean Sea lies along the axis of an east-west belt of seismic activity extending from Burma westward through Asia and the Caucasus to the Azores. The western Mediterranean Sea is, however, a zone of minor seismic activity (Gutenberg and Richter, 1954). Most of this activity in the western Mediterranean region occurs in two zones marginal to the western Basin and Tyrrhenian Sea. Several earthquake epicenters have been located in the coastal region of North Africa

and the Alboran Basin, and in the zone interior to the arcuate structure forming the southernmost part of Italy and Sicily. The strongest recorded shock originating in this area was the Messina earthquake of 1908; its magnitude, according to Gutenberg and Richter (1954), was not greater than 7.5. Volcanism is present in the interior arc extending from Naples through the Lipari Islands and into Sicily. Seismic activity in the region bordering the western Mediterranean to the north and northwest is extremely low.

Previous Geophysical Studies

Seismic Refraction. Previous direct investigation of the crustal structure underlying the Mediterranean Sea has been limited to a few reconnaissance refraction profiles which were too short to obtain energy arrivals from deep high-velocity layers. Gaskell, et al (1958) report the results of three refraction stations made in the eastern Mediterranean Sea (Ionian Basin) during the 1950-1952 cruise of HMS CHALLENGER. Results for all three stations indicate that the Ionian Basin is floored by a thin layer of low velocity sediments underlain by material having intermediate velocities in the range 4.2 to 4.7 km/sec. Two additional unreversed profiles in the Ionian Basin reported by Ewing and Ewing (1959) are in agreement with these results. Results of three other unreversed

refraction profiles located in the Tyrrhenian Sea, in the western Mediterranean Basin west of Corsica, and in the Alboran Basin, have also been reported by Ewing and Ewing (1959).

Results of a single short profile established by CHAIN and WINNARETTA SINGER in 1959 have been recently published by Leenhardt (1962). This profile directly adjoins the northwest end of Profile 4 (Plate 1) and will be discussed in detail later. Two reversed refraction profiles have been reported by Muraour, et al (1962) in the Gulf of Lyon. Muraour (personal communication) has also obtained a profile between Cape Corsica and the Italian coast, but the data are as yet unpublished.

Seismic Reflection. Several reflection experiments have been conducted in the Mediterranean Sea by Weibull (1947, 1955); the preliminary results of these experiments were discussed by Petterson (1946). Continuous reflection measurements were made from CHAIN in 1961 under the direction of J. B. Hersey, E. Hays, and D. Caulfield of the Woods Hole Oceanographic Institution. The results are not yet published.

Surface Waves. No studies of surface wave dispersion occurring over western Mediterranean travel paths have been published. Knopoff and Press (1960) have published a proposal for such a

study; the experimental measurements were carried out during the summer of 1961 (Knopoff, personal communication) but their results have not been published to date.

Gravity Measurements. Gravity measurements in the western Mediterranean have been reported by several investigators (Cassinis, et al, 1934, 1935; Pelissier, 1939; Vening Meinesz, 1932). Coster (1945) has made isostatic computations (Vening Meinesz regional isostatic system) and published gravity maps of the western Mediterranean region based on these pendulum measurements. Worzel (1959) reports two traverses across the Tyrrhenian Sea and two traverses through the Strait of Gibraltar and Alboran Basin made with the Graf Sea Gravimeter.

Despite occasional uncertainties in some of the early pendulum measurements, certain broad regions of positive or negative free air anomalies can be outlined. A belt of negative free air anomalies (-60 to -80 mgals) parallels the southeast coast of southern Italy and Sicily. A second belt of negative anomalies (-40 to -100 mgals) is coincident with the Betic-Rif System in the region of Gibraltar; Worzel (1959) measured a double negative anomaly on each of two parallel tracks passing through the Strait of Gibraltar. A belt of positive free air anomalies extends from the coast of Spain north-eastward through the Balearic Islands. The northern half of the

western Mediterranean Basin has a nearly zero free air anomaly, measured values ranging from +11 to -9 mgals in this region.

Several speculative syntheses of the gravity data and their interpretation in terms of tectonics of the western Mediterranean Sea have been made by various authors (Coster, 1945; van Bemmelen, 1952; Hoffman, 1952; and Cizancourt, 1948, 1953). Studies of the gravity field of the adjoining land areas have been made by Lejay and Coron, (1950, 1953), and Coron (1954). No completely reliable gravity data has been taken over the same region covered by the refraction profiles to be discussed here.

LOCATION OF GEOPHYSICAL OBSERVATIONS

Location of Seismic Refraction Stations

Profiles 193-199, taken during the course of a seismic reconnaissance survey made by ATLANTIS and VEMA during the International Geophysical Year, are rather widely spaced throughout the western Mediterranean region. The locations of the profiles are shown in Figure 1 and again on Plate 1, and the geographic coordinates (latitude and longitude) for each profile are listed in Table 1. Four additional profiles, numbered 2, 3, 4, and 5 were obtained in 1959 by scientists of the Woods Hole Oceanographic Institution; two research vessels, the CHAIN (Woods Hole Oceanographic Institution) and the WINNARETTA SINGER (Musée Océanographique de Monaco) participated in this study. The locations of these stations are also shown in Figure 1 and, in greater detail, on Plate 1, and the geographic coordinates are listed in Table 2.

Geographically the profiles may be grouped as follows:

a) Tyrrhenian Sea - Profile 193 is located in the south central Tyrrhenian Basin; water depth along the profile section exceeds 3.3 km.

b) Western Mediterranean Basin (South) - A single profile, 194, consisting of two unreversed segments, is located midway between

Sardinia and the Balearic Islands at approximately 39°N latitude.

This is the only seismic measurement obtained in the southern half of the basin.

c) Western Mediterranean Basin (North) - Profiles 195, 2, 4, and 5 are all located in deep water in the northern half of the basin. Profile 195 extends in a north-south direction and is located approximately midway between the Gulf of Lyon and the Balearic Islands. Profile 5, located about 90 km. to the east of Profile 195, is aligned in a northwest- southeast direction. Profile 4 extends in a northwest- southeast direction from a point seaward of Cape Camarat to a point northwest of Porto, Corsica. The most northeasterly basin profile extends from a point offshore due south of San Remo, Italy, to the vicinity of Cape Corse.

d) Continental Shelf and Slope - Profile 3 is located at the extreme northeast margin of the basin across the approaches to the Gulf of Genoa. The profile trends almost east-west and crosses the two deep embayments extending northwesterly into the continental slope. Water depth varies from 0.8 to 2.30 km. along the profile section.

e) Balearic Platform - Two profiles, 197 and 198, are oriented north-south and midway between Spain and the Balearic Islands from

slightly north of the latitude of Valencia to the latitude of Cape Nao.

f) Western Mediterranean Basin (Southwest) - Profile 198 is located southwest of the Balearic Islands in 2.8 km. of water. The seismic section starts about 15 km. from the steep slope south of the Balearic platform and extends southwesterly toward the central portion of the basin.

Profile 199 is located at the extreme southwesterly margin of the basin in about 2 km. of water; it is almost 100 km. due west of Oran, Algeria.

Location of Seismic Reflection Profiles

Seismic reflection data have been used to supplement and extend the refraction information whenever possible. Two explosive reflection profiles, Profile 1 and Profile 2, obtained on CHAIN Cruise 7 in 1959, are located midway between Menorca and the Gulf of Lyon. Continuous Seismic Profiler (CSP) recordings (Hoskins and Knott, 1961; Hersey, in press) made on CHAIN Cruise 21 in 1961 cover much more extensive area (Plate 1). One such profile extends almost continuously from the southern end of Profile 197 northward to the southern end of Profile 196, and then northeastward along the axis of the trough between the Balearic Islands and Spain. This CSP profile ends north of Mallorca. A second CSP

profile extends from midway between Profiles 5 and 4 northeastward to the midpoint of Profile 2. A third CSP section, only a few kilometers in length, is located in the vicinity of Profile 2.

Navigational Accuracy

Ships' positions during the refraction study were determined from celestial observations and dead reckoning except when visual and/or radar bearings could be taken on landmarks. Thus the absolute positions given for end points of the profiles may be subject to considerable error. The positions given are the best estimates obtained when navigational data for both ships were reconciled. The results may be in error by as much as ± 5 km. (± 3 miles) for profiles 194, 198 and 199. The error in position for the remaining profiles is less.

Absolute distance between shot point and receiver was obtained from the travel time of the direct water wave. The travel time of the direct water wave, D , multiplied by the sound velocity in the surface sound channel gives the range between shot point and receiver. The uncertainty in the determination of the range is $dR = C_0 dD + D dC_0$ where R =range in meters. Assuming the travel time, D , is known to $\pm .005$ seconds and the velocity is known to ± 2 m/sec., the uncertainty in the range determination is $dR = \pm 7.5 \pm 2D$ meters.

TABLE 1 - Geographic Location - Profiles 193 to 199
(July 24 - July 31, 1958)

<u>No.</u>	<u>Ship</u>	<u>Latitude</u>	<u>Longitude</u>
193	VEMA (NE)	39°43'N	12°05'E
	ATLANTIS (SW)	39°35.5'N	11°45'E
194	ATLANTIS	38°51'N	6°41.5'E
	End (NW)	39°01.5'N	6°27'E
	End (SE)	38°43'N	6°56'E
195	VEMA (N)	41°40'N	5°01'E
	ATLANTIS (S)	41°10'N	5°01'E
196	VEMA (N)	39°40'N	1°02'E
	ATLANTIS (S)	39°22'N	0°55'E
	End (S)	39°10'N	0°50'E
197	VEMA (NE)	39°02'N	0°52'E
	ATLANTIS (SW)	38°47'N	0°43'E
198	VEMA (N)	37°50.5'N	0°57'E
	ATLANTIS (S)	37°24'N	0°41'E
199	ATLANTIS (E)	35°58'N	1°39'W
	End (W)	35°49'N	2°12'W

TABLE 2 - Geographic Location - Profiles 2 to 5
(1 July - 10 July, 1959)

<u>Section</u>	<u>Ship</u>	<u>Profile 2</u>			
		<u>Northwest</u>		<u>Southeast</u>	
		<u>Latitude</u>	<u>Longitude</u>	<u>Latitude</u>	<u>Longitude</u>
2.1	W. S.	43°33.5'N	7°53.5'E	43°26.5'N	8°09'E*
2.2	W. S.	43°27'N	8°09.5'E*	43°21'N	8°26'E
2.3	CHAIN	43°29.5'N	8°09'E	43°25'N	8°31'E*
2.4	CHAIN	43°24'N	8°37'E*	43°20'N	8°52.5'E
2.5	W. S.	43°21.5'N	8°39'E	43°17'N	8°55.5'E*
2.6	W. S.	43°17.5'N	8°54'E*	43°14'N	9°08'E
2.7	W. S.	43°28'N	8°03'E*	43°17.5'N	8°56'E
2.8	W. S.	43°33'N	7°52.5'E	43°14.5'N	9°08.5'E*

<u>Section</u>	<u>Ship</u>	<u>Profile 3</u>			
		<u>Northwest</u>		<u>Southeast</u>	
		<u>Latitude</u>	<u>Longitude</u>	<u>Latitude</u>	<u>Longitude</u>
3.1	W. S.	43°57'N	8°23.5'E	43°52'N	8°33'E*
3.2	W. S.	43°52'N	8°33'E*	43°46'N	8°46.5'E
3.3	CHAIN	43°51'N	8°37'E	43°46'N	8°48'E*
3.4	CHAIN	43°46'N	8°48'E*	43°38.5'N	9°00.5'E
3.5	W. S.	43°45'N	8°49.5'E	43°38.5'N	9°01.5'E*
3.6	W. S.	43°36'N	9°01'E*	43°30'N	9°12'E
3.7	W. S.	43°48.5'N	8°36.5'E*	43°36'N	9°01'E
3.8	W. S.	43°52'N	8°33.5'E	43°36'N	9°05'E*

Profile 4

<u>Section</u>	<u>Ship</u>	<u>Northwest</u>		<u>Southeast</u>	
		<u>Latitude</u>	<u>Longitude</u>	<u>Latitude</u>	<u>Longitude</u>
4.1	W. S.	42°55'N	7°04'E	42°48.5'N	7°14.5'E*
4.2	W. S.	42°48.5'N	7°14.5'E*	42°40'N	7°31'E
4.3	CHAIN	42°47'N	7°16'E	42°40.5'N	7°34.5'E*
4.4	CHAIN	42°41'N	7°35'E*	42°35'N	7°50'E
4.5	W. S.	42°52.5'N	7°36.5'E	42°33'N	7°50.5'E*
4.6	W. S.	42°32.5'N	7°50.5'E*	42°27'N	8°02.5'E
4.7	W. S.	42°46.5'N	7°18'E*	42°32'N	7°51'E
4.8	W. S.	42°50.5'N	7°06'E	42°30.5'N	7°52'E*

Profile 5

<u>Section</u>	<u>Ship</u>	<u>Northwest</u>		<u>Southeast</u>	
		<u>Latitude</u>	<u>Longitude</u>	<u>Latitude</u>	<u>Longitude</u>
5.1	W. S.	41°54.5'N	6°07'E	41°49'N	6°16'E*
5.2	W. S.	41°48.5'N	6°15'E*	41°41'N	6°26'E
5.3	CHAIN	41°47.5'N	6°14'E	41°40.5'N	6°25'E*
5.4	CHAIN	41°40'N	6°25'E*	41°28.5'N	6°43'E
5.5	W. S.	41°39.5'N	6°30'E	41°29'N	6°49'E*
5.6	W. S.	41°28'N	6°42'E*	41°21.5'N	6°53'E
5.7	W. S.	42°01.5'N	5°57'E*	41°28'N	6°42'E
5.8	W. S.	41°56'N	6°05'E	41°27.5'N	6°49'E*

W. S. - WINNARETTA SINGER

* Denotes receiving location for that segment of profile.

METHODS AND TECHNIQUES

General Procedure

The methods and operational techniques of marine explosion seismology used by the geophysics groups of Woods Hole Oceanographic Institution and Lamont Geological Observatory have been discussed in considerable detail in the literature (Ewing, et al (1939); Officer (1958); Officer, et al (1959); and Drake, et al (1959)).

The refraction measurements obtained in 1958 were standard two-ship profiles, although not all profiles were reversed. Profile 194 consisted of an end to end shot line and a single receiving location. Profile 199 was shot in one direction only and is consequently unreversed. The remaining 1958 stations were completely reversed, except for a segment of Profile 197. The 1960 investigation was conducted somewhat differently. In order to study the sediment structure in detail, as well as the deep crustal structure, the profile sections and shooting procedure were modified. Each of these profiles (2, 3, 4, and 5) was made up of three overlapping end to end profiles and a much longer superposed reversed profile. The sequence of events in establishing these profiles is illustrated schematically in Figure 3. Initially WINNARETTA SINGER hove to at a preselected receiving location. CHAIN then fired shots along the desired course line up to and past

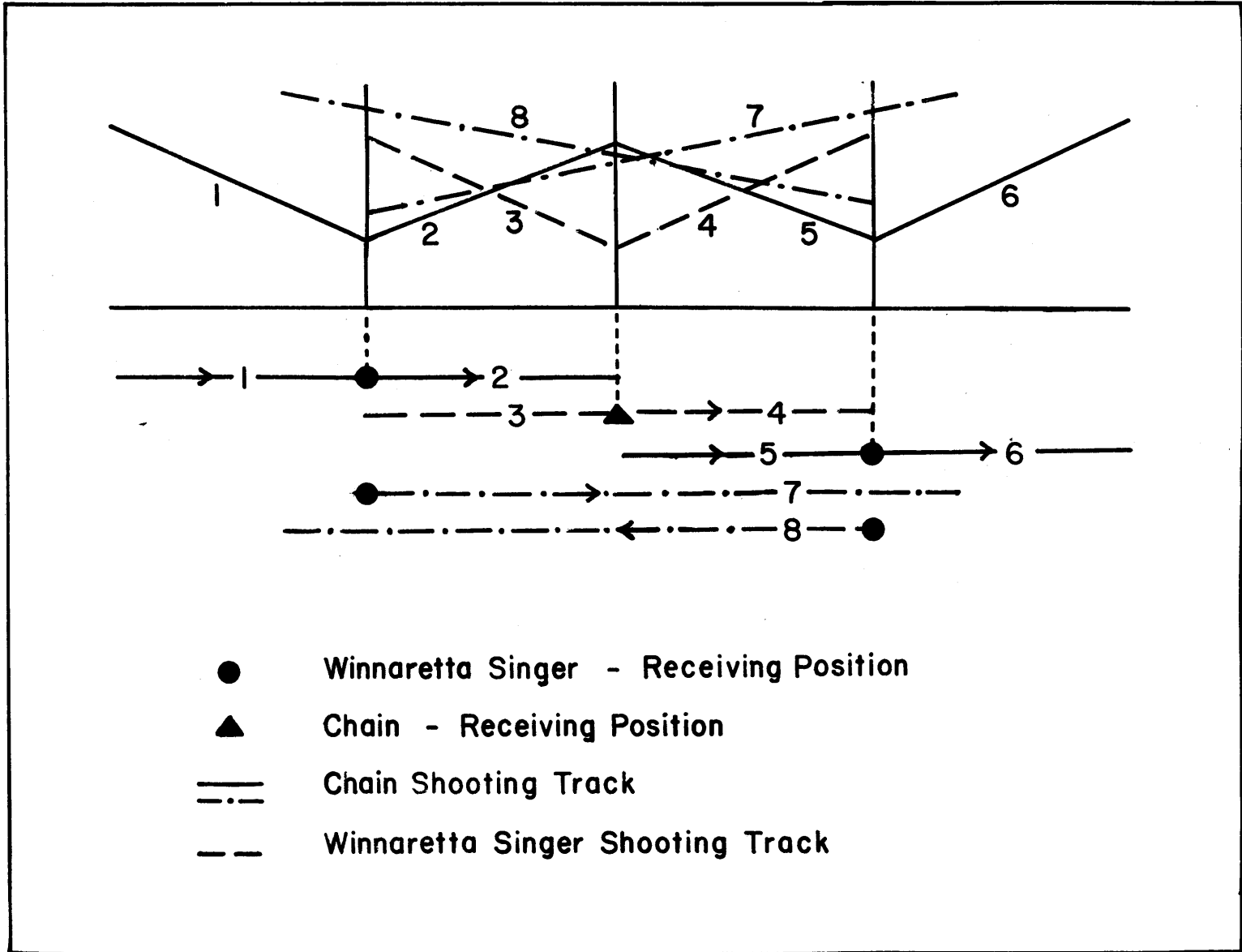


Figure 3. Diagram of Procedure (Profiles 2, 3, 4, and 5)

the WINNARETTA SINGER (Sections 1 and 2). CHAIN then hove to and WINNARETTA SINGER proceeded to fire the shots establishing Sections 3 and 4. The process was repeated once more to establish Sections 5 and 6, again with the WINNARETTA SINGER acting as the receiving ship. The short sections of the profile were shot with small charges (3 lbs. to 96 lbs.) fired at short range intervals. At the conclusion of the three end to end profiles the two exterior listening positions were reoccupied and the long reverse profile (7-8 in Figure 3) was completed; large charges (144 lbs. - 300 lbs.) were used to extend the measurements to ranges adequate to obtain refractions from the deep crustal horizons and the crust-mantle interface. Ideally the completed profile can be treated as two short reversed profiles (2-3 and 4-5) adjoined on either end by unreversed short profiles (1 and 6).

Measurements

The refraction and reflection seismograms were recorded photographically. The instrumentation used in the detection and recording of the acoustic signals has been discussed in detail by Officer, et al (1959). Included on the seismogram of each shot are signal traces from two hydrophones filtered for various frequency bands and gain settings, a radio trace for recording the shot instant transmitted by the shooting ship, and a timing trace. Typical seismograms are illustrated in

Figures 4, 5, 6, 7, and 8.

Auxiliary data were also obtained to aid in the reduction of the seismic data. The horizontal surface sound velocity, C_0 , used in the range computations, is sensitive to the temperature of the surface isothermal layer; therefore bathythermograph lowerings were made at intervals along each profile section during the shooting run. Continuous underway thermistor recordings were made along the sections of profile shot by CHAIN. Direct sound velocity measurements made with the National Bureau of Standards sound velocimeter (Greenspan and Tschiegg, 1957) supplemented these determinations (Hays, 1961).

Precision echo soundings were made as routine underway observations. These measurements have been valuable, (1) in increasing the physiographic knowledge of the sea floor and (2) in providing the data necessary for making reasonable topographic corrections to the seismic travel time data when necessary.

Data Reduction

The data were reduced using the methods outlined by Officer and Wuenschel (1951) and Sutton and Bentley (1953). The measured travel time data were corrected for shot instant (travel time from shot point to shooting ship), surface of reference (shot and receiving

points corrected to sea level), and topography (sloping bottom).

The corrected travel time data were plotted on conventional travel time graphs (travel time versus range in seconds of water travel time). The apparent velocities and time intercepts were established by visually fitting straight lines to the observed points. Additional control for determining reasonable fits to the data was provided by the travel time at the reverse point on a reversed profile and by the zero range time intercept for adjoining end-to-end profiles.

Compressional velocities and layer thicknesses were computed from the apparent measured velocities and intercepts following the method of Ewing, et al (1939). Unreversed sections of a profile were computed assuming horizontal layering unless noted otherwise in the discussion of results. The apparent velocity and intercept data were reduced to compressional velocities and thicknesses on a Recomp II computer.

PROFILE 195-ATLANTIS SEISMOGRAMS

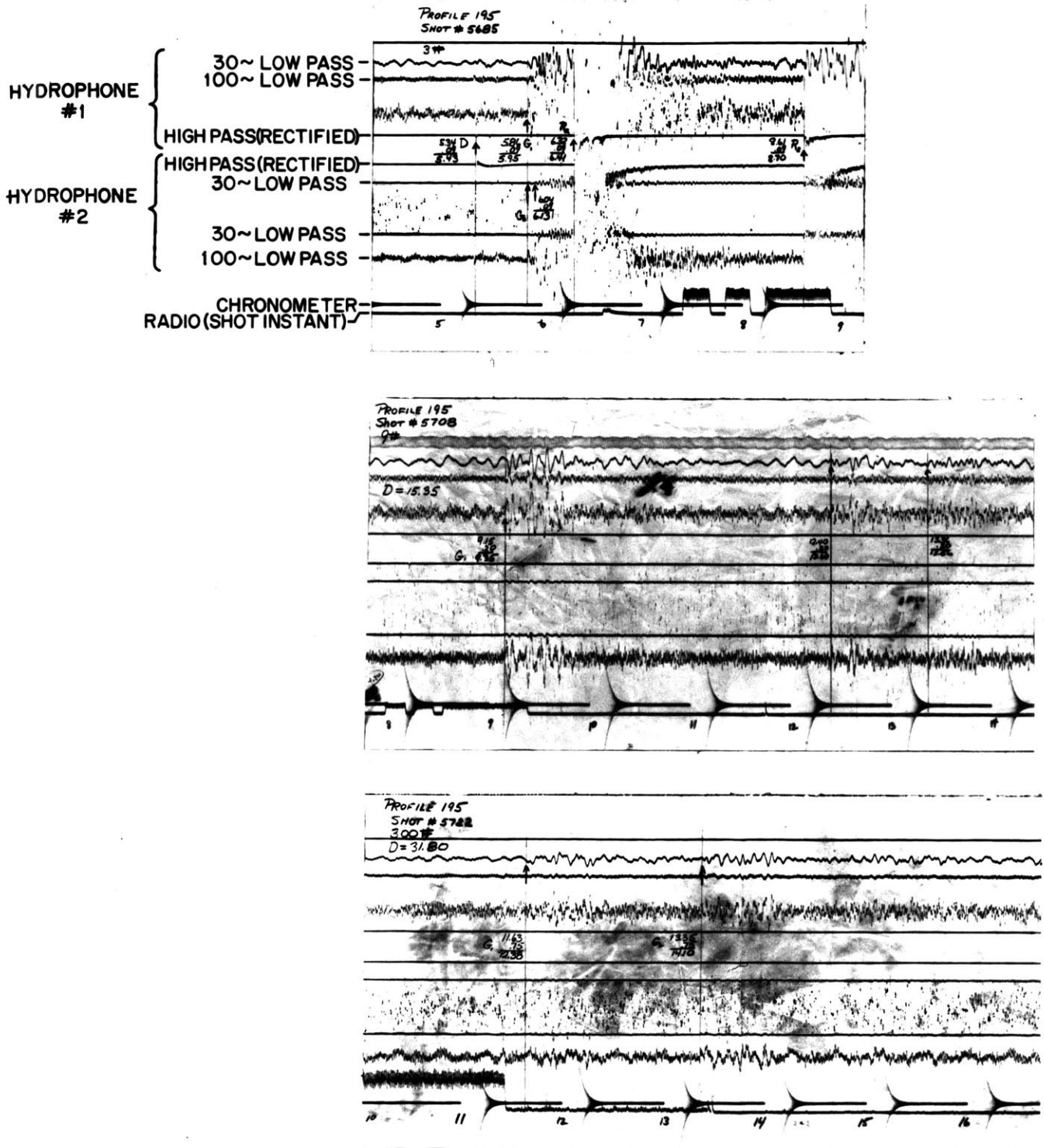
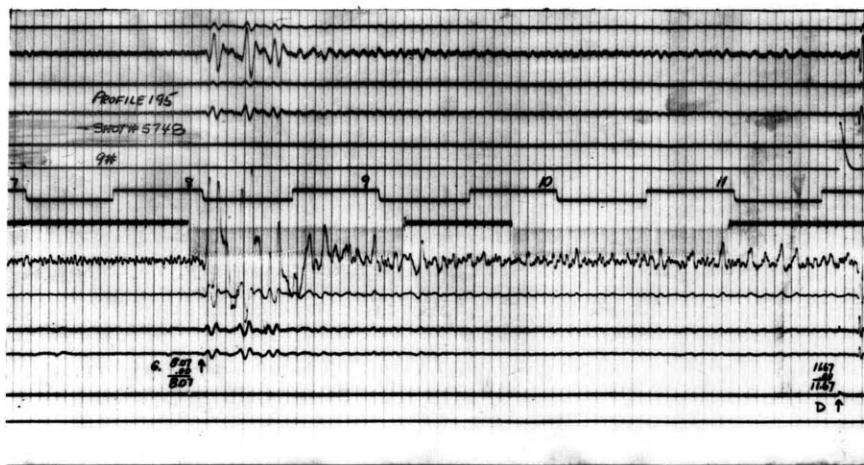
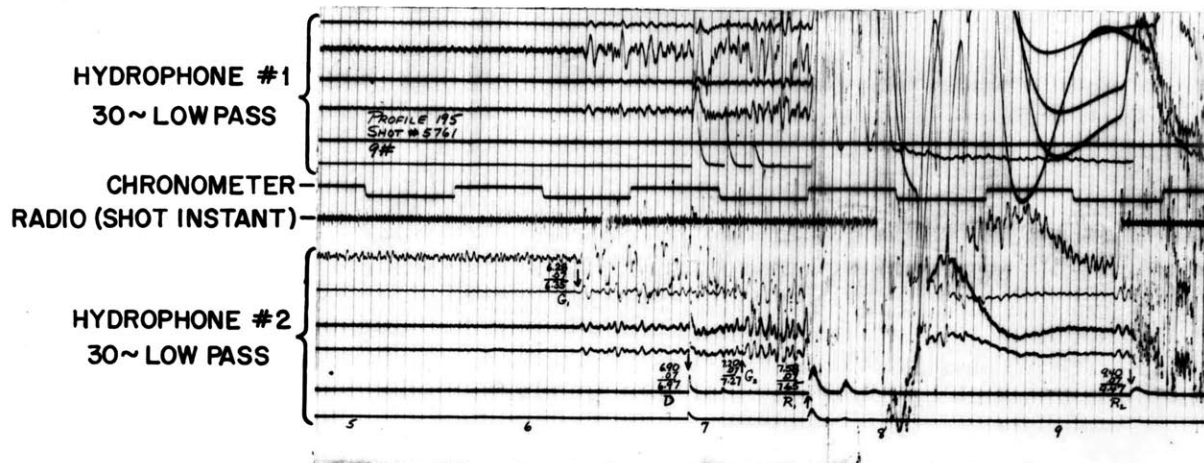


Figure 4.

PROFILE 195-VEMA SEISMOGRAMS



PROFILE 2.5-WINNARETTA SINGER SEISMOGRAMS

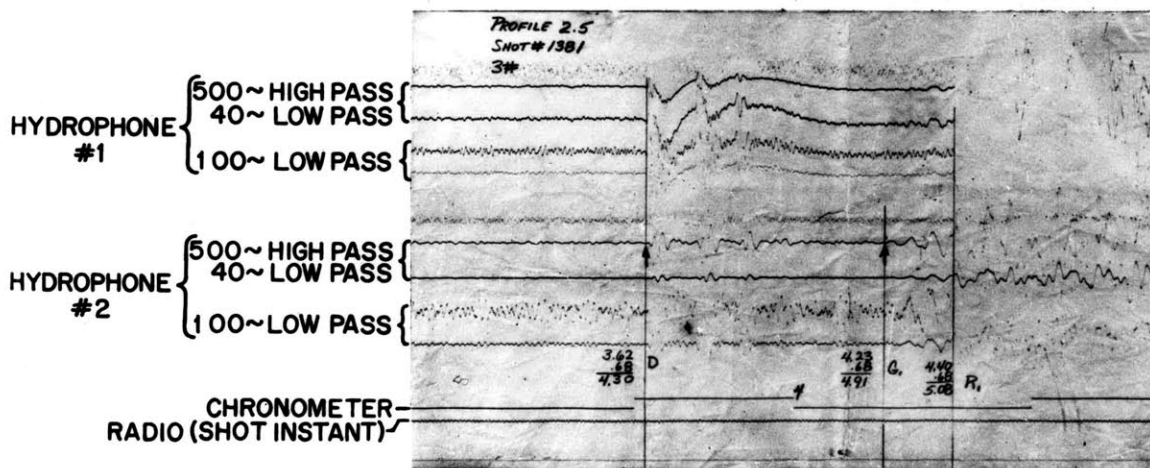


Figure 5.

PROFILE 2.5 (CONTINUED)

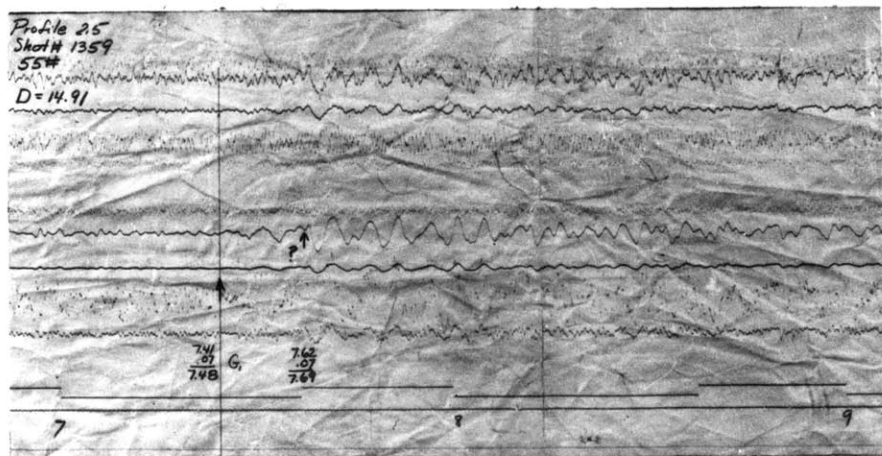
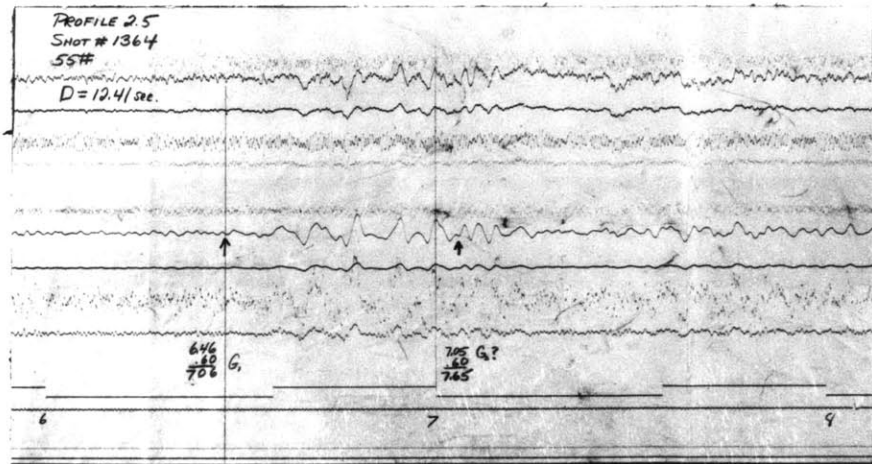
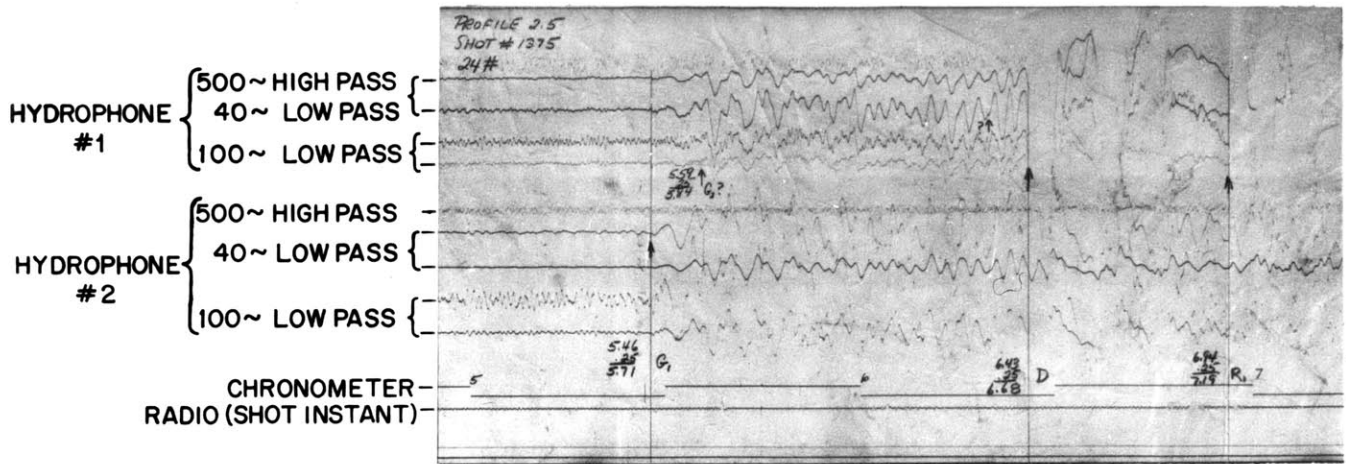
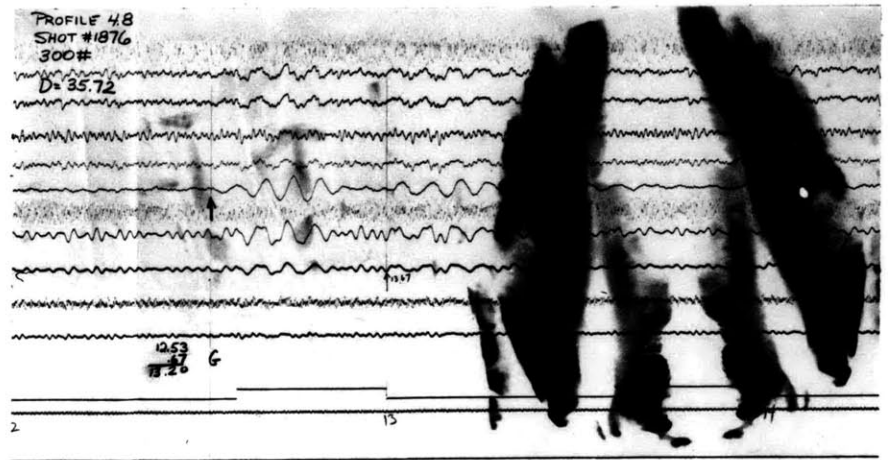
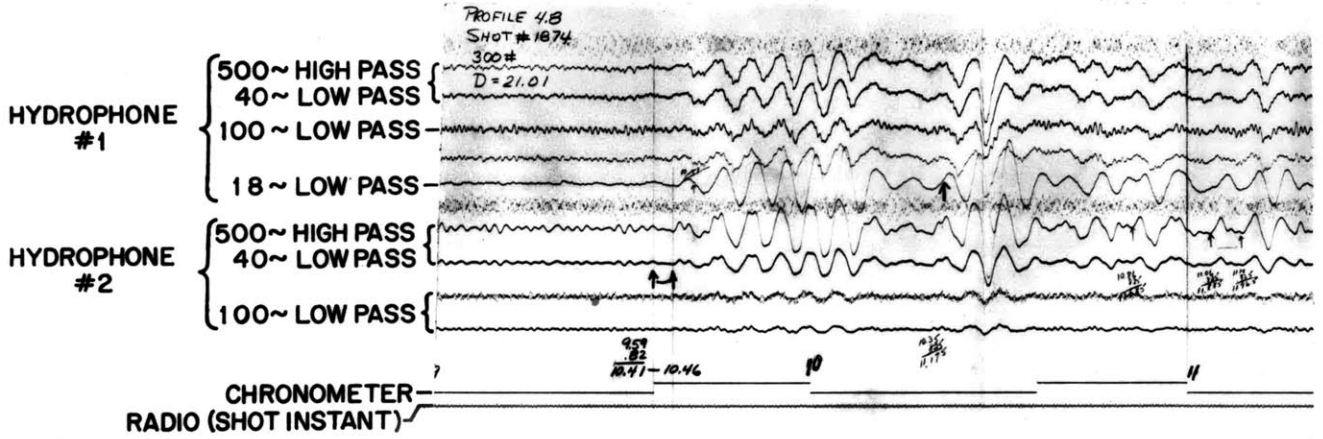


Figure 6.

PROFILE 4.8-WINNARETTA SINGER SEISMOGRAMS



PROFILE 5.7-WINNARETTA SINGER SEISMOGRAMS

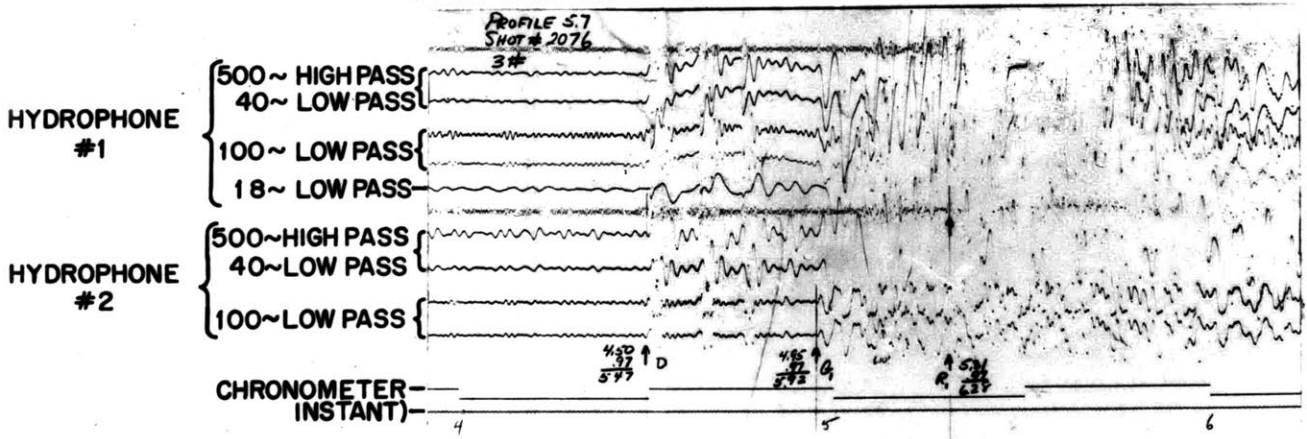


Figure 7.

PROFILE 5.7 (CONTINUED)

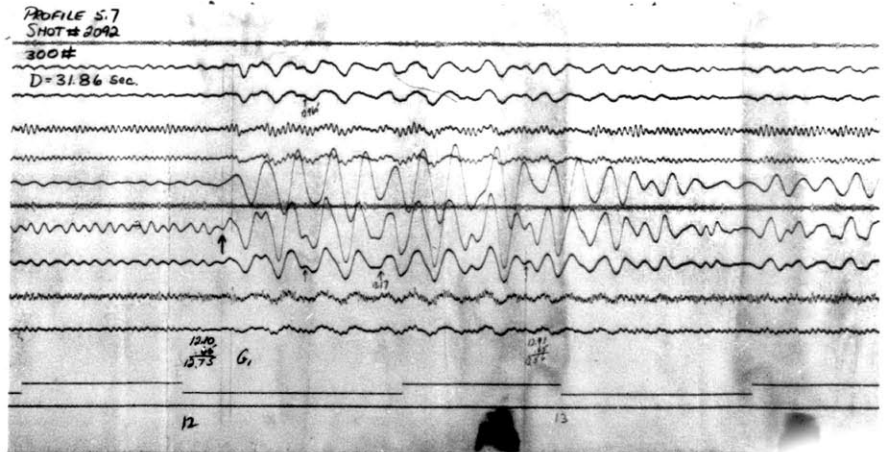
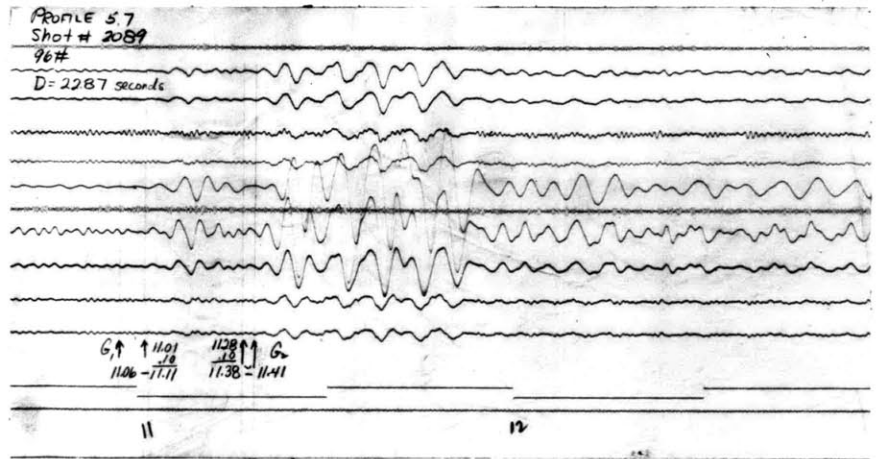
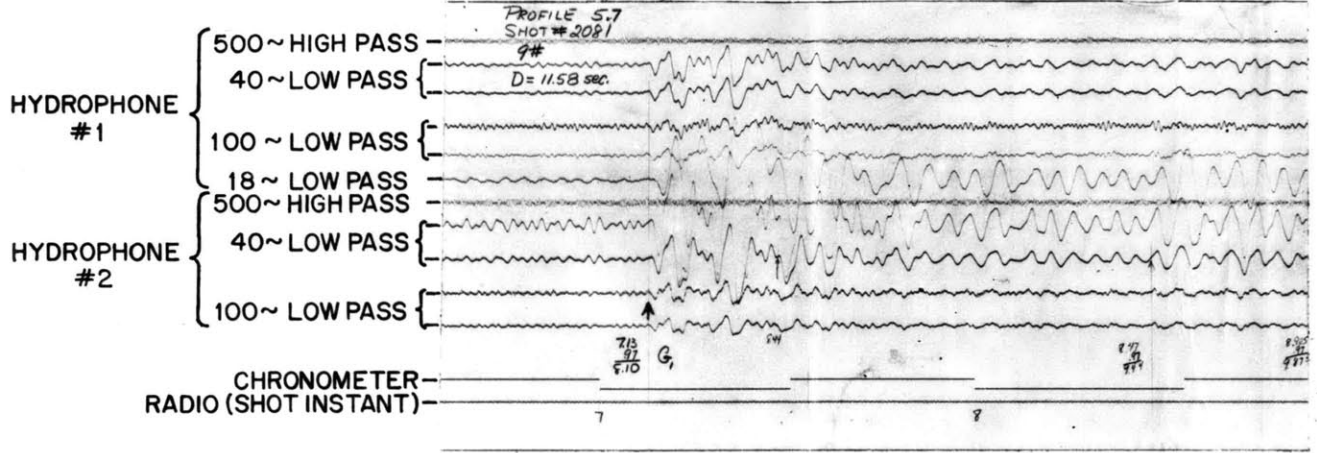


Figure 8.

GEOPHYSICAL RESULTS

Notation

The seismic refraction measurements are presented as travel-time graphs in Figures 9 to 19. The velocities, layer thicknesses, and depths computed from these travel-time graphs are presented in Tables 3 to 7. The average horizontal near-surface water velocity, C_0 , and the vertical water velocity, \overline{C}_v , used in the computations are listed in Table 9.

The travel-time graphs are plots of the travel time of the initial onset of refracted and/or reflected energy pulse trains (ordinate) as a function of distance (abscissa). The ordinate and abscissa are scaled in seconds. To obtain the range in kilometers the abscissa must be multiplied by C_0 , the surface water velocity (Table 9). In the profiles discussed here, C_0 varies from 1.51 to 1.53 km/sec; for a rapid estimate of range, a value of $C_0 = 1.50$ km/sec can be used with the introduction of only a small error.

The refraction arrivals are plotted as circles on the travel-time graph. First and second bottom reflections have been plotted as open triangles; sub-bottom reflections (Profiles 198 and 4.1), where identified, are plotted as inverted triangles. Each line shown on the travel-time graph has its associated slope and intercept expressed in the form of a linear equation: $T = T_0 + D/C$ where D is the distance in kilometers,

C is velocity in km/sec, T_0 is the zero intercept in seconds, and T is the travel time in seconds of the arrival in question. The inverse slope of the line, C , is the apparent wave velocity of the arrival measured along the sea surface.

The bathymetric sections along the profile are shown beneath the travel-time graph. The depth scale is shown in meters (left) and fathoms (right). Distance in kilometers along the profile is also shown beneath the travel-time graph.

The data from the six short sections making up an individual profile (Profile 2 to 5) are presented as three end-to-end travel-time graphs in Figures 16 to 19. These short sections are numbered with the profile and section number: e. g. 4.6 (Profile 4, Section 6). The section numbers are sequenced 1 through 6 from left to right in the figure. Geographically, Section 1 is the most westerly segment of the profile and section 6 the most easterly. Section numbers 7 and 8 are reserved for the long reversed profile. Unless otherwise noted in the text, Sections 2 and 3 make a reversed profile as do Sections 4 and 5.

Notation used in Tables 3 to 7 is as follows. The velocity measurements and layer thicknesses are tabulated in km/sec respectively. A velocity value enclosed in parentheses, i. e. (1.80), indicates that this velocity has been assumed. A velocity value enclosed in brackets, i. e. [3.44], indicates that the velocity measurement

is unreversed.

In the computational procedure for an unreversed profile several options are available. The velocity computations can be made assuming (1) all refracting horizons are horizontal or (2) all refracting horizons are parallel to the sea floor or (3) a combination of (1) and (2). When the adjoining profile indicates almost flat lying layers beneath the sea floor, the assumption of horizontal refracting horizons has been used. This procedure has been followed on Sections 1 and 6 of Profiles 2, 4 and 5.

The results for 3.2 - 3.3 and 3.4 - 3.5 indicate that the layers parallel the topography, at least to a first approximation. Therefore Sections 3.1 and 3.6 have been computed assuming that the refracting horizons parallel the topographic base line. Other modifications in the computational procedure are listed in the footnotes associated with each table.

The computed velocity - depth sections for Profiles 193 to 199 are shown in Figures 9 to 15 below the travel-time graphs. The velocity-depth sections for Profiles 2 to 5 are shown in Figures 16 to 19.

The lowest velocity measured on the travel-time graph seldom corresponds to refraction from the sea floor interface. Therefore, in the computations it is necessary to assume a velocity for that

material lying between the sea floor and the first refracting horizon. In those cases where this overlying layer appears to be extremely thin (less than 100 meters), the water velocity \overline{C}_v has been used for all material between sea level and the first refracting horizon. In the majority of the profiles, however, a somewhat higher assumed velocity, 1.80 - 2.00 km/sec, has been used in the computations. The choice of this velocity has negligible effect on the computed depths to the deeper horizons.

Results

Profile 193 - Tyrrhenian Sea (Table 3, Figure 9). The agreement between reverse points for the lowest velocity lines is poor and consequently the station has been treated in the computations as two unreversed profiles.

No unconsolidated sediment velocities were measured at either end of the profile; a velocity of 1.80 km/sec was assumed for this layer. Velocities of 4.36 km/sec (SW) and 3.92 km/sec (NE) were measured for material lying at shallow depths below the sea floor. Velocities of 7.28 km/sec and 6.96 km/sec were measured for the basement material; the depths to the top surface of this layer are 6.29 km. and 5.68 km. respectively.

Previous measurements in this region are limited to a single refraction station (D-10) reported by Ewing and Ewing (1959). This profile is located 60 miles to the north of Sicily and about 120 miles east of Profile 193. Their data show a refraction horizon with a velocity 4.9 - 5.7 km/sec at a depth of 0.9 - 1.2 km. below sea level. Unfortunately the profile crosses over a sea mount and they were unable to extend the range sufficiently to obtain refractions from deeper layers. In contrast with D-10, the results for Profile 193 show a markedly lower velocity for the first detectable refracting horizon. This layer, 2 to 2.6 km. thick, is underlain by high velocity (6.96 to 7.28 km/sec) material; a similar high velocity layer was not detected at D-10.

Results obtained on Profile 193 cannot be directly related to the structure of the Tyrrhenian Basin; the profile is isolated from regions of geologic control. Nevertheless, some inferences may be drawn by analogy with similar seismic sections obtained in regions of known geologic structure. Officer, et al (1952) obtained velocity-depth sections on portions of the Bermuda Platform which are similar to the results obtained in Profile 193. They tentatively identified the low velocity material (4.00 - 4.50 km/sec) as a layer of volcanics, sediments, and pyroclastics. This layer overlies a high velocity basement (7.19 km/sec) which they suggested as

possibly consisting of gabbro or related basic rock material. Drake, et al, (1959), obtained similar high velocities (7.1 km/sec) at shallow depths below the sea floor in the central part of the Red Sea. B ath (1960) measured a velocity of 7.38 km/sec on Iceland; this material was overlain by a thick layer of basalts (15.7 km.) having a velocity of 6.71 km/sec. The areas cited above are well established as volcanic. The known volcanism north of Sicily and the known presence of numerous sea mounts in the Tyrrhenian Sea suggest a basic rock material for the 6.96 - 7.28 km/sec layer.

Profile 194 - Western Mediterranean Basin (South) - (Table 3, Figure 10). Profile 194 has been treated both as an unreversed and as a reversed (end to end) profile in the computations. A velocity of 1.80 km/sec was assumed for the unconsolidated sediment layer. The first sediment velocity directly measured is 2.66 km/sec, the top of this layer closely paralleling the sea floor. The underlying material has a measured velocity of 3.44 km/sec (NW) and 3.89 km/sec (SE). The 2.66 km/sec material thins to the southeast as indicated by the measured thickness of 0.92 km. (SE) and 1.25 km. (NW). The indicated dip for this layer (end to end computation) is 3.71° downward to the northwest. A structural section based on the end to end computation indicated that this layer should intersect the sea

floor midway along the southeastern section of the profile. The echo-sounding records show no evidence to support this possible interpretation; however such evidence could be concealed under the relatively thin veneer of recent sedimentation. The 3.89 - 3.44 km/sec layer thickens appreciably to the southeast toward Sardinia. Computed thicknesses for this layer are 3.69 km. and 2.44 km. respectively for the southeast and northwest sections of the profile. The two layers having velocities 2.66 km/sec and 3.44 - 3.89 km/sec probably represent semiconsolidated and consolidated sediments. Underlying these layers is material having a velocity of 5.23 - 5.26 km/sec. The top interface for this layer shows a dip of approximately 2° (from horizontal) downward to the southeast.

The highest velocity measured, 7.21 - 7.24 km/sec, is based on limited data (see Appendix A - Profile Evaluation); computed depths to this interface are 9.74 (NW) and 10.20 km. (SE).

The results for this profile do not correlate with those measurements made in this basin further to the north. The high velocity found at this station is similar to that obtained on Profile 193, but the depth to this layer is approximately 3 km. deeper than was obtained for the Tyrrhenian Sea profile.

There is no evidence available to indicate whether the 5.23 km/sec material represents consolidated sediments, metasediments, or an igneous rock.

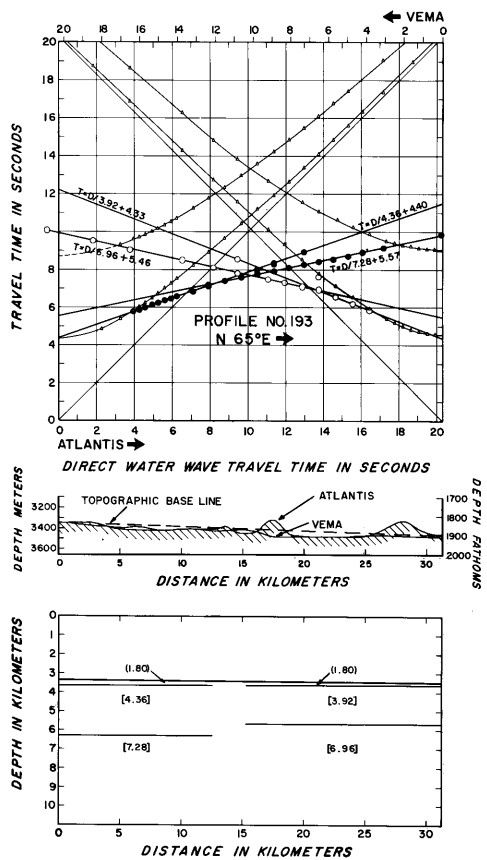


Figure 9.

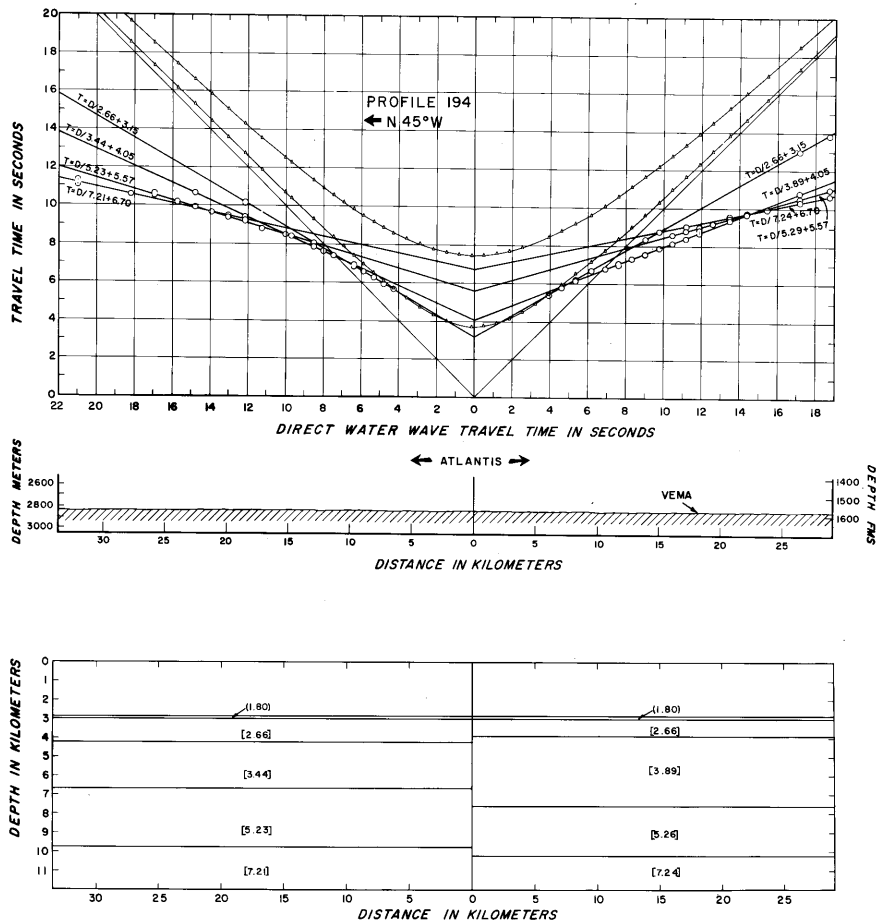


Figure 10.

Profile 195 - Western Mediterranean Basin (North) - (Table 3,

Figure 11). A thin layer of unconsolidated sediment having a velocity of 2.03 km/sec and a thickness of 0.35 km. (S) and 0.59 km. (N) is the first layer detected; the refractor appears to coincide very nearly with the bottom. This layer is underlain by a second layer of sediment having a velocity of 2.91 km/sec and moderately uniform thickness, 0.85 km. (S) and 0.71 km. (N).

This semi-consolidated or consolidated material is underlain by material having a velocity of 4.20 km/sec. This layer appears to be extremely uniform in thickness (2.18 to 2.28 km.) over the entire section. It is underlain by material having a velocity of 4.93 km/sec and a thickness of 3.08 km. (S) and 3.98 km. (N). The material having velocities 4.20 and 4.93 km/sec represents two layers of material having a total thickness of 5.36 km. at the south and 6.16 km. at the north end of the profile. At station D-11 not far distant from this profile, Ewing and Ewing (1959) obtained a velocity of 4.79 km/sec (unreversed); they computed a minimum thickness of 4.4 km. for this layer. Their layer of velocity 4.79 km/sec is probably equivalent to the composite layer having velocities, 4.20 and 4.93 km/sec which we have measured on Profile 195. The total thickness of these layers, 5.36 km. (S) to 6.16 km. (N), clearly indicates that the previous profile in the

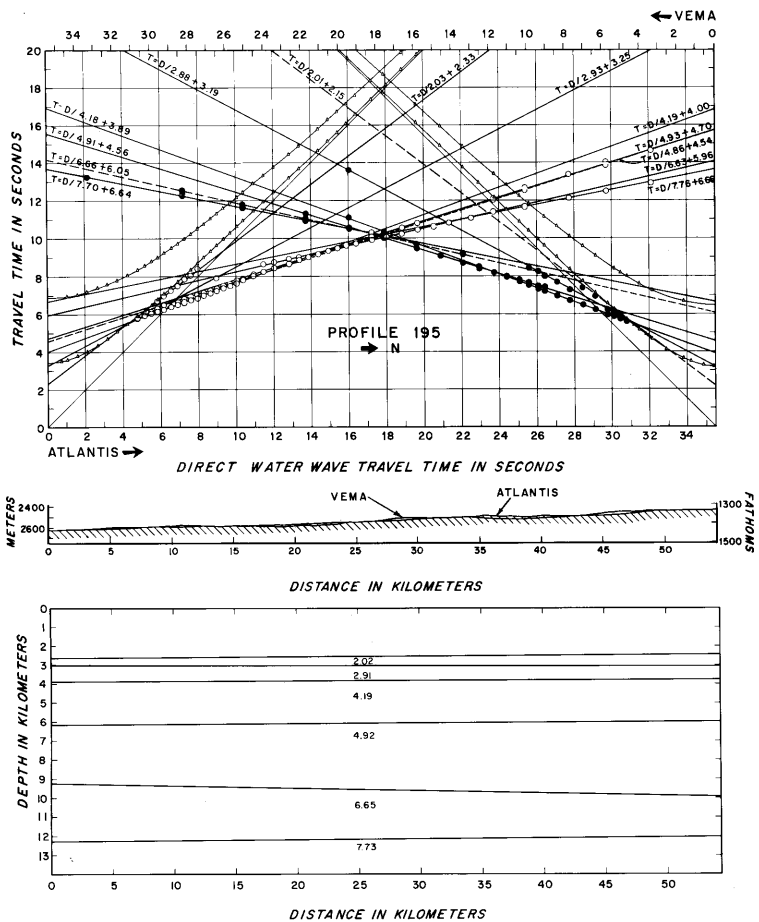


Figure 11.

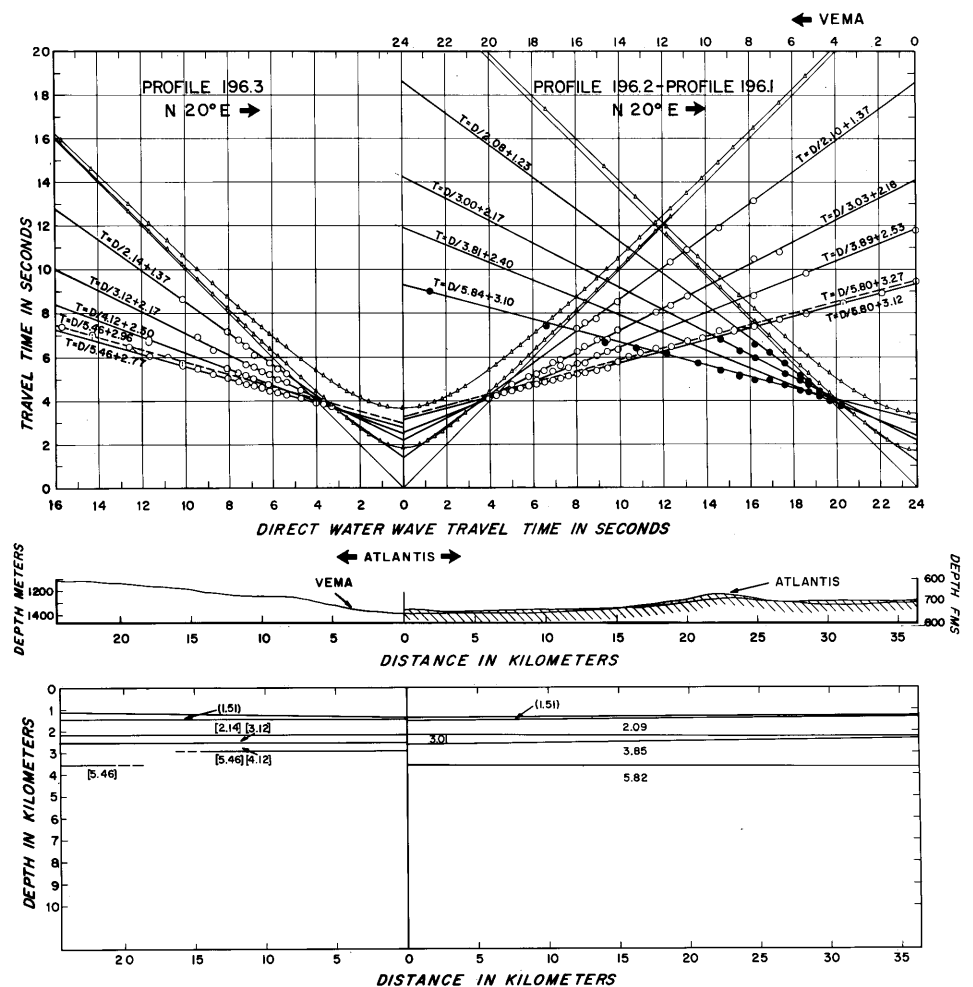


Figure 12.

area was not long enough to obtain refractions from the base of these two layers.

Two layers having higher velocities, 6.67 km/sec, and 7.76 km/sec have been measured on this profile. The 6.67 km/sec velocity material, frequently identified with the oceanic crustal layer, has a thickness of 3.03 km. at the south and thins to 2.10 km. at the north. Depths to the 7.76 km/sec interface are 12.27 km. (S) and 12.03 km. (N). The velocity, 7.76 km/sec, is considered to represent mantle material in this region although this velocity is slightly lower than commonly associated with the mantle.

Profiles 196, 197 - Balearic Platform - (Table 3, Figures 12 and 13). Profiles 196 and 197 form a semi-continuous seismic section about 100 km. in length extending in a south-southwesterly direction between the Balearic Islands and Cape San Antonio, Spain. The profiles cross the seaward extension of the Betic Cordillera at an angle normal to the tectonic axis of this folded mountain chain. The northernmost section, Profile 196.1 - 196.2, has been treated as a reverse profile; the southernmost section, 196.3, has been computed as an unreversed station.

A velocity of 1.51 km/sec was assumed for the thin layer of sediment overlying the first detectable refraction horizon. The first layer measured on Profile 196.1 - 196.2 has velocity 2.09 km/sec

and thickness varying from 0.90 km. (N) to 0.60 km. (S). The unreversed velocity for the equivalent horizon on Profile 196.3 is 2.14 km/sec; its computed thickness is 0.71 km. The underlying material has a velocity of 3.01 km/sec (196.1 - 196.2) and 3.12 km/sec (196.3). This layer is thin, decreasing in thickness from 0.46 km. (S) to 0.08 km. (N). It lies above material having a velocity of 3.85 km/sec (196.1 - 196.2) and 4.2 km/sec (196.3). The 3.85 km/sec layer has a thickness of 1.35 km. at the north and 0.95 km. at the south; the corresponding thickness for the 4.12 km/sec layer on 196.3 is 0.41 - 1.03 km. The layer appears to thicken substantially (1.03 km.) at the extreme south end of the profile as indicated by the offset in the velocity line establishing the next refraction horizon (Figure 12).

The highest velocity measured on the profile is 5.82 km/sec for the reversed section (196.1 - 196.2) and 5.46 km/sec for the unreversed section (196.3). The computed depths to this horizon are 3.55 km. (S) and 3.67 km. (W) on the reversed section of the profile. The well-defined offsets in this velocity line both to the north (196.2) and south (196.3) indicate the existence of considerable topographic relief on this surface. The 0.35 sec. disparity in the zero intercept for this velocity line measured on sections 196.2 and 196.3 is further evidence for the existence of uneven topography along the surface of

this layer. Computations based on the intercepts of the offsets as shown on the travel-time plot (dashed lines) indicate relief of at least 0.4 to 0.6 km. No conclusion based on the present data can be reached regarding possible tectonic origin for this irregular structure.

Profile 197 has been treated as two unreversed stations. As on Profile 196, the measured travel times are indicative of topographic relief on the upper surfaces of the 4.76 and 6.58 km/sec layers.

A velocity of 1.80 km/sec has been measured at the north for the unconsolidated sediment layer; the same velocity, 1.80 km/sec, has been assumed for the first layer at the south end of the profile. It lies above material having a velocity of 3.49 km/sec (N) and 3.78 km/sec (S); layer thickness varies from 0.29 km. (N) to 0.38 km. (S).

The next layer, velocity 4.71 - 4.76 km/sec, thickens appreciably from north (1.81 km.) to south (3.53 km.). The measurement at the south end of the profile shows considerable scatter in the travel times for energy refracted from this layer. Surprisingly, the VEMA (N) measurements show no similar variations for data lying on the comparable velocity lines. The scatter in the ATLANTIS data indicates possible irregular relief on the surface of this layer.

Underlying this layer is material of velocity of 6.85 - 6.58 km/sec; the depths to this layer are 3.58 km. (N) and 5.36 km. (S).

These two profiles, 196 and 197, if directly correlated, show marked increase in layer velocities from north to south except in the unconsolidated sediment layer (2.14 to 1.80 km/sec). The thin layer underlying the unconsolidated sediments shows an increase in velocity from 3.01 to 3.78 km/sec; in the next layer the velocities increase from 3.85 to 4.12 to 4.76 km/sec. The basement horizon shows more variability in velocity but the southward trend of increasing velocities at comparable depths is still evident; the measured velocities are 5.84 and 5.46 km/sec (Profile 196) and 6.85 - 6.58 km/sec (Profile 197). This increase in velocity may be an indication of an increasing degree of metamorphism as the axis of the Betic Cordillera is approached.

The total thickness of the section between the sea floor and the top of the high velocity layer is nearly uniform over the entire length of Profile 196: 2.39 km. at the north (196.1), 2.18 km. at the south (196.2), and 2.17 km. at the most southerly end of 196.3. On Profile 197 the layer of velocity 4.71 - 4.76 km/sec almost doubles in thickness from north to south. The total thickness of the section to basement increases from 2.90 km. (N) to 4.59 km. (S). This increase in section thickness is almost entirely due to

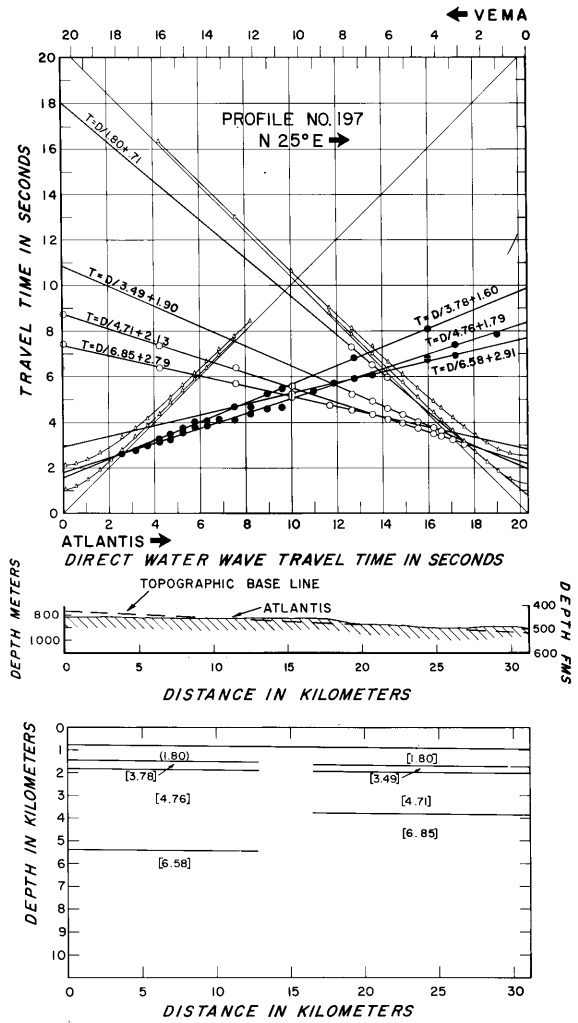


Figure 13.

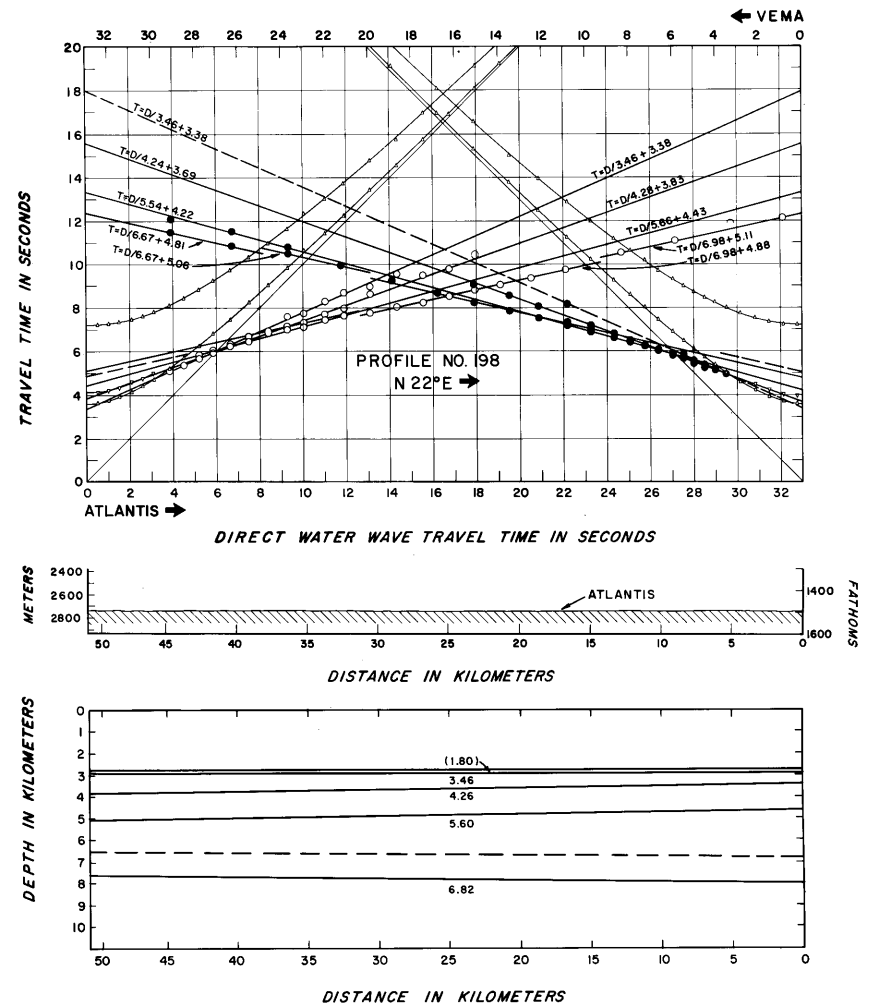


Figure 14.

the thickening in the 4.71 - 4.76 km/sec layer and is coincident with the gradual shallowing of the bottom toward the south.

Profile 198 - Western Mediterranean Basin (Southwest) -

(Table 3, Figure 14). A velocity of 1.80 km/sec has been assumed for the unconsolidated sediment layer; its thickness is uniform (0.17 - 0.18) along the profile. The first underlying layer has a velocity of 3.46 km/sec; its thickness increases from 0.50 km. at the north to 0.91 km. at the south. The evidence does not preclude the possibility that the layer may pinch out to the north, although its presence at the south end of the profile is well established.

The next layer, velocity 4.26 km/sec, is extremely uniform throughout the section: 1.19 km. at the north and 1.26 km. at the south.

Two higher velocities, 5.60 km/sec and 6.82 km/sec, have been determined on this profile. The velocity lines which determine the 6.82 km/sec measurement show significant offsets which do not reverse properly. Using the minimum and maximum time intercepts at zero range for these velocity lines, thickness computations give minimum and maximum values for the thickness of the 5.60 km/sec material: 2.19 - 3.41 km. at the north and 1.39 - 2.56 km. at the

south. (The minimum depth is shown as a dashed line on the velocity-depth section (Figure 14)). There is evidence for the existence of relief on the surface of the 6.82 km/sec layer, although it is not clear whether the relief is the result of faulting or folding. No mantle velocities were identified on this profile.

The 3.46 km/sec material probably represents consolidated sediment or metasediment. The unconsolidated sediments (assumed velocity, 1.80 km/sec) are extremely thin here. Recent sedimentation in this region appears to have been negligible. The 4.26 km/sec material probably represents a consolidated sediment or metasediment, also. Similarly the 5.60 km/sec material could represent consolidated sediment, metasediment, or perhaps rocks of volcanic or igneous origin.

Profile 199 - Western Mediterranean Basin (Southwest) - (Table 3, Figure 15). Three velocities, 2.89, 5.10 and 7.70 km/sec, all unreversed measurements, are well determined on this profile. A velocity of 1.80 km/sec was assumed for the unconsolidated sediments. The semiconsolidated or consolidated sediment (2.89 km/sec) layer has a thickness of 1.65 km. The 5.10 km/sec material has a thickness of 3.34 km. The highest velocity measured is 7.70 km/sec; the depth to the interface is 7.75 km.

The extremely shallow depth determination, the fact that the

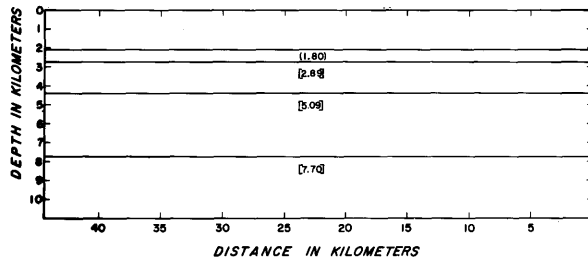
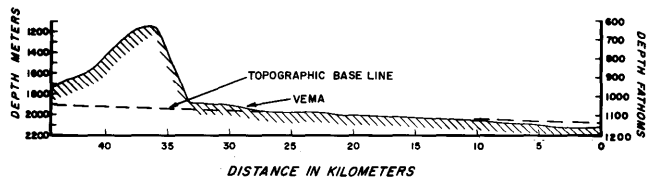
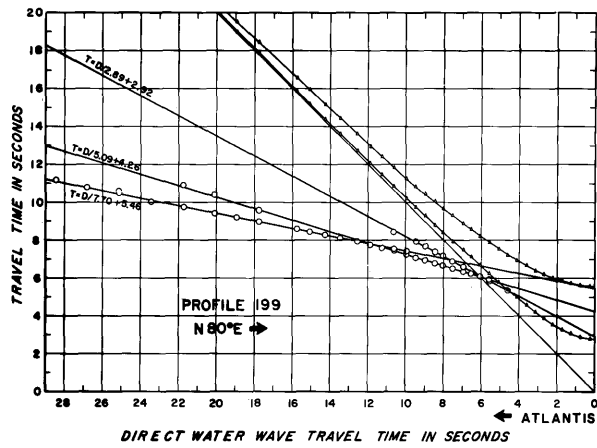


Figure 15.

measurement is unreversed, and the relatively short length of the profile suggest that an interpretation of the high velocity material as representative of mantle should be viewed with suspicion. In addition, an interpretation of this profile must take into account its geographical location midway between the Betic Cordillera of Spain and the Tellian Rif mountains of Morocco and Algeria. These bordering regions to the north and south are known to consist of tightly folded sediments which have been overthrust to the north and south. It is almost certain that the tectonic activity of this area has included both the intrusion and extrusion of igneous or volcanic material. Outcrops of known Tertiary volcanics are numerous on the African coast directly south of the location of Profile 198. Consequently, the 7.70 km/sec apparent velocity is probably to be associated with basic intrusives introduced during periods of orogenesis rather than directly with mantle.

Table 3 Profiles 193-199
Seismic Velocities, Layer Thicknesses, and Depths
(in km/sec and km.)

Profile	V	T _a	D _a	V	T _b	D _b
193	1.53	3.35	3.35	1.53	3.48	3.48
ATLANTIS	(1.80)	0.30	3.65	(1.80)	0.14	3.62
(SW)	[4.36]	2.64	6.29	[3.92]	2.06	5.68
	[7.28] ⁽¹⁾			[6.96] ⁽¹⁾		
				VEMA		
				(NE)		

Table 3 (continued)

Profile	V	T _a	D _a		V	T _b	D _b
194 ATLANTIS ⁽²⁾ (NW)	1.53 (1.80) [2.66] [3.44] [5.23] [7.21]	2.84 0.14 1.25 2.44 3.07	2.84 2.98 4.23 6.67 9.74	ATLANTIS ⁽²⁾ (SE)	1.53 (1.80) [2.66] [3.89] [5.29] [7.24]	2.84 0.14 0.92 3.69 2.61	2.84 2.98 3.90 7.59 10.20
195 ATLANTIS (S)	1.52 (1.52) 2.02 2.91 4.19 4.92 6.65 7.73	2.63 0.06 0.33 0.84 2.27 3.07 3.02	2.63 2.69 3.02 3.86 6.13 9.20 12.22	VEMA (N)		2.43 0.05 0.58 0.71 2.17 3.97 2.09	2.43 2.48 3.06 3.77 5.94 9.91 12.00
196.1-196.2 VEMA (N)	1.51 (1.51) 2.09 3.01 3.85 5.82	1.28 0.06 0.91 0.07 1.35	1.28 1.34 2.25 2.32 3.67	ATLANTIS (S)		1.37 0.13 0.64 0.46 0.95	1.37 1.50 2.14 2.60 3.55
196.3 ATLANTIS (S)	1.51 (1.51) [2.14] [3.12] [4.12] [5.46]	1.37 0.09 0.71 0.34 0.41 1.03	1.37 1.46 2.17 2.51 2.92 3.54 ⁽³⁾				
197 VEMA (N)	1.51 1.51 (1.80) [3.49] [4.71] [6.85]	0.95 0.03 0.77 0.29 1.81	0.95 0.98 1.75 2.04 3.85	ATLANTIS (S)	1.51 (1.80) [3.78] [4.76] [6.58]	0.77 0.00 0.68 0.38 3.53	0.77 0.77 1.45 1.83 5.36

Table 3 (continued)

Profile		V	T _a	D _a		T _b	D _b
198	VEMA	1.52	2.74	2.74	ATLANTIS	2.74	2.74
	(N)	(1.80)	0.17	2.91	(S)	0.18	2.92
		3.46	0.50	3.41		0.91	3.83
		4.26	1.19	4.60		1.26	5.09
		5.60	2.19	6.79		1.39	6.48
			3.41	8.01 ⁽⁴⁾		2.52	7.61
		6.82					
199	ATLANTIS	1.52	2.08	2.08			
		(1.80)	0.68	2.76			
		[2.89]	1.65	4.41			
		[5.09]	3.34	7.75			
		[7.70]					

V - Velocity in km/sec

T_a, T_b - Layer thickness in km.

D_a, D_b - Depth to layer in km.

N, S - North, South end of profile.

() - Assumed velocity.

[] - Unreversed data.

(1) - Reversed velocity - 7.12 km/sec.

(2) - Profile 194 (end to end) - ATLANTIS received both NW and SE sections of profile at same position.

(3, 4) - Travel time graph shows offset in this velocity line; depth computed for maximum and minimum time intercepts.

Profile 2 - Western Mediterranean Basin (North) - (Table 4,

Figures 16 and 20).

Topography. Topographic corrections have been made where necessary; the topographic base lines are dashed on the bathymetric profile for each section (Figure 16).

The northwest end of the profile (Sections 2.1, 2.2, 2.3) is located over the abyssal plain; the southeast end of the profile (Sections 2.4, 2.5, 2.6) is located on the continental slope. The boundary

zone between the two physiographic provinces, marked by an abrupt change in topography of more than 365 meters (200 fathoms), is also accompanied by an equally marked change in the velocity-depth structure as determined by seismic measurements.

The profile extends northwesterly from near Cape Corse toward the southern coast of France. The profile crosses two distinct physiographic provinces, the almost flat abyssal plain to the south of the Cote d'Azur and the continental slope to the southeast toward Corsica. Water depth varies smoothly from 2560 meters (1400 fathoms) near the central portion of the profile to 2377 meters (1300 fathoms) at the northwest end. The southeasterly end of Section 2.1 shows about 100 meters (55 fathoms) of relief superposed on the average bottom slope. An abrupt shallowing from 2560 meters (1400 fathoms) to 2195 meters (1200 fathoms) occurs at the eastern end of Section 2.4. The water depth then increases slightly once more before shallowing gradually to less than 1830 meters (1000 fathoms) northeast of Corsica.

Sections 2.1, 2.2, 2.3. A velocity of 1.80 km/sec was assumed for the unconsolidated sediment layer. This layer overlies material of velocity 3.36 km/sec (Sections 2.2, 2.3). The comparable velocity obtained on Section 2.1, 3.60 km/sec, is unreversed. The thickness of this material increases gradually from 1.09 km.

(SE) to 1.77 km. (NW) toward the coast of France. It in turn is underlain by a thick layer of material having velocities of 4.08 km/sec (Sections 2.2, 2.3) and 4.21 km/sec (Section 2.1). At the southeast end of Sections 2.2, 2.3 near the margin of the abyssal plain this layer has a thickness of 3.34 km.; the layer thins to 2.54 km. toward the northwest (Section 2.1). Beneath the 4.08 - 4.21 km/sec layer is material of velocity 5.67 km/sec. The highest velocity measurements on this section, 6.65 km/sec (Section 2.2) and 6.77 km/sec (Section 2.1) are unreversed. If the 6.65 km/sec material is assumed flat lying, then the thickness of the overlying material is 3.37 km. under the receiving position for Section 2.2; this is in good agreement with the 3.05 km. thickness measured on Section 2.1. Evidence for these velocities, 6.65 and 6.77 km/sec is based entirely on second arrival evidence on these short profiles but convincing additional evidence for the existence of material in this velocity range is furnished by the long reverse profile (Sections 2.7, 2.8).

Sections 2.4, 2.5, 2.6. Beneath the unconsolidated sediments is material having a velocity of 3.22 km/sec (Sections 2.4, 2.5). It increases in thickness from 0.69 km. (NW) to 0.99 km. (SE). Velocities of 4.59 (Sections 2.4, 2.5) and 4.67 (Section 2.6) km/sec have been measured for the underlying material.

This layer is in turn underlain by material having a velocity of 5.99 km/sec (Sections 2.4, 2.5). At the northwest end of this section a clearly defined offset of approximately 0.20 seconds is present in the lines defining this velocity on the travel time graph. The early arrivals defining this offset occur for shots fired in the region coincident with abrupt change in topography. Computations of thickness for the 4.59 km/sec material give 0.57 km. (NW) and 2.38 km. (SE); this computation assumes that the 3.22 km/sec material forms a continuous horizon throughout the entire length of Sections 2.4, 2.5. If the 3.22 km/sec material is missing at the northwest end of the profile, as seems quite probable, then the 4.59 km/sec layer is over 1 km. thick here. The topographic rise in the vicinity of the receiving location for Section 2.4 may be composed entirely of the 4.59 km/sec material except for a thin surface veneer of recent sediments.

The results obtained in Section 2.6, with a single exception, are consistent with those obtained on Sections 2.4 and 2.5. The 6.41 km/sec velocity measured on Section 2.6 is appreciably higher than the 5.99 km/sec velocity measured to the northwest on the adjoining sections. Secondly the depth to this layer, 4.30 km., is almost 2 km. shallower than that measured for the high velocity layer at the southeast end of Sections 2.4, 2.5. This marked discrepancy

in computed depth to the deep horizon where Sections 2.5 and 2.6 join has not been resolved by the present seismic refraction data.

The northwest half of the profile (Sections 2.1, 2.2 and 2.3) do not correlate in a simple way with the sections to the southeast (Sections 2.4, 2.5, and 2.6). A possible correlation would identify the 5.67 km/sec material (Sections 2.2, 2.3) with the 5.99 km/sec material (Sections 2.4, 2.5). If this identification is correct, then the region between the two reversed profiles and that in the vicinity of the northwest end of Section 2.4 must represent a zone of displacement. The depths to the top surface of the 5.67 - 5.99 km/sec material, 7.42 and 4.00 respectively, indicate a vertical displacement of approximately 3 km. in this region. The block of material to the northwest has moved downward relative to that to the southeast. Two separate pieces of evidence are available to support this hypothesis. The abrupt break in topography has already been mentioned. Secondly, reflection records (Continuous Seismic Profiler) taken in the immediate vicinity of this region give clear indication that the region has been tectonically disturbed. A photograph of the reflection record is shown in Figure 24 and the location of the reflection run shown in Plate 1. That portion of the reflection profile made between 2235, 1 October and 0025, 2 October parallels the direction of Profile 2, but is 2 to 4 km. south of the refraction

line. The record, over this portion of the traverse, shows uniformly parallel reflecting horizons identifiable to at least a depth of 550 meters (300 fathoms) beneath the bottom (assumed velocity 4800 ft/sec); the beds are interrupted by crescent shaped zones (noted in the photograph) where the incident sound appears to be entirely absorbed or scattered. These zones may well represent small sea mounts now buried under sediments. The sediments show clearly defined reflecting horizons which turn gently upward as the flank of the seamount is approached. No other deformation of the sediments can be seen in the records. Hersey (1962) has noted similar behavior on the flanks of Caryn Peak and has attributed the upward curvature of the reflecting horizons to differential compaction of the sediments. At 0.40 and 0.65 seconds after the bottom reflection, two strong reflections may be clearly identified. Identification of these two reflecting horizons with a particular refraction horizon is not possible at the present time; the deepest reflector however is a minimum of 495 meters (270 fathoms) below the bottom (velocity assumed 4800 ft/sec). If twice the velocity of water is assumed, more nearly in agreement with the velocity measured in the refraction experiment, the depth to this reflector is doubled and becomes nearly 1 km. This places this reflector near the base of the 3.36 km/sec layer or possibly the top surface of the 4.08 km/sec material measured on

Sections 2. 2, 2. 3. Shortly before the ship changed course to 000 °T an extremely strong series of reflections (at least four reflectors) appear suddenly on the reflection record at a depth of 310 meters (170 fathoms) below the bottom. Identification with either of the reflectors previously discussed cannot be made from the present evidence. At 0025 the ship was headed directly north toward the northwest end of Sections 2. 4, 2. 5; the abrupt discontinuity in sediment structure was not crossed again. The strong reflector persisted until a further course change to the northwest was made at 0150. Although the reflector continues at about the same depth, the surface appears irregular and weakly reflecting over a portion of the traverse. Shortly after the course change to the northwest, the bottom topography changes abruptly. The water depth shallows by 365 meters (200 fathoms) and the topography becomes rough and irregular. Again the shallow reflecting horizons appear to lap gently up on the side of this irregular surface. No evidence of bedding below this reflecting surface can be detected. The refraction and reflection evidence taken together indicate both a zone of major vertical displacements and very possibly associated volcanic activity. The undisturbed nature of the overlying sediments, except for effects of compaction, indicate that the tectonic activity must have taken place prior to the laying down of these sediments.

Section 2.7, 2.8. This profile has been computed as two unreversed profiles. The results obtained on Section 2.7 are in good agreement with the results obtained on the shorter profiles (Sections 2.1, 2.2, 2.3). The 7.12 km/sec velocity is higher than that measured for the same layer on the shorter profiles. In addition, a mantle velocity, 8.05 km/sec, has been measured on Section 2.7. Section 2.8, consisting of only 5 shots, was not extended to sufficient range to obtain refraction arrivals from the mantle.

Table 4 Profile 2
Seismic Velocities, Layer Thicknesses, and Depths
(in km/sec and km.)

Section		V	T _a	D _a		T _b	D _b
2.1	W. S.	1.53	2.44	2.44			
		(1.80)	0.39	2.83			
		[3.60]	1.77	4.60			
		[4.21]	2.56	7.16			
		[5.66]	3.05	10.21			
		[6.77]					
2.2-2.3	W. S.	1.53	2.44	2.44	CHAIN	2.55	2.55
		(1.80)	0.49	2.93	(SE)	0.44	2.99
		3.36	1.24	4.17		1.09	4.08
		4.08	2.54	6.71		3.34	7.42
		5.67	3.37	10.17 ⁽¹⁾			
		[6.63] ⁽¹⁾					

Table 4 (continued)

Section		V	T _a	D _a		V	T _b	D _b
2.4-2.5	CHAIN	1.53	2.67	2.67	W. S. (SE)		2.09	2.09
		(1.80)	0.07	2.74		0.52	2.61	
		3.22	0.69	3.43		0.99	3.60	
		4.59	0.57	4.00 ⁽²⁾		1.70	5.30 ⁽²⁾	
			1.35	4.78 ⁽²⁾		2.38	5.98 ⁽²⁾	
		5.99						
2.6	W. S.	1.53	2.09	2.09				
		(1.80)	0.46	2.55				
		[3.42]	0.94	3.49				
		[4.67]	0.81	4.30				
		[6.41]						
2.7-2.8	W. S.	1.53	2.38	2.38	W. S. (SE)	1.53	2.09	2.09
		(1.80)	0.42	2.80		(1.80)	0.81	2.90
		[3.43]	1.68	4.48		[5.14]	7.60	10.50
		[4.04]	2.32	6.80		[6.74]		
		[5.61]	3.53	10.33				
		[7.12]	2.73	13.06				
		[8.05]						
2.7-2.8	Alternate	1.53	2.38	2.38		2.55	2.55	
		(1.80)	0.61	2.99		0.51	3.06	
		3.37	1.34	4.33		0.98	4.04	
		4.02	2.38	6.71		3.22	7.26	
		5.64	3.98	10.69		3.16	10.42	
		6.92	2.40	13.09 ⁽⁴⁾				
			2.24	12.93 ⁽⁵⁾				
		[7.73] ⁽⁴⁾						
		[7.88] ⁽⁵⁾						

- (1) Interface assumed horizontal
- (2) Offset; two depth computations
- (3) Fictitious profile for purposes of computation;
Section 2.8 replaced with results of Section 2.5.
- (4) Unreversed high velocity; interface assumed parallel
to preceding interface.
- (5) Unreversed high velocity; interface assumed horizontal.

Profile 3 - Continental Shelf and Slope (Table 5, Figures 17 and 21).

Topography. Profile 3, the northernmost of all the refraction stations, is aligned in a northwest-southeast direction across the approaches to the Gulf of Genoa (Plate 1). It crosses extremely rugged topography, the water depth varying between 900 and 2400 meters along the section; the bottom slope exceeds 4° over much of the profile. The bathymetry along the profile section and the base lines used in the topographic correction are shown in Figure 17.

Topographic corrections (Sutton and Bentley, 1953) have been applied to all the arrivals shown on the travel time graph. The corrections have been made for differences in the travel path in water only, i. e., the bottom topography is assumed to exist in all the layers from which refractions were obtained. The choice of a topographic base line was controlled by the slope present in the topography. No attempt was made to force the topographic base lines to coincide at the ends of adjoining profiles. Sections 3. 2 and 3. 3 were corrected to a single base line as were Sections 3. 4 and 3. 5 in order to permit reverse computations. Sections 3. 7 and 3. 8 were also corrected to a single base line.

The topographic corrections to the measured travel time range from 0 to ± 0.30 seconds on the short segments of the profile; the

corrections on Section 3.7 and 3.8 range from 0 to ± 0.80 seconds. Confidence in the topographic correction may be tested at least empirically. Although the scatter in the data points is reduced appreciably, some scatter is still present, particularly in the highest velocity line measured. The reverse points on Sections 3.2, 3.3 and Sections 3.4, 3.5 agree within 0.10 seconds after the topographic correction has been made.

Despite the uncertainties introduced by topography, a moderately consistent interpretation is obtained for this profile. The computed velocity-depth section (Table 5, Figure 21) is to some extent artificial; it should be considered as a first approximation only to the true structure. Thickness and depth computations for this profile are directly related to the topographic base line, not the true water depth.

Sections 3.1 to 3.6. The first velocity measured along the Section varies from 3.15 km/sec (Sections 3.4, 3.5) to 3.55 km/sec (Section 3.1). The thickness of this layer varies from a maximum of 1.44 km. (Section 3.1) to a minimum of 0.56 km. (Sections 3.4, 3.5). This layer thins markedly near the middle of the profile in the region of the topographic high where Sections 3.3 and 3.4 adjoin.

The measured velocities for material underlying this layer are 5.04 km/sec (Section 3.1), 5.31 km/sec (Sections 3.2, 3.3), 5.39 km/sec (Sections 3.4, 3.5), and 5.75 km/sec (Section 3.6). The velocities measured on Sections 3.1 and 3.6 are computed on the assumption that the layers parallel the bottom topography. The measured apparent velocities on Sections 3.1 and 3.6 are 6.41 km/sec and 6.77 km/sec respectively. On both these profiles the shots were fired up dip from the receiving position. The final computed velocities, 5.04 km/sec and 5.75 km/sec, are in fair agreement with the velocities computed on Sections 3.2, 3.3 and Sections 3.4, 3.5. The assumption that the refracting layer parallels the topography therefore seems reasonable on this profile.

Similar arguments can be applied to the overlying layer. The measured apparent velocities obtained on Sections 3.1 and 3.6, 4.13 km/sec and 3.78 km/sec respectively, when computed for layering parallel to the topographic base line, become 3.54 km/sec and 3.46 km/sec, values which are in good agreement with the 3.43 and 3.15 km/sec velocities obtained on Sections 3.2, 3.3 and Sections 3.4, 3.5 respectively.

A velocity of 1.80 km/sec was assumed for the unconsolidated sediment layer except on Sections 3.4, 3.5.

An apparent velocity of 2.10 km/sec measured on Section 3.4 and an assumed velocity of 2.24 km/sec (Section 3.5) were used to obtain the reverse velocity of 2.17 km/sec shown in the velocity-depth section (Figure 21). On Section 3.6 a velocity of 2.45 km/sec (apparent velocity 2.58 km/sec) was measured. The 2.17 km/sec and 2.45 km/sec material could represent the same layer; the topography and steep slopes along the section make it impossible to resolve this problem unambiguously.

Sections 3.7, 3.8. The long reverse profile, Sections 3.7, 3.8, adds little information to that obtained on the short sections. No low velocities were measured. A velocity of 5.79 km/sec, somewhat higher than that obtained on the short sections, was measured for the basement. Depth computations, assuming the existence of two overlying layers having velocities of 1.80 km/sec (0.40 km.) and 3.30 km/sec, yield results comparable to these obtained on the short profiles.

A single arrival at a range of 35 seconds on Section 3.7 indicates the possibility that a refraction was obtained from a deeper layer. In conjunction with a single second arrival at shorter range a line having apparent velocity 7.90 km/sec can be drawn to permit computation of a minimum depth to the possible deeper horizon. Assuming this interface is horizontal the computed velocity and

depth are 7.69 km/sec and 11.82 km. (Table 5). This interpretation is not very satisfactory; the arrival in question may be an arrival from the basement or another deeper intermediate velocity layer, but it is extremely doubtful that it represents a refraction from the mantle.

Structure Along the Profile. Profile 3 contrasts markedly with the profiles located to the southwest in the basin. The location of the profile on the continental slope, the highest velocity measured (5.3 - 5.4 km/sec), the shallow depth to this layer (2 to 3 km.), and the probable thickness of the layer (>10 km.) argue strongly for associating this profile with continental structure. Muraour (personal communication) recently obtained a velocity of approximately 5.4 km/sec at shallow depths on two profiles extending from the vicinity of Cape Corse to the Italian mainland. His results are in excellent agreement with the measurements reported here for Profile 3.

The bathymetric chart for the northeastern part of the Ligurian Sea by Debrazzi and Segre (1960) shows two deep embayments extending from the abyssal plain toward shallow water. The two embayments are separated by a ridge which gradually shallows toward the northeast. Profile 3 is directed almost normal to this structure and crosses both embayments and the ridge. This single seismic

section cannot define the entire structure. However, a reasonable hypothesis can be based on the present data: the topography of the sea floor in this region is controlled by warping of the basement material (5.04 - 5.79 km/sec). The evidence indicates that the 3.15 - 3.55 km/sec material was laid down on a relatively flat basement surface and was then warped at the same time as the basement was deformed. The evidence would suggest that the two embayments are structurally controlled by two broad synclines separated by an anticlinal ridge, all plunging gently to the southwest.

Table 5 Profile 3
Seismic Velocities, Layer Thicknesses, and Depths
(in km/sec and km.)

Section		V	T _a	D _a		T _b	D _b
3.1*	W.S.	1.52	1.78	1.78			
		(1.80)	0.28	2.06			
		[3.54]	1.44	3.50			
		[5.04]					
3.2-3.3	W.S. (NW)	1.52	2.29	2.29	CHAIN (SE)	0.79	0.79
		(1.80)	0.40	2.69		0.36	1.15
		3.43	0.91	3.60		0.99	2.14
		5.31					

Table 5 (continued)

Section	V	T _a	D _a			T _b	D _b
3. 4-3. 5	CHAIN (NW)	1. 52	1. 13	1. 13	W. S. (SE)	1. 89	1. 89
		(1. 52)	0. 04	1. 17		0. 00	1. 89
		2. 17	0. 54	1. 71		0. 46	2. 35
		3. 15	0. 56	2. 27		1. 30	3. 65
		5. 39					
3. 6*	W. S.	1. 52	2. 09	2. 09			
		(1. 80)	0. 19	2. 28			
		[2. 45]	0. 55	2. 83			
		[3. 46]	1. 02	3. 85			
		[5. 75]					
3. 7-3. 8	W. S. (NW)	1. 52	2. 25	2. 25	W. S. (SE)	1. 93	1. 93
		(1. 80)	(. 40)	2. 65		(. 40)	2. 33
		(3. 30)	1. 08	3. 73		1. 53	3. 86
		5. 71	8. 09	11. 82 ⁽¹⁾			
		[7. 69] ⁽¹⁾					

* Profile 3. 1 and 3. 6 - Velocities are unreversed; computations assume the layers parallel the topographic base line and velocities are computed accordingly.

(1). Minimum depth computation: this velocity is based on a single first arrival and one possible second arrival; the velocity line is dashed on the travel time plot to indicate its speculative nature.

Profile 4 - Western Mediterranean Basin (North) - (Table 6, Figures 18 and 22).

Sections 4. 1 to 4. 8. The results obtained on Profile 4 differ in major detail from those obtained in neighboring profiles

both to the north (Profile 2) and south (Profile 5).

The first interface from which refraction arrivals were obtained coincides closely with the sea floor; this layer has a measured velocity of 2.39 - 2.46 km/sec on Sections 4.1 through 4.6; its thickness increases slightly from northwest to southeast, ranging from 0.35 km. (Sections 4.1 and 4.2) to 0.50 (Section 4.4) to 0.98 km. (Section 4.6).

This layer is underlain by material of velocity 3.16 to 3.44 km/sec; it thins markedly toward the middle of the section. Evidence for material of this velocity is excellent on Section 4.2 and 4.5. Similar evidence for this layer on Sections 4.3 and 4.4 is either missing or masked by arrivals from the next refraction horizon. The layer is clearly very thin or entirely absent in this region. Its thickness varies from 1.91 km. (Section 4.2) to 0.50 - 0.77 km. (Sections 4.3 and 4.4); it again increases in thickness to the southwest to 1.92 km. (Section 4.5).

Velocities of 4.17 km/sec and 4.25 km/sec were measured for the next underlying layer over the central portion of the profile. A slightly higher velocity, 4.55 km/sec, was measured on Section 4.6, at the southeast end of the profile. This layer thickens near the midpoint of the profile to 4.35 - 4.77 km. (Sections 4.3 and 4.4); the thickening is coincident with the thinning in the overlying 3.43 - 3.44 km/sec material. The 4.17 - 4.25 km/sec layer thins to approximately

3.0 - 3.5 km. to the northwest and southeast. Except for a moderate slope indicated on Sections 4.7, 4.8, the base of the layer is almost horizontal as shown by the thickness determinations.

A velocity of 5.87 - 6.05 km/sec was measured for the underlying material along Sections 4.2 to 4.5. The unreversed measurement on Section 4.7 gave a velocity of 6.07 km/sec. The 5.88 km/sec velocity shown on Sections 4.7, 4.8 (Figure 22) was obtained by using the data for Sections 4.7 and 4.5 in a reverse computation; only a single velocity, 7.99 km/sec, was measured on Section 4.8. The 5.88 to 6.07 km/sec velocity is substantially lower than the velocity measured at comparable depth to the northeast and southwest on Profiles 2 and 5 and is significantly lower than the velocity normally associated with oceanic crustal material.

The highest velocity measured, 7.96 km/sec, is poorly determined on Section 4.7 but well determined on Section 4.8. Depth to the top of the material having this velocity is a little over 11 km. throughout the section.

Comparison of the velocity-depth determinations on Sections 4.7, 4.8 with the results obtained on the short profiles, Sections 4.1 to 4.6, emphasize the advantages in combining short detailed profiles with a long profile. The thinning of the 3.42 km/sec layer and thickening of the 4.17 - 4.25 km/sec layer are not indicated in the data.

obtained from the long profile; this detail is seen only on the short profiles.

Results of Leenhardt (1962). The results of a short reversed profile established by CHAIN and WINNARETTA SINGER and extending from the northwest end of Profile 4 toward Nice have been recently published by Leenhardt (1962). These results are compared with those of Section 4.1 in Table 7.

Leenhardt suggests that the semiconsolidated sediments (2.0 km/sec) are Plaisancian (Lower Pliocene) and that the high velocity material (4.2 km/sec) may well be Mesozoic limestones or older metamorphic rocks. The results of Leenhardt's profile are in excellent agreement with the results obtained in Section 4.1. The total thickness of unconsolidated sediment (1.80 and 2.38 km/sec, Section 4.1) is 0.50 km.; Leenhardt obtains 0.53 km. for his profile. The unconsolidated sediment velocity, 2.76 km/sec, measured by Leenhardt is slightly lower than the 3.16 km/sec velocity obtained on Section 4.1, but again the thickness of these corresponding layers is equal. An apparent velocity of 4.19 km/sec was measured on Section 4.1 and also on the south end of Leenhardt's profile.

Leenhardt's profile extends almost to the base of the continental slope. It is significant that the layered structure observed in the central portion of the basin extends without major change or

Table 6 Profile 4
Seismic Velocities, Layer Thicknesses, and Depths
(in km/sec and km.)

Section		V	T _a	D _a		T _b	D _b
4. 1	W. S.	1. 53	2. 65	2. 65			
		(1. 80)	0. 15	2. 80			
		[2. 38]	0. 35	3. 15			
		[3. 16]	1. 30	4. 45			
		[4. 19]	3. 46	7. 91			
		[6. 50]					
4. 2-4. 3	W. S. (NW)	1. 53	2. 65	2. 65	CHAIN	2. 72	2. 72
		(1. 80)	0. 07	2. 72	(SE)	0. 08	2. 80
		2. 46	0. 35	3. 07		0. 73	3. 53
		3. 42	1. 91	4. 98		0. 48	4. 01
		4. 17	3. 45	8. 43		4. 35	8. 36
		6. 05					
4. 4-4. 5	CHAIN (NW)	1. 53	2. 72	2. 72	W. S.	2. 73	2. 73
		(1. 80)	0. 14	2. 86	(SE)	0. 00	2. 73
		2. 39	0. 50	3. 36		0. 77	3. 50
		3. 44	0. 62	3. 98		1. 92	5. 42
		4. 25	4. 77	8. 75		2. 07	7. 49
		5. 87					
4. 6	W. S.	1. 53	2. 73	2. 73			
		[2. 35]	0. 88	3. 61			
		[3. 23]	0. 98	4. 59			
		[4. 55]	2. 94	7. 53			
		[6. 50]					
4. 7-4. 8	W. S. (NW)	1. 53	2. 61	2. 61	W. S.	2. 73	2. 73
		(1. 80)	0. 06	2. 67	(SE)	0. 00	2. 73
		2. 36	0. 61	3. 28		0. 81	3. 54
		3. 34	2. 04	5. 32		1. 56	5. 10
		4. 36	3. 03	8. 35		2. 50	7. 60
		5. 88	2. 71	11. 06		3. 74	11. 34
7. 96							

Table 7 - Comparison of Results: Section 4. 1 and Profile of Leenhardt, 1962

Section 4. 1 (Unreversed Profile)

42°48.5'N; 07°14.5'E* (Southeast)
42°55'N; 07°04'E (Northwest)

Velocity km/sec	Depth km.	Thickness km.
1.53	2.65	2.65
(1.80)	0.15	2.80
[2.38]	0.35	3.15
[3.16]	1.30	4.45
[4.19]	3.46	7.91
[6.50]		

Leenhardt Profile

42°51'N; 07°07.5'E (South)* 42°59'N; 07°10'E
(North)*

Velocity km/sec	Depth km.	Thickness km.	Velocity km/sec
1.53	2.45	2.45	1.53
[1.97]	0.53	2.98	
[2.76]	1.32	4.30	
[4.19] ⁽¹⁾			[4.78] ⁽¹⁾

* Receiving position for profile

() Velocity assumed

[] Unreversed measurement

(1) Reversed velocity - 4.47 km/sec; 1°20' slope
downward to north

transition to such close proximity of the continental margin. This evidence suggests that the change from the structure observed underlying the basin to that underlying the continent must be very abrupt.

Profile 5 - Western Mediterranean Basin (North) - (Table 8, Figures 19 and 23).

Sections 5.1 to 5.8. Profile 5 is located over the extremely flat abyssal plain; water depth along the profile decreases from 2758 meters (1508 fathoms) at the southeast to 2542 meters (1390 fathoms) at the northwest as the Rhone delta is approached.

The unconsolidated sediment velocity along this profile ranges from 2.02 km/sec (Sections 5.4, 5.5) to 2.15 km/sec (Section 5.1). On those sections where it is in evidence, the top of the layer having this velocity appears nearly coincident with the sea floor as determined by the echo sounding profile. The maximum thickness of the material along the section is 0.63 kilometers.

Underlying the unconsolidated sediment is material having velocity 2.52 to 2.55 km/sec. On Section 5.1 this layer has a velocity of 2.79 km/sec but the measurement is unreversed. The layer thickness is remarkably uniform over the entire section,

varying from 0.63 km. (Section 5.1) to 0.73 km. (Section 5.5). It is underlain by material of velocities ranging from 3.55 km/sec to 3.83 km/sec. The thickness of this layer is relatively uniform, varying from 1.25 km. to 1.63 km. along the section except for the region where Sections 5.3 and 5.4 overlap. Computed thicknesses here are 1.04 km. (Section 5.3) and 2.07 km. (5.4); this disagreement may be ascribed to complications in the structure underlying Sections 5.2, 5.3 as evidenced by considerable scatter in the data points on the travel-time graph for the next higher velocity line.

The next velocity measured varies from 4.70 to 4.76 km/sec. This layer is more irregular than the overlying layers and thickens gradually from southeast (3.18 km.) to northwest (4.40 km.). The presence of structure in this layer is evidenced by the large "sag" in the 4.70 km/sec velocity line on the travel-time graph for Section 5.2. In addition, the 4.71 km/sec velocity line on Section 5.3 fails to reverse with the corresponding line on Section 5.2 and its zero intercept differs by 0.19 seconds with the corresponding zero intercept of Section 5.4.

The 4.70 - 4.76 km/sec layer overlies material of velocity 6.56-6.63 km/sec (Section 5.2. to 5.6); a velocity of 6.10 km/sec is measured on the unreversed segment (Section 5.1). The depth to the top of this layer is nearly uniform along the central section of the profile

(Section 5. 2 to 5. 5) varying from 7. 98 to 8. 34 km. A velocity of 6. 54 km/sec was determined on Sections 5. 7, 5. 8. A gradual thickening from 4. 15 km. (SE) to 5. 05 km. (NW) is indicated.

A mantle velocity of 7. 72 km/sec was measured on the long reverse profile, Section 5. 7, 5. 8. Depth to the interface increases from 12 km. at the southeast to 14 km. at the northwest.

The 6. 56 - 6. 63 km/sec velocity is measured, typically, at moderately shallow depths below the sea floor in the deep ocean; here it has often been termed the oceanic crust. The layer overlying this material is moderately thin (1 - 2 km.) in the deep ocean. The thickness of the overlying material measured on this profile (2. 7, 2. 8) varies from 5. 20 to 6. 40 km., a thickness substantially greater than normally encountered in the deep ocean.

Table 8 Profile 5
Seismic Velocities, Layer Thicknesses, and Depths
(in km/sec and km.)

Section		V	T _a	D _a	T _b	D _b
5. 1	W. S.	1. 53	2. 62	2. 62		
		[2. 15]	0. 50	3. 12		
		[2. 79]	0. 63	3. 75		
		[3. 66]	1. 26	5. 01		
		[4. 74]	4. 40	9. 41		
		[6. 10]				

Table 8 (continued)

Section		V	T _a	D _a		T _b	D _b
5. 2-5. 3	W. S.	1. 53	2. 62	2. 62	CHAIN	2. 65	2. 65
	(NW)	(1. 53)	0. 05	2. 67	(SE)	0. 00	2. 65
		2. 05	0. 63	3. 30		0. 31	2. 96
		2. 55	0. 24	3. 54		0. 72	3. 68
		3. 55	1. 25	4. 79		1. 04	4. 72
		4. 70	3. 51	8. 30		3. 26	7. 98
		6. 56					
5. 4-5. 5	CHAIN	1. 53	2. 62	2. 62	W. S.	2. 72	2. 72
	(NW)	(1. 53)	0. 02	2. 64	(SE)	0. 05	2. 72
		2. 02	0. 25	2. 89		0. 22	2. 99
		2. 52	0. 71	3. 60		0. 73	3. 72
		3. 83	2. 07	5. 67		1. 34	5. 06
		4. 76	2. 49	8. 16		3. 28	8. 34
		7. 71					
5. 6	W. S.	1. 53	2. 72	2. 72			
		(1. 53)	0. 02	2. 74			
		[2. 03]	0. 29	3. 03			
		[2. 53]	0. 65	3. 68			
		[3. 71]	1. 63	5. 31			
		[4. 70]	3. 18	8. 49			
		[6. 56]					
5. 7-5. 8	W. S.	1. 53	2. 52	2. 52	W. S.	2. 72	2. 72
	(NW)	(2. 00)	0. 49	3. 01	(SE)	0. 28	3. 00
		2. 54	0. 55	3. 56		0. 80	3. 80
		3. 71	1. 04	4. 60		1. 05	4. 85
		4. 53	4. 32	8. 92		3. 07	7. 92
		6. 54	5. 05	13. 97		4. 15	12. 07
		7. 72					

Table 9
Values of C_O and $\overline{C_V}$

Profile	C_O (km/sec)	$\overline{C_V}$ (km/sec)
193	1.53	1.53
194	1.53	1.53
195	1.525	1.52
196	1.53	1.51
197	1.53	1.51
198	1.53	1.52
199	1.53	1.52
2	1.525	1.53
3	1.525	1.52
4	1.525	1.53
5	1.525	1.53

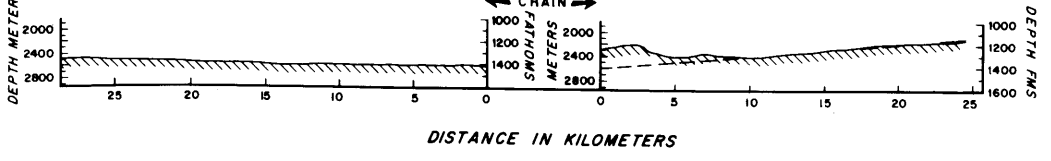
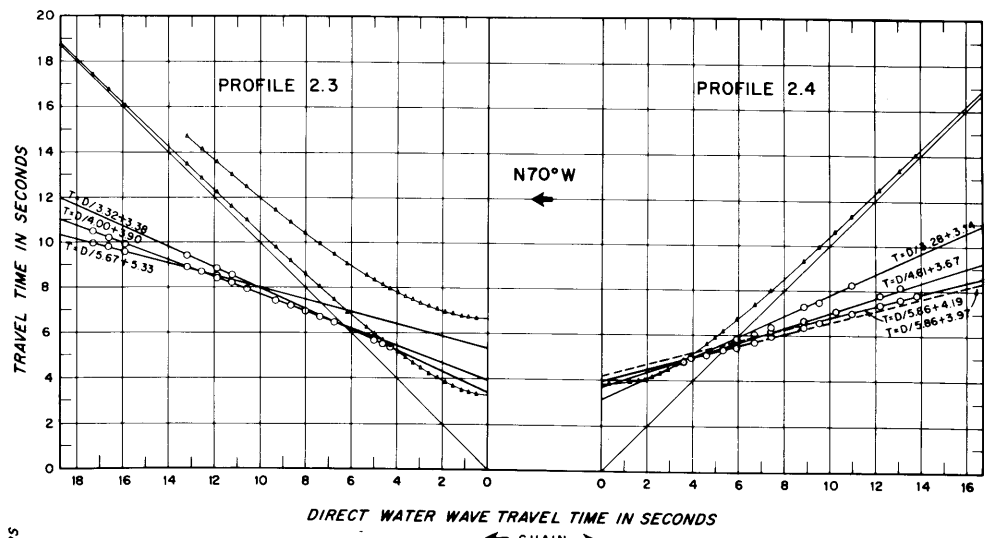
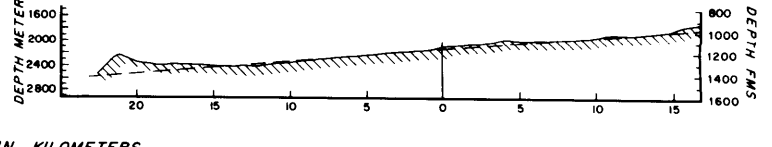
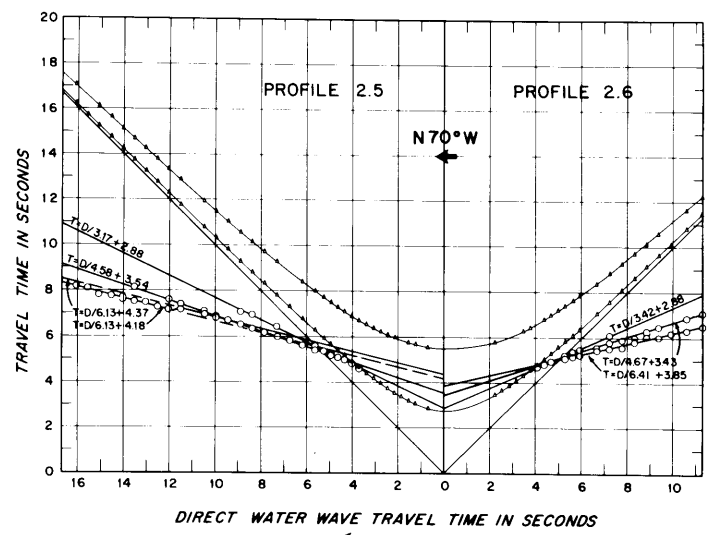
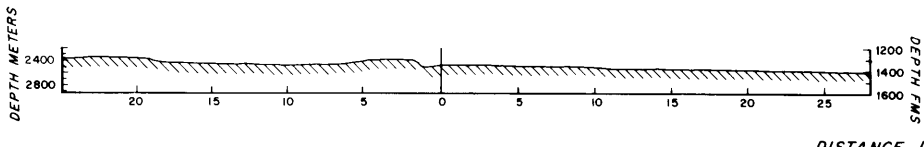
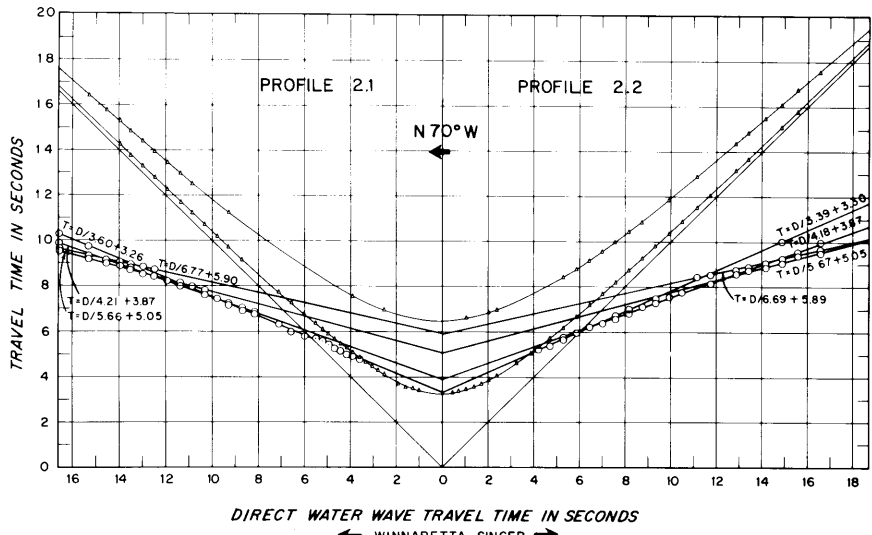
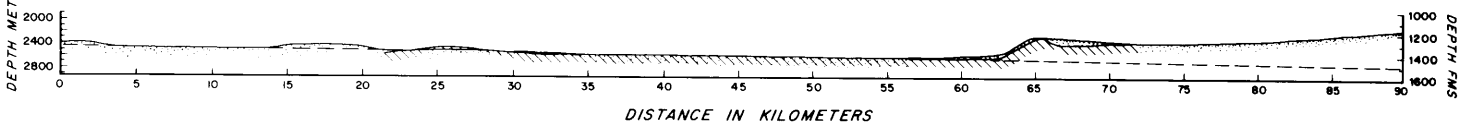
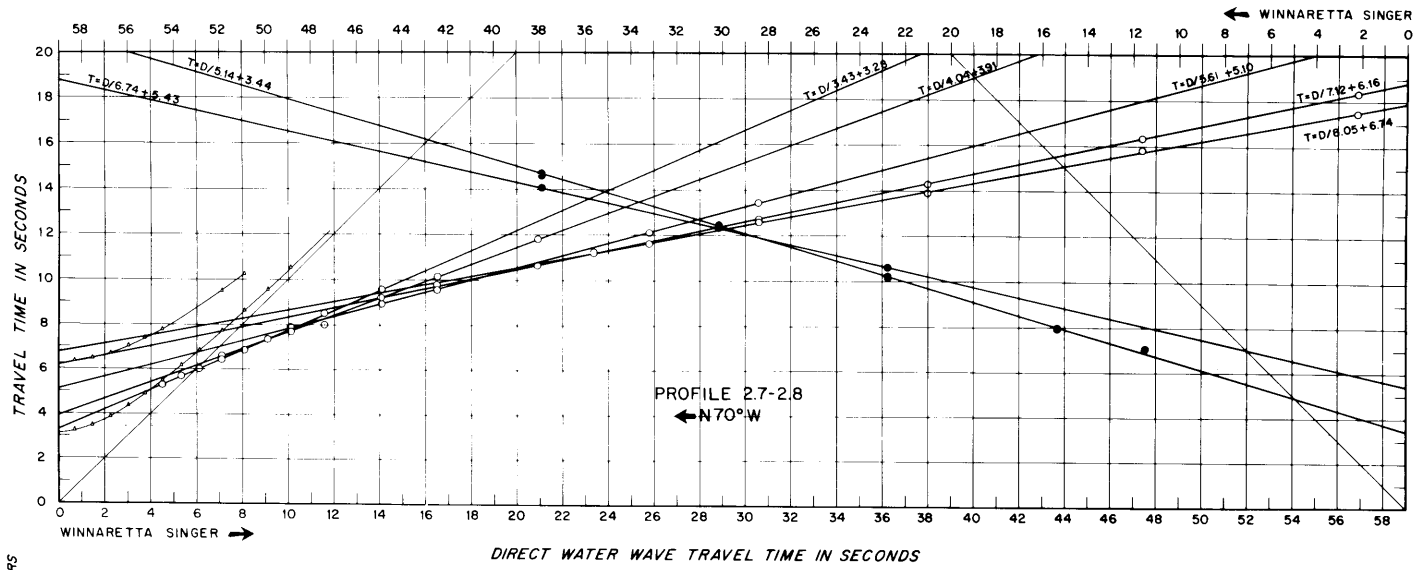


Figure 16.

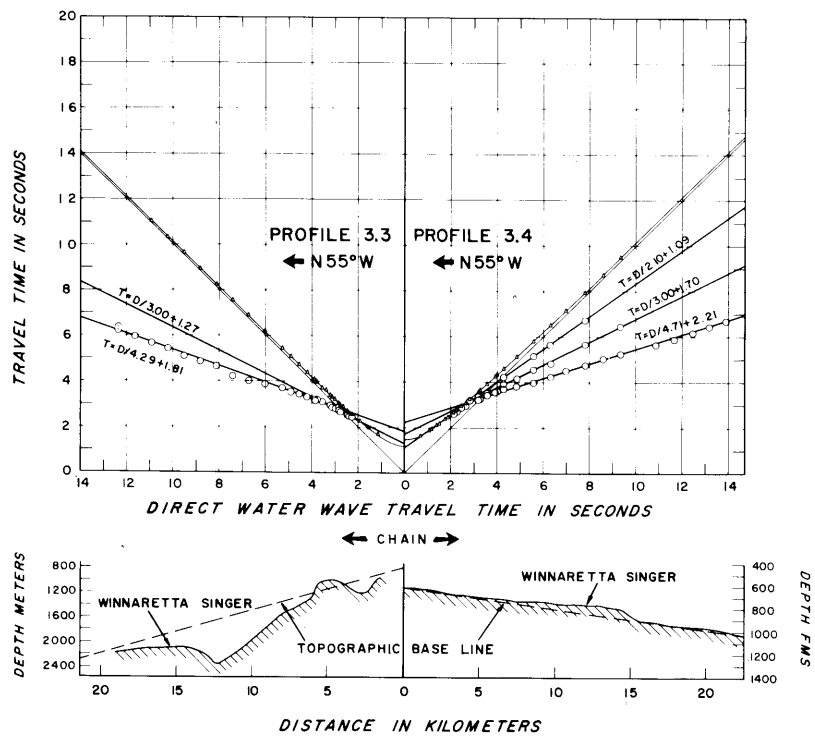
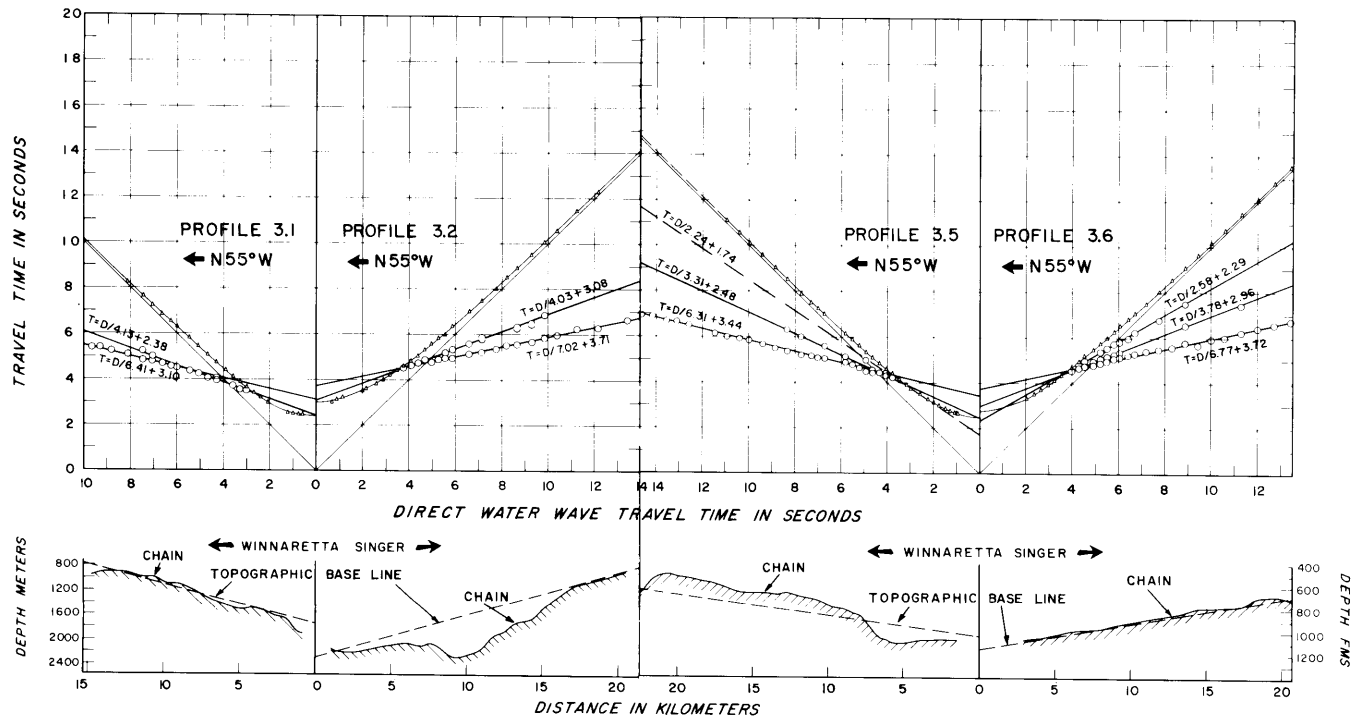
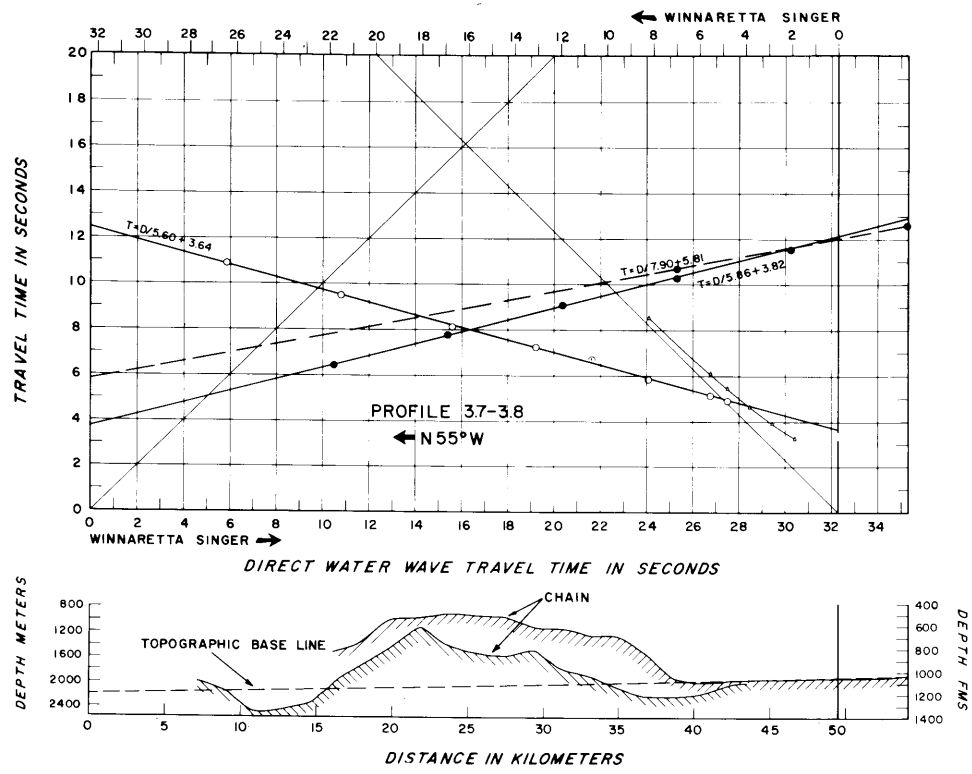


Figure 17.

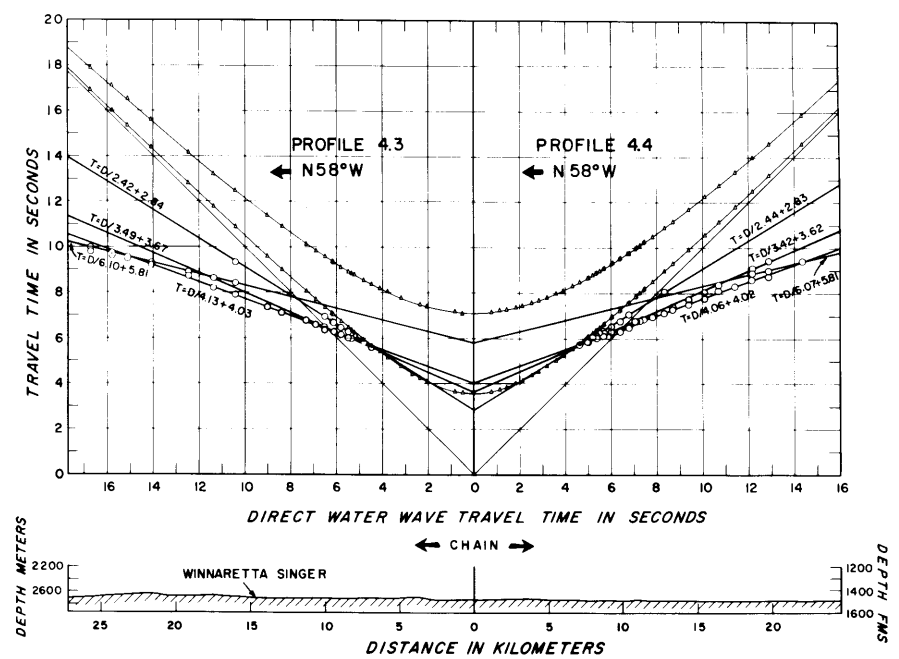
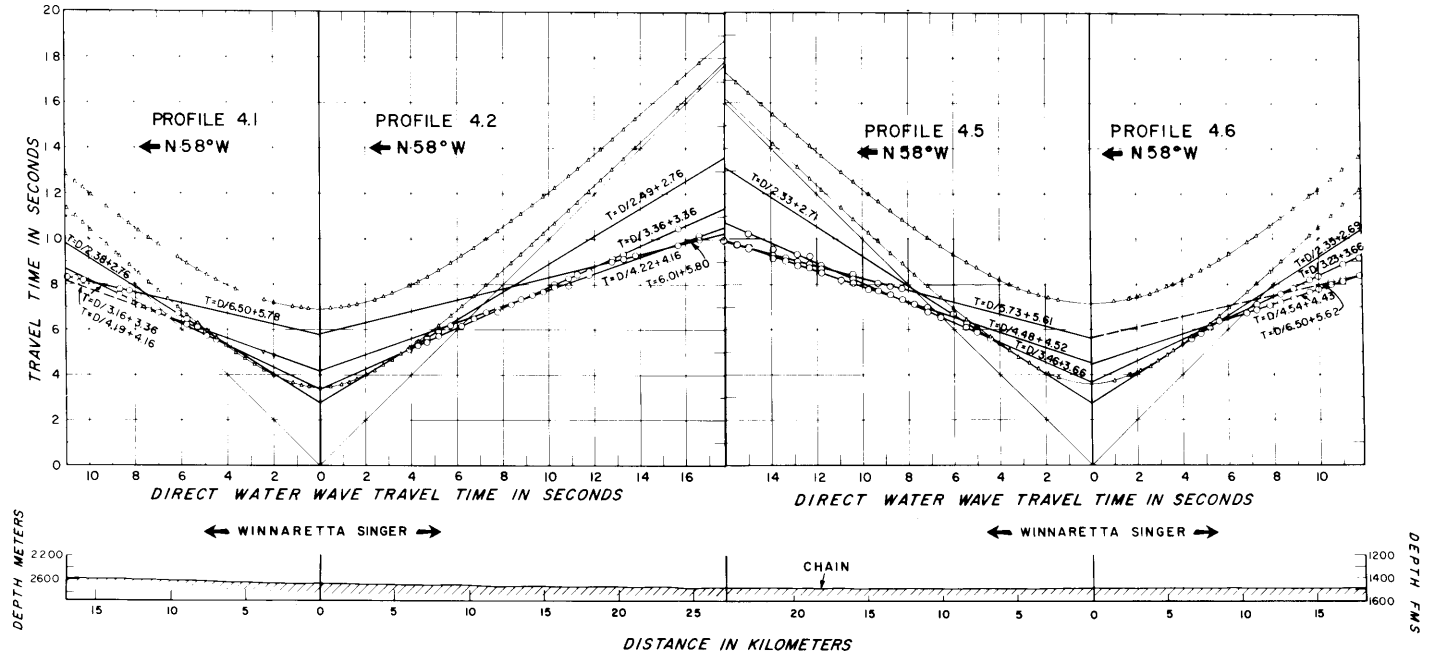
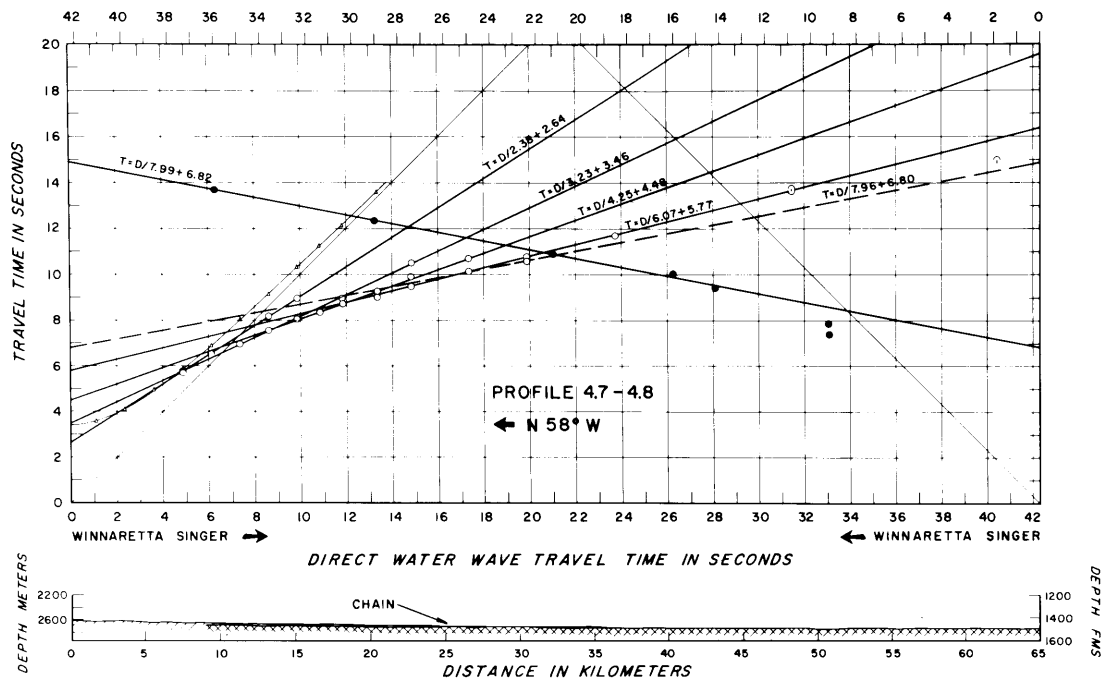


Figure 18.

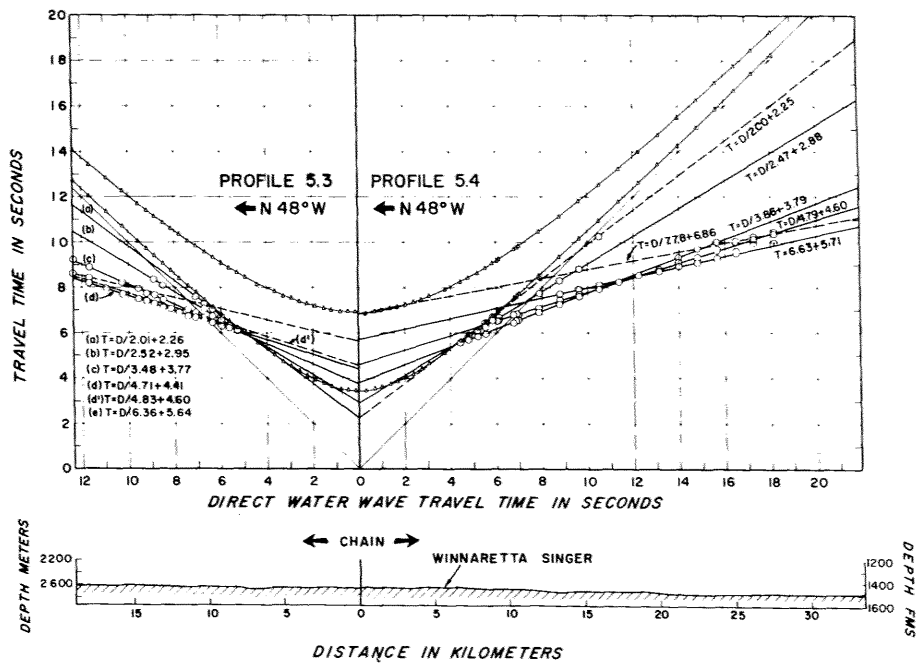
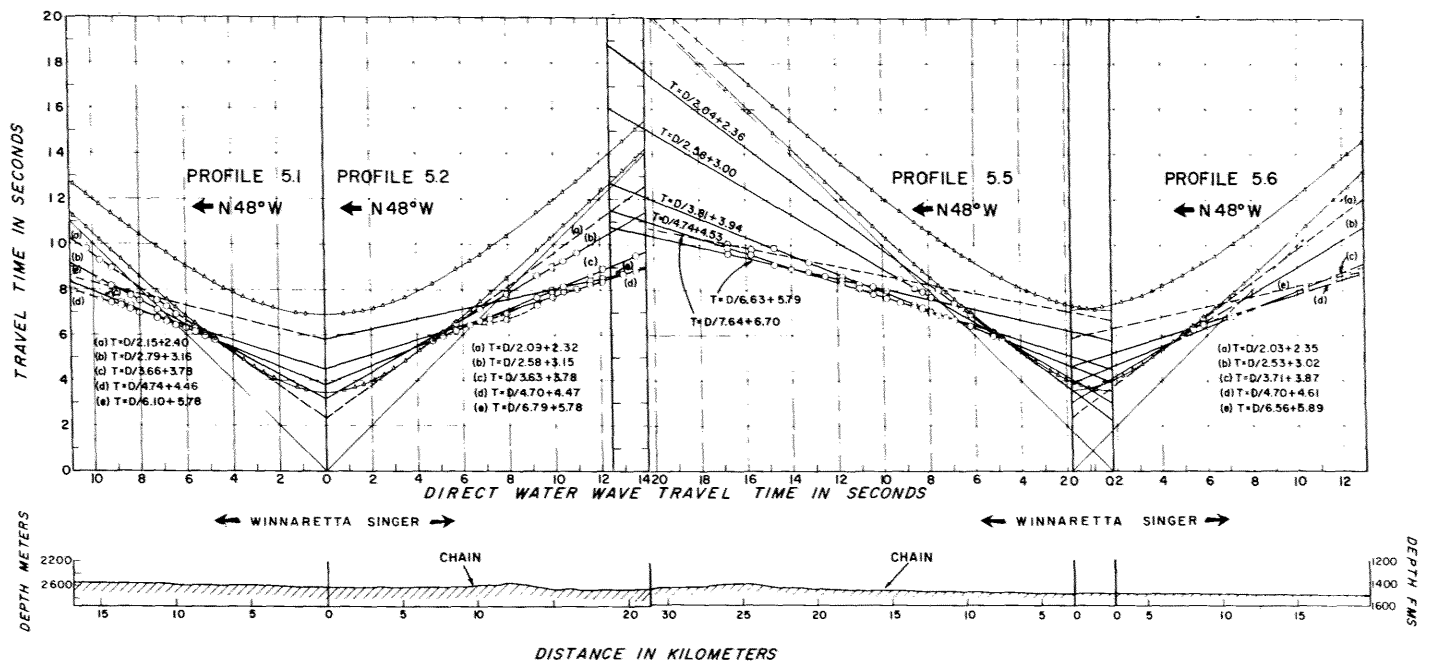
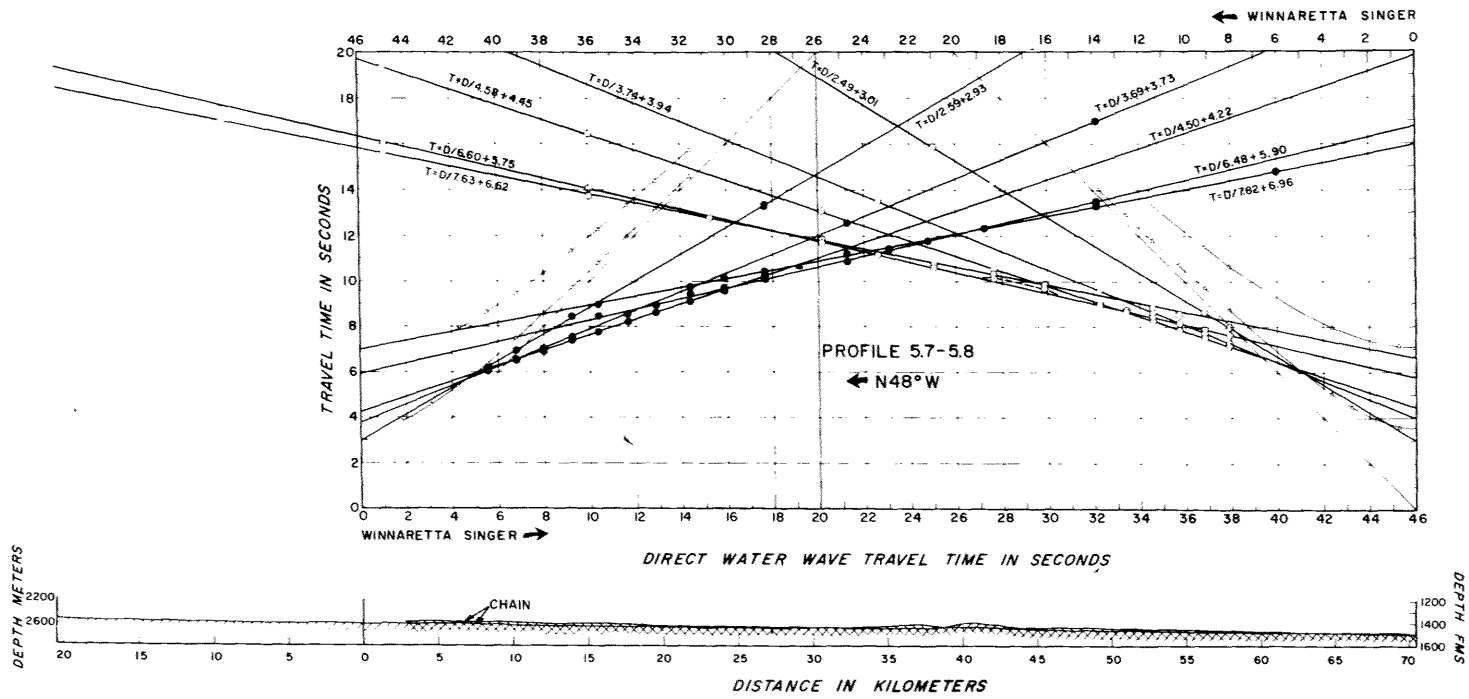


Figure 19.

PROFILE 2
VELOCITY-DEPTH SECTION
VELOCITY (KM/SEC)

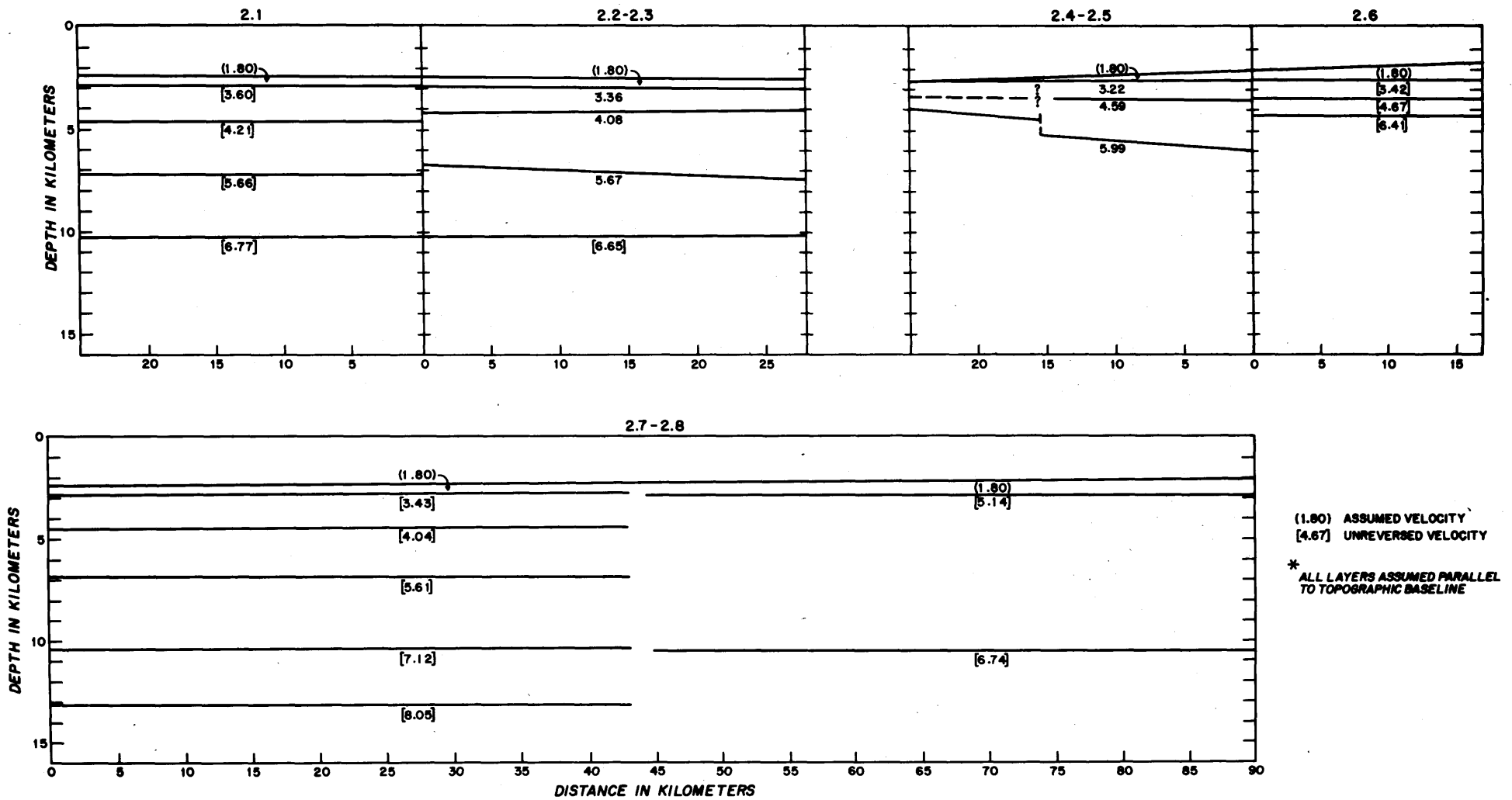


Figure 20.

PROFILE 3
VELOCITY-DEPTH SECTION
 VELOCITY (KM/SEC)

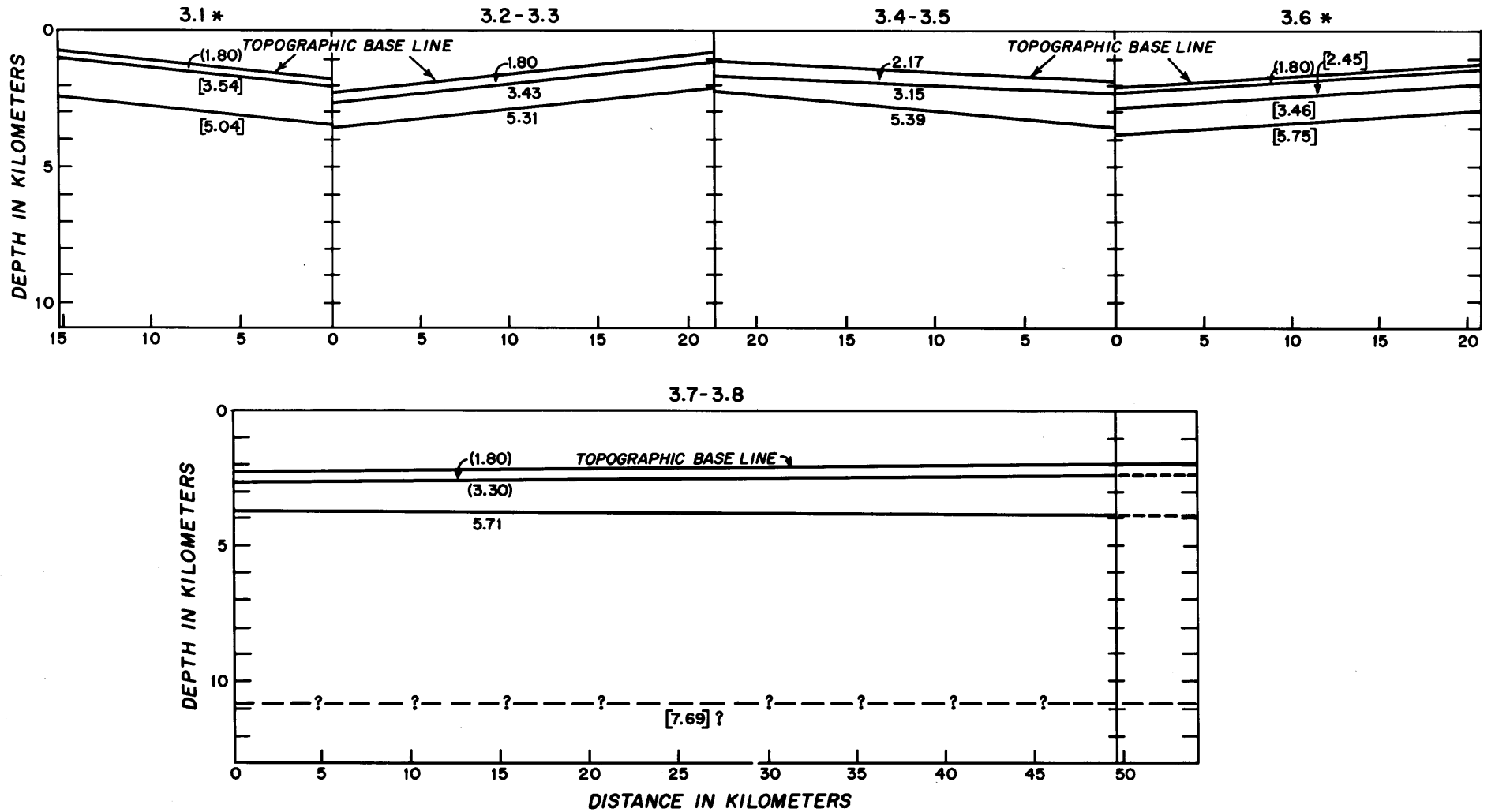


Figure 21.

PROFILE 4
 VELOCITY-DEPTH SECTION
 VELOCITY (KM/SEC)

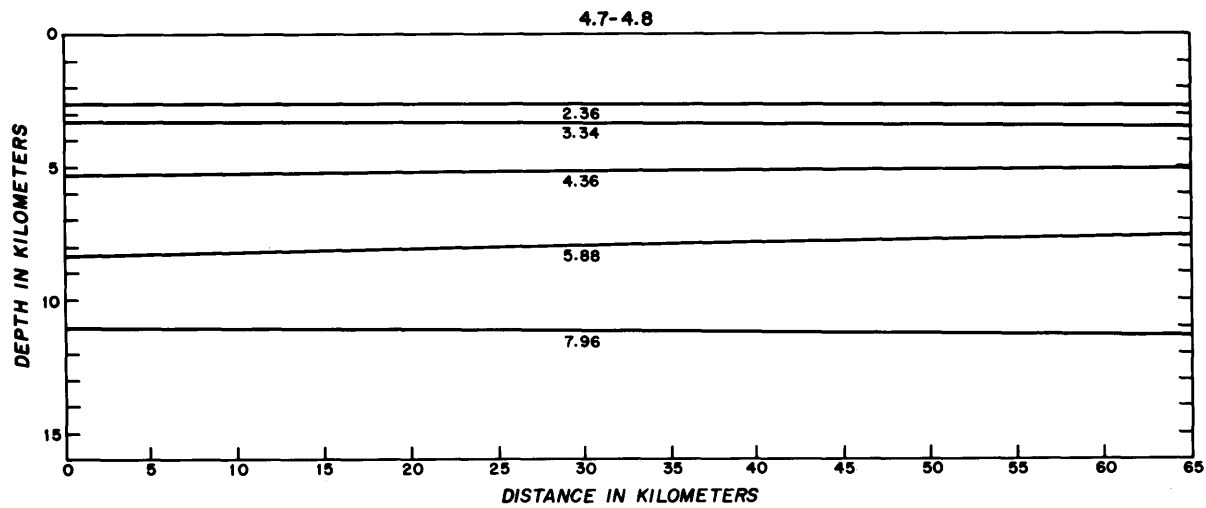
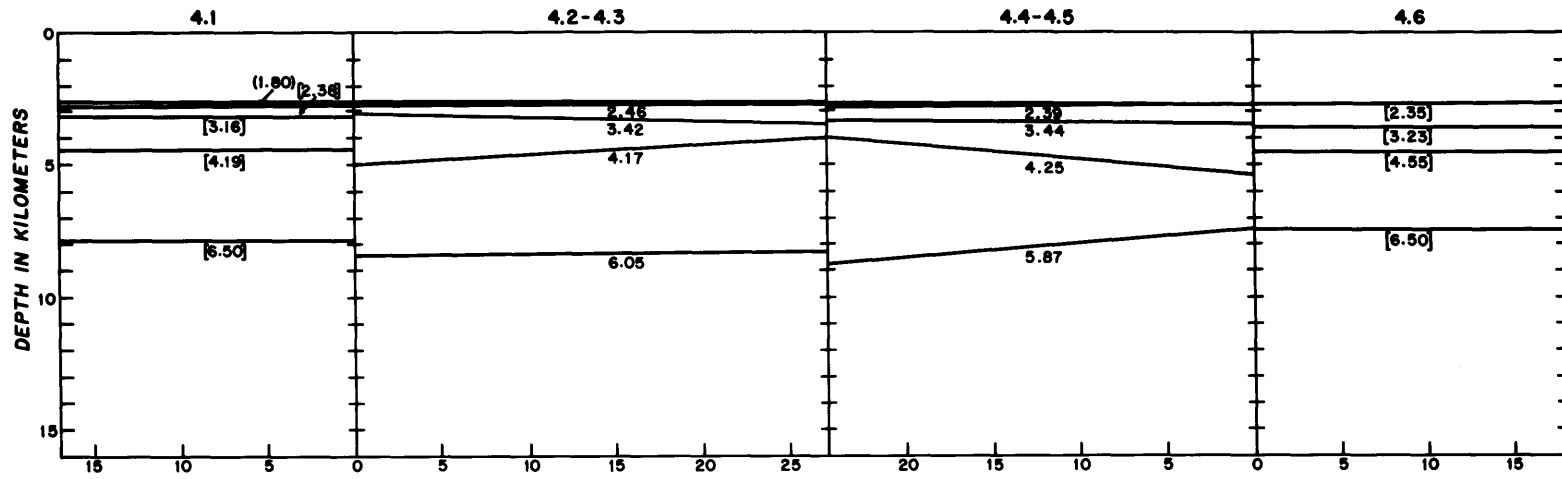


Figure 22.

PROFILE 5
VELOCITY-DEPTH SECTION
 VELOCITY (KM/SEC)

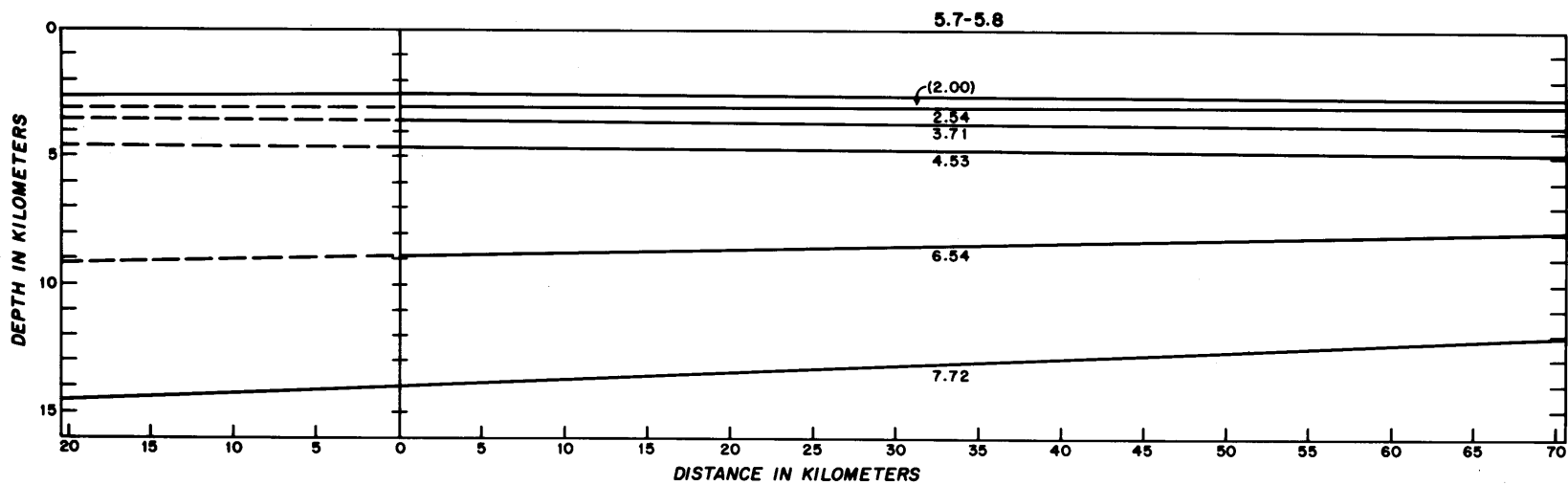
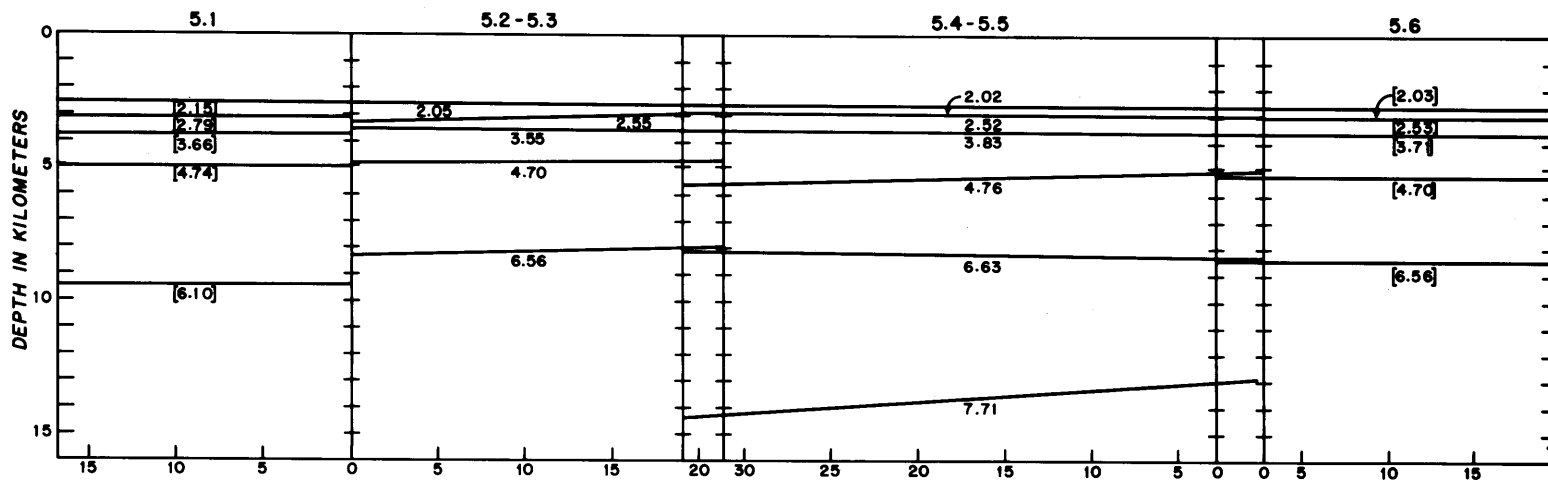


Figure 23.

REFLECTION PROFILE (CSP) - SPARK SOURCE
CHAIN CRUISE 21-1, 2 OCTOBER, 1961
WATER DEPTH: 1370 FATHOMS (2,490 METERS)

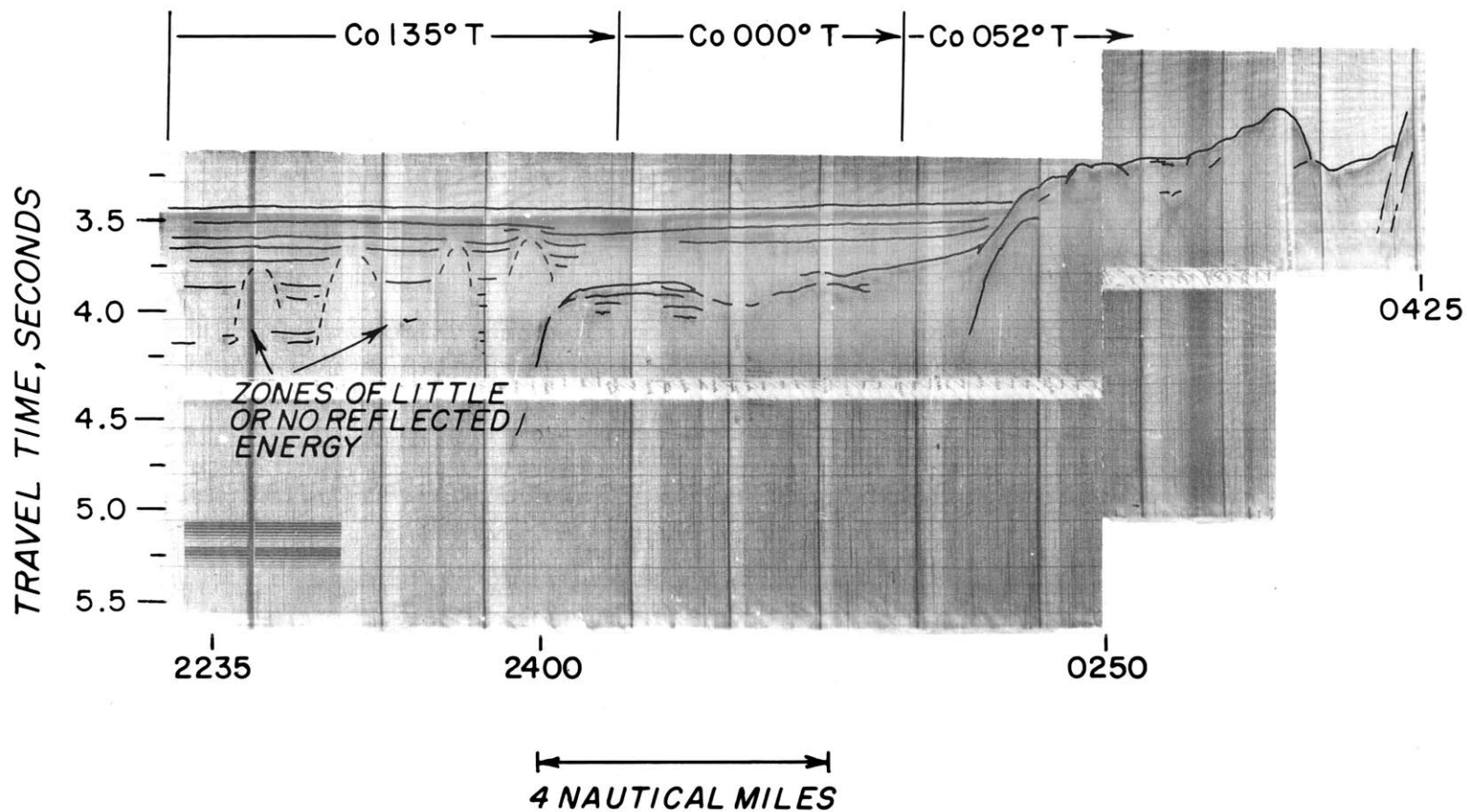


Figure 24.

DISCUSSION OF RESULTS

Structure Cross Section

A structure cross section based on the seismic refraction evidence has been constructed and is presented in Plate 2. The line of the section runs northeast from Profile 197 across the basin and onto the continental shelf in the region of the Gulf of Genoa (Plate 1). The section intersects the midpoint of Profiles 3, 4, 5, and 195 and passes through the northwest end of Profile 2 (Sections 2.2, 2.3). Since it is based chiefly on profiles located normal to the section line it has been necessary to extrapolate the results of a given profile to that of another profile over several tens of kilometers. Although transitions from one profile to another may not be known in complete detail, the major features illustrated by the section may be drawn with confidence.

The observed velocities, for purposes of discussion, are grouped as follows: unconsolidated and semiconsolidated sediments with velocity 2.5 km/sec, intermediate velocity materials with velocities 3.4 to 6.0 km/sec, high velocity crust with velocity 6.6 to 7.0 km/sec, and mantle, velocity 7.7 km/sec.

Mantle, High Velocity and Intermediate Velocity Crust. The crust under the western Mediterranean Basin is characterized

by an extremely shallow depth to mantle. The Mohorovicic discontinuity is found at a depth of approximately 10.5 km. near the central part of Profile 5; its depth increases to 13 to 14 km. both to the southwest and northeast in the direction of the Balearic Islands and the coast of Italy respectively. A velocity of 7.7 km/sec was obtained on Profile 195 and 5 and 8.0 km/sec on Profiles 4 and 2; the measurement on Profile 2 is, however, unreversed. The 7.7 km/sec mantle velocity determinations on Profile 195 and 5 are excellent; such a velocity is somewhat lower than usually expected for mantle. Similar low values for mantle velocity have been obtained in other areas where they are intimately associated with mantle velocity determinations of 8.0 km/sec or greater. For example, Ewing, et al (1960) obtained a velocity of 7.8 km/sec associated with neighboring velocities of 8.1 and 8.2 km/sec in the Colombian Basin and Bunce and Fahlquist (1962) obtained a 7.7 km/sec velocity associated with 8.0 km/sec velocities on adjoining profiles on the Outer Ridge north of the Puerto Rico Trench. The 7.7 km/sec velocity (Profiles 195, 5) when considered in relation to the 8.0 km/sec determination on Profiles 2 and 4, may therefore be reasonably regarded as associated with mantle material. It is not known whether this value (7.7 km/sec) obtained in the western Mediterranean is indicative of any characteristic changes in the mantle material as the western margin of the basin

is approached or whether it merely represents normal inhomogeneity to be expected in the mantle. Depths to the Mohorovičić discontinuity are similar to those measured in the deep ocean.

Material having a velocity of 6.6 km/sec has been found overlying mantle material at three stations, Profiles 195, 5, and 2. The thickness of this layer varies from 2 to 3 km. along the section, reaching a thickness of slightly over 3 km. in the region northeast of the Balearic Islands. At Profile 4 a velocity of 5.8 to 6.0 km/sec was obtained at depths comparable to the 6.6 km/sec determinations; no 6.6 km/sec material was detected at this station. Since the seismic profiles are located normal to the section line, the transition from 5.8 - 6.0 km/sec material found on Profile 4 to the 6.6 km/sec material found to the northeast and southwest of this profile cannot be detailed. The top surface of the 6.6 km/sec layer closely parallels the configuration of the Mohorovičić discontinuity; it has a minimum depth of approximately 8 km. at Profile 5 where the depth to mantle is a minimum, and increases to a depth of about 10 km. both to the northeast and southwest. The section so far described has definite oceanic characteristics. However, it has a shallower water depth (2.5 - 2.8 km.) than a typical oceanic region; it has an unusually thick section of intermediate velocity material (3.4 to 6.0 km/sec), and it has a somewhat thinner layer of 6.6 km/sec material

than normally found in the deep ocean basins.

A thick section of material having an intermediate velocity, 3.4 to 6.0 km/sec, is present beneath the basin. In the central part of the basin in the region of Profiles 195, 5 and D-11 (Ewing and Ewing, 1959), the thickness of this material varies from 4.5 to 5.5 km; the section of intermediate velocity material thickens substantially both to the southwest and to the northeast as the edge of the basin is approached.

At Profile 4, further to the northeast, material of intermediate velocity makes up almost the entire crustal section. The 3.4 km/sec material thins to 0.5 km. in this region and is underlain by 4.5 km. of material of velocity 4.2 km/sec. This layer is in turn underlain by over 2.5 km. of material of velocity 5.8 to 6.0 km/sec; the 6.6 km/sec layer is either altered in velocity and composition, missing, or so thin, it has gone undetected at this station. The 3.4 and 4.2 km/sec layers extend in an uninterrupted fashion northward to the base of the continental slope (see Geophysical Results, Profile 4, page 73). At Profile 2 (Sections 2.1, 2.2, 2.3) the intermediate velocity section has thickened to 7 km. The top surface of the 5.7 km/sec layer shoals gradually to the northeast as Profile 2 is approached.

Significance of 5.7 - 6.0 km/sec Material. Identification of the 5.7 to 6.0 km/sec material with a specific rock type is a matter of speculation. This velocity can be associated with a wide variety of rock types: granite, gneiss, a variety of metamorphic rocks, and even dense limestones (Birch, 1960). Similar velocities are commonly encountered in the rocks making up the basement complex on the continents.

Several geologists, including Kuenen (1959) and Bourcart (1960), have hypothesized on the basis of geologic evidence that continental structures were continuous across the northern Ligurian Sea from France to Corsica from the Cretaceous up to the Miocene. Bourcart (personal communication, 1958) suggests that this granite ridge extends from the vicinity of Cape Antibes southeasterly to Corsica below the present sea floor. The selection of the locations of Profile 2 and 4 was guided by this consideration.

Topographically there is some suggestion of a broad submarine ridge extending east southeast from Cape Antibes (Debrazzi and Segre, 1960), which might reflect a continuation of continental type basement complex. The separation of this portion of the Ligurian Sea into two distinct basins, one to the north of the ridge and one to the south, is not very marked topographically. The difference in elevation between the basins and the dividing ridge is less

than 100 meters. More detailed soundings are desirable in this region to verify this separation. Nevertheless, the elongate nose extending southeast from Cape Antibes is very pronounced in the near shore bottom topography. Profile 2 is located just to the north of the ridge and closely parallels its axis; Profile 4 is well to the south of the ridge.

West of Profile 2 and northwest of Profile 4, the Maures-Esterel Massif, extending along the French coast from Cape Antibes to Toulon, is made up of granite, gneisses, schists, and slightly metamorphosed shales and quartzites (Gignoux, 1950; Goguel, 1955). The Massif of Mercantour (Hercynian), composed of gneiss, schist, and granite, is located less than 50 km. north of Nice. A seismic profile extending from Briançon in the Maritime Alps southward to Nice (Rothe', 1958) measured a velocity of 6.07 km/sec at a depth of about 2 km. and over a range interval of 12 to 150 km.

The most northwesterly end of Profile 4 (Section 4.1) and the short profile reported by Leenhardt (1962) are located less than 50 km. southeast of the Maures-Esterel Massif. If the 5.7 to 6.0 km/sec material present at Profiles 2 and 4 is indicative of sialic rocks similar to those found in the Massif, then these rocks are now at depths of 7 to 8 km. below sea level in the Ligurian Sea.

Direct seismic evidence on Profile 2 (see Geophysical Results, Profile 2, page 62) indicates a downward displacement of the basin floor of 2 to 3 km. Bourcart (1958) theorizes that the present continental slope south of France is the result of downbending of the crustal rocks. If the 5.7 to 6.0 km/sec material does represent continental basement rocks, the conclusion that this portion of the western Mediterranean is downwarped or downfaulted at least 2 to 3 km. is inescapable. The seismic results, particularly the evidence for the thick section of intermediate velocity material, support this point of view.

Continental Margin. Turning to the northeast, Profile 3, is located on the continental margin adjoining the basin. The water depth as noted previously (Figure 17) varies between 1 and 2.5 km. along the profile. Velocities of 3.4 and 5.4 km/sec were measured here. The 3.4 km/sec material is about 1 km. thick along the section, a thickness which agrees remarkably well with that found for the 3.4 km/sec material to the southwest (Profile 2). The highest velocity measured at Station 3 is 5.4 km/sec.

It is difficult to extrapolate between Profiles 2 and 3 since the intervening region crosses the continental margin and slope. It is not known whether the 3.4 km/sec material measured at both these stations represents the same horizon. Furthermore, if the two

layers are identical, the present seismic evidence cannot indicate how the displacement of this layer between Profiles 2 and 3 takes place. Lack of intervening data precludes confirmation of any interpretation in terms of faulting or downwarp of the basin. However, further to the southeast on Profile 2 (Sections 2.4, 2.5) evidence for the existence of faulting or downwarping of the Basin is excellent. Along the section between Profiles 2 and 3 a relative vertical movement of almost 2 km. would bring the 3.4 km/sec horizons on the two profiles into juxtaposition. The underlying materials, velocities 4.1 and 5.4 km/sec, do not correlate.

Unconsolidated and Semiconsolidated Sediments. Unconsolidated and semiconsolidated sediment velocities have been measured at several points along the crustal section. In the central portion of the Basin (Profiles 195, 5, 4), velocities ranging from 2.0 km/sec to 2.9 km/sec are observed. At the extreme northeast end of the Basin (Profiles 2, 3) a sediment velocity of 1.80 km/sec has been assumed. The section has been extended across the Basin in a southwest direction and along the axis of the broad trough north of the Balearics to the vicinity of Profiles 196 and 197. Evidence for the reflection horizon (dashed line on Plate 2) is based on two explosive reflection profiles (Plate 1 and Figure 25) and on Continuous Seismic Profiler data (Plate 1). The reflection data indicate

REFLECTION PROFILE - CHAIN CRUISE #7

POSITION 41° 11' N, 3° 30' E
CHARGE SIZE - 9# (FIRED AT SURFACE)
LOW PASS FILTER - 18 TO 40 c.p.s.
WATER DEPTH - 2120 meters

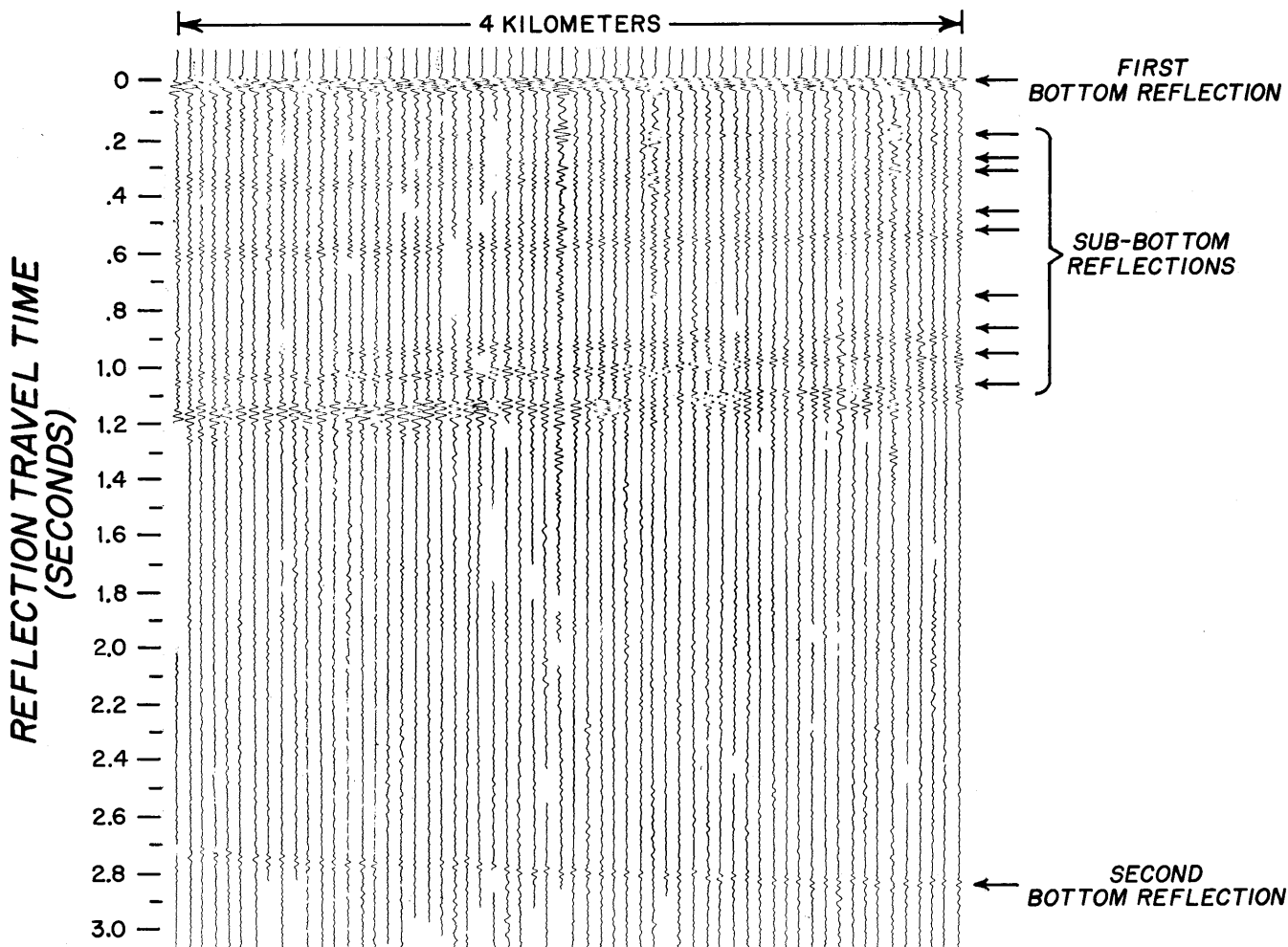


Figure 25.

exceptionally strong reflector recorded at travel times varying from 0.80 to 1.50 seconds after the bottom reflection. This reflector probably marks the discontinuity between the low velocity (< 3.0 km/sec) material and the intermediate velocity materials. The reflecting horizon appears to be continuous from Profiles 196 and 197 all the way along the axis of the trough and out into the basin.

The interface shown in the crustal section (Plate 2) has been drawn under the assumption that the average sediment velocity is 2.5 km/sec. The depth computations indicate excellent agreement with the top surfaces of the 3.85 km/sec layer (Profile 196) and the 4.2 km/sec layer (Profile 195). Sediment thickness increases gradually from about 0.5 km. near the edge of the continental margin to over 1.2 km. in the center of the basin in the vicinity of Profile 195. Further to the southwest along the section the sediment thickness increases to about 1.75 km. and then thins again as shallow water is approached to the west of the Balearic Islands. An assumed velocity less than 2.5 km/sec would decrease the thickness of these sediments; an average velocity greater than 2.5 km/sec would correspondingly increase the thickness. At present no velocity data are available in this region.

Significant Features: Summary. The significant features of this structure cross section based on seismic observation may be

summarized as follows:

(1) Depth to the Mohorovičić discontinuity in the central part of the basin is less than 12 km, and increases toward the basin margins.

(2) A thick section of intermediate velocity material is present throughout the northern part of the basin.

(3) As the basin margin is approached to the northwest the crustal layers decrease in velocity at comparable depths; 4.2 to 3.4 km/sec at a depth of 4 km.; 4.9 to 4.7 to 4.1 km/sec at a depth of 5 to 8 km.; 6.6 to 5.8 km/sec at a depth of 8 km; and 7.7 - 8.0 to 6.8 - 7.1 km/sec at a depth of 11 km.

(4) A velocity increase at shallow depth (5.4 km/sec at 2 km. depth) occurs at the continental margin.

(5) The seismic evidence supports the conclusion that the crustal material underlying the basin has been displaced downward at least 2 to 3 km. to its present position.

Comparison with European Crustal Structure

The western Mediterranean Basin is adjacent to continental Europe. It is therefore of interest to compare the results obtained in this crustal study in the central part of the western Mediterranean

with those obtained on the European continent, both in the Alps and elsewhere. Several crustal studies, using both earthquake and explosion seismic techniques, have been carried out in Europe since the conclusion of World War II. Willmore (1949) presented the results obtained in North Germany from the Heligoland explosion; Rothé (1947) reported the results obtained at the French stations for the same explosion. Caloi (1957) discussed both results obtained from earthquakes and large explosions with particular reference to central and southern Europe. Caloi (1958) extensively reviewed the seismic crustal studies for central Europe and published a seismic-geologic section extending from north Germany southward to the Po Valley. Rothé (1958) reviewed the results of several seismic experiments conducted in Germany and France since 1946.

The results obtained for the Heligoland explosion in north Germany by Willmore (1949) are summarized in Table 10. The notation commonly used in earthquake seismology to denote compressional wave velocities is followed here:

- | | |
|--|--|
| P_s = Sediment velocity | P_g = Basement velocity
(granite) |
| P^* = Velocity of Conrad layer | |
| P_n = Velocity associated with top of the mantle | |

Table 10. Results of Heligoland Explosion

North Germany (after Willmore (1949))

<u>Phase</u>	<u>Vel</u> (km/sec)	<u>Thickness</u> (km.)	<u>Phase</u>	<u>Vel</u> (km/sec)	<u>Thickness</u> (km.)
P _s	4.4	6.7	P _s	4.4	5.9
P _g	5.95	20.7	P _g	5.57	8.3
			P*	6.50	15.7
P _n	8.18		P _n	8.18	
		Total 27.4			Total 29.9

The available data are satisfactorily interpreted by the first model but the second model, including the P* (Conrad discontinuity) velocity, is not precluded.

The results of the Haslach experiment in southern Germany and France have been summarized by Rothé (1958) and are presented in Table 11.

Table 11. Results of Haslach Experiment

J. P. Rothé and E. Peterschmitt (1950)			O. Förtsch (1951)		
<u>Vel</u>	<u>Thickness</u>	<u>Depth</u>	<u>Vel</u>	<u>Thickness</u>	<u>Depth</u>
5.63	2.4	2.4	5.88	4-6	4-6
P _g 5.97	17.7	20.1	6.00	11.5	15.5-17.5
P* 6.54	10.1	30.2	6.55	17-18	32.5-35.5
P _n 8.15			8.34		

Refraction studies in the Paris Basin, (Beaufils, et al, 1956 and Geneslay, et al, 1956), obtained a velocity of 6.0 km/sec, later identified with Paleozoic basement consisting of schists and granites, at a depth of 2170 - 3180 meters.

Two studies located nearer to the region of the western Mediterranean are of particular significance. A profile, 26 km. in length obtained in 1949 (Beaufils, et al, 1956), extends southeasterly to the Mediterranean Sea in the neighborhood of Arles; all the receiving stations were near sea level. The highest velocity obtained was 6.0 km/sec; depth to this layer was only 2 km. The layer was tentatively identified with the Paleozoic basement. Of perhaps considerably more significance was the series of experiments carried out by the Comite National Français de Géodesie et Géophysique (Section de Seismologie) in the western Alps (Tardi, 1956). Results of this study have been reported by Tardi (1957) and reviewed by Rothé, J. P. (1958). In this experiment, three seismic lines radiate east, west, and south of the shot point located in the internal (Briançonnaise) zone of the western Alps. The southerly profile extends from northwest of Briançon southeasterly to Nice on the Mediterranean. At shot ranges two velocities were identified, 4.5 km/sec and 5.2 to 5.5 km/sec. At ranges greater than 12 km. and extending to Nice (150 km.) only a single velocity, P_g , 6.07 km/sec was measured.

Depth to this horizon was only 2 km. P^* and P_n were not identified on this profile, possibly due to poor energy coupling of the explosive source with the ground. On the westerly profile extending through the Belle Donne Massif and to the Rhône River, there is some indication of a discontinuity at a depth of 25 km. (Conrad?) with an associated velocity of 6.7 km/sec. This compares with a depth of approximately 20 km. at Haslach; P_n was not observed. These studies did not fix the depth to the Mohorovičić discontinuity under the western Alps. Caloi (1958) gives results for a section extending from North Germany to the Po Valley (Table 12). His total crustal thicknesses, including the granite and "basalt and/or gabbro" layers, are as follows:

Table 12 Crustal Thickness (after Caloi, 1958)

Aggregate Thickness of Crust

Wurtemberg	30 km.
Po Valley	30 km.
South Alps	40 - 45 km.
Central Appenines	50 - 55 km.

In summary, the European continental crust, in non-mountainous areas, appears to be roughly 30 km. thick; under the Alps and Appenines there is a substantial thickening, perhaps to as much as 55 to 60 km. Under the north German plain and in the Black Forest region, the

the Conrad discontinuity is associated with a velocity of 6.5 km/sec at depths varying from 10 to 15 km. The question of the existence of the Conrad layer underlying most of Europe is still debated. The most recent Alpine studies (H. Closs, personal communication, 1962) still leave the existence of a discrete, well-defined Conrad layer open to question. However, the existence or non-existence of a Conrad layer will not alter the total crustal thickness by any large amount.

A reasonable comparison of the western Mediterranean Basin data and a typical European crustal section is made in Table 13.

Table 13 Comparison of European and western
Mediterranean Crustal Thickness

<u>Western Mediterranean</u>			<u>Central Europe</u>		
<u>Vel</u> km/sec	<u>Thickness</u> km.	<u>Depth</u> km.	<u>Vel</u> km/sec	<u>Thickness</u> km.	<u>Depth</u> km.
1.5	2.5	2.5	1.8 - 5.0	2	2
1.8 - 5.0	5.5	8.0	6.0	18	20
6.6	3.0	11.0	6.7	10	30
7.7 - 8.0			8.1		

The structural transition between the western Mediterranean Basin and continental Europe is abrupt; the changes in crustal structure occur over the relatively short lateral distance of 50 to 75 km, that is, between the present 2500 meter bathymetric contour roughly

outlining the abyssal plain and the present continental margin. The margins of the western Basin are bounded by steep slopes and a very narrow continental shelf. This marginal zone, very pronounced physiographically, must also mark very significant changes in the deep crustal structure. Attempts to trace seismic horizons from the basin to the continent across this transition region are futile on the basis of the present data. The data reported here only serve to focus attention once more on the gap in our understanding of the transition from deep ocean to continent.

Comparison of Oceanic, Intermediate and Continental Crust

The crust underlying the Mediterranean Sea has very definite similarities to oceanic crustal structure; the existence of a layer of material having a velocity of 6.6 km/sec and the shallow depth to the Mohorovičić discontinuity have already been discussed. In Figure 30 the velocity - depth structure of the western Mediterranean is directly compared with the crust underlying a typical deep ocean basin (western Atlantic), a continental land mass (Europe - Asia), and an area of intermediate crustal structure (Venezuelan Basin). The data were taken from the following sources: (1) western Mediterranean Basin (this paper) - Profiles 2, 4, 5, 194, 195, 198 and 199; (2) western Atlantic Basin (Ewing and Ewing, 1959) - Profiles A156-28, A173-4, A157-29, 30, 31, 32, 33, G-15, E-1, A150-4, 5, 6, G-3,

4, 5, 10, 11, 12, 13, 14, D-2, 15, 16, and F-1; (3) Venezuelan Basin (Officer, et al, 1957) - Profiles 2, 7, 8, 9, 31, 32 and 33; (Officer, et al, 1959) - Profiles 10-56, 24-56, 26-56 and 27-56; and (4) Continental Europe - Asia - Crustal data from several sources (tabulated by Steinhart and Meyer, 1960). Measurements made on the Aves Swell and near the Antilles Arc were excluded from consideration with the Venezuelan Basin data. Similarly, data from high plateaus and mountains were excluded from the Eurasian data.

The regional data defining the curves of Figure 30 are shown independently in Figures 26, 27, 28 and 29. The curves are an integrated composite of the results obtained from several profiles in each region. To a first approximation they can be considered as representing a gross average of the velocity - depth properties within the crust in the selected areas. The curves are not intended to imply continuous changes of velocity with depth, i. e., velocity gradients, although such gradients probably exist.

Comparison of the individual curves (Figure 30) suggests several observations that can be made. The pronounced difference between continental structure and that of the deep ocean and intermediate areas is obvious. The velocity associated with continental structure increases slowly with depth from its near surface value of 5.5 to 6 km/sec. Velocities associated with oceanic and intermediate

areas increase rapidly with depth until the mantle is reached.

The individual curves for the western Mediterranean (Figure 26) and Venezuelan Basin (Figure 27) show a nearly continuous distribution of data points indicative of the wide variety of velocity layering present in these basins. The Mediterranean profiles, although few in number, clearly demonstrate this effect, thus reflecting the complex stratigraphy and geologic history of the region. In contrast the western Atlantic Basin data (Figure 28) stress the uniformity and relatively simple layering found over wide areas in the deep sea. Even the addition of more recent refraction and reflection data, demonstrating the existence of material having a velocity of 4 to 5 km/sec in oceanic areas (Ewing and Ewing, 1959; Nafe and Drake, 1960; and Bunce and Fahlquist, 1962) would not alter this conclusion appreciably.

The presence of material of velocity 6.6 to 7.0 km/sec at depths of only 6 to 7 km. below sea level in oceanic areas is emphasized in the results shown in Figure 30. Despite the 1.5 km. difference in water depth between the western Mediterranean Sea and the Caribbean Sea (Venezuelan Basin) comparable depths (7 to 9 km.) to a velocity of 6 to 7 km/sec are exhibited, a depth 1 to 2 km. greater than that found in oceanic areas. Mantle velocity of 8.0 km/sec is reached at 12 km. depth on the western Atlantic Basin curve. The western Mediterranean Basin curve closely approaches the western Atlantic data

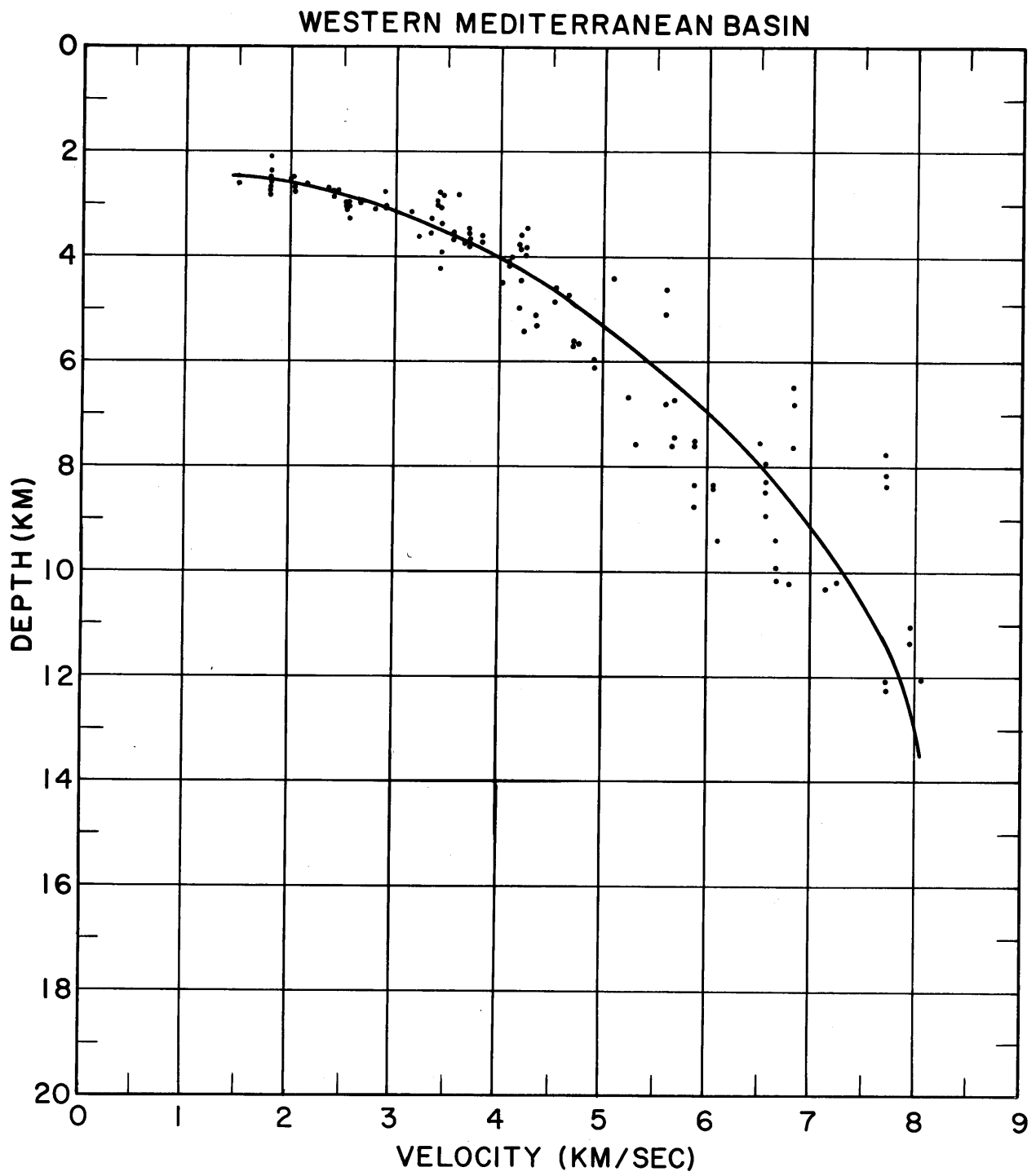


Figure 26. Velocity-Depth Structure - Western Mediterranean Basin

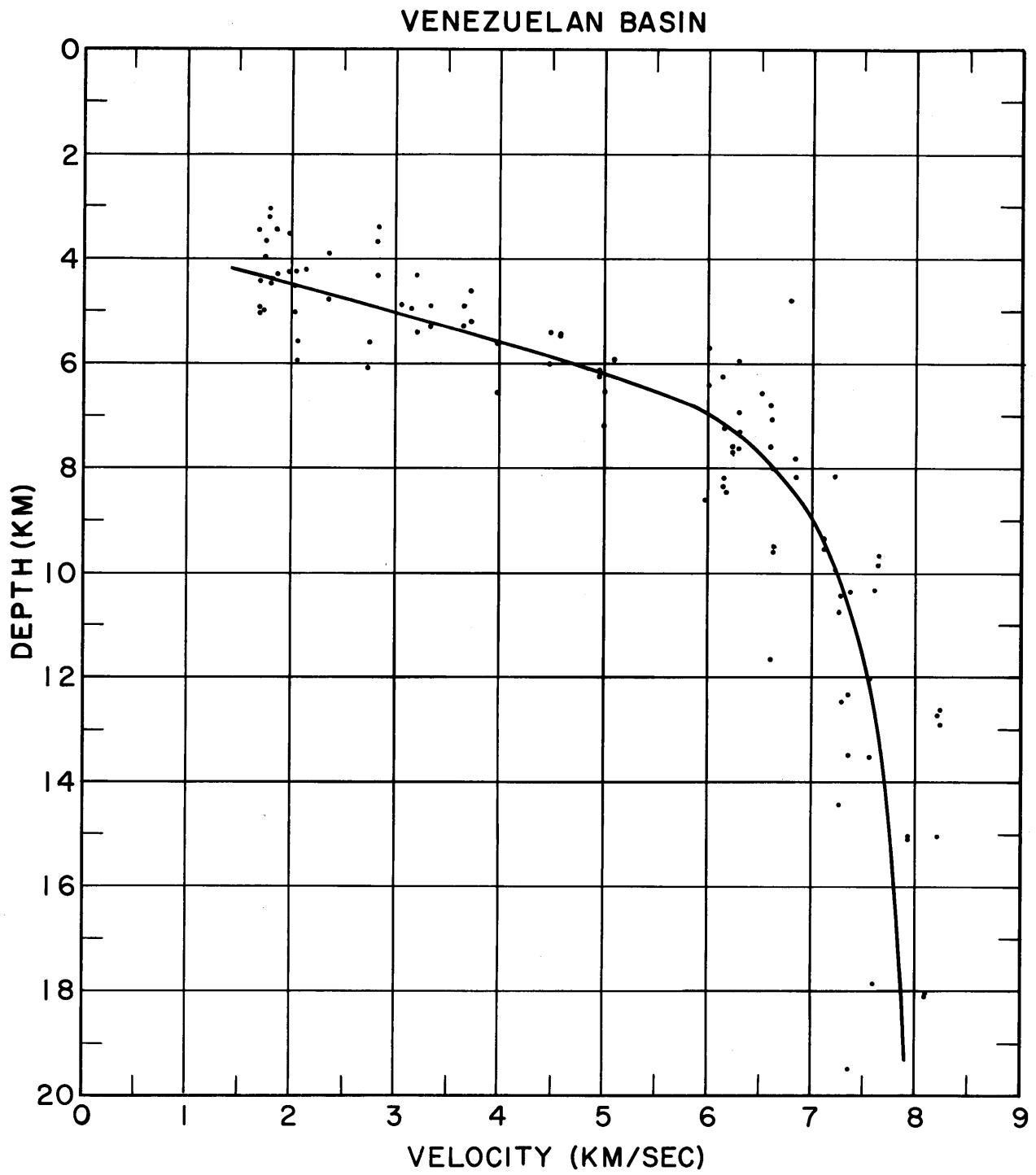


Figure 27. Velocity-Depth Structure - Venezuelan Basin

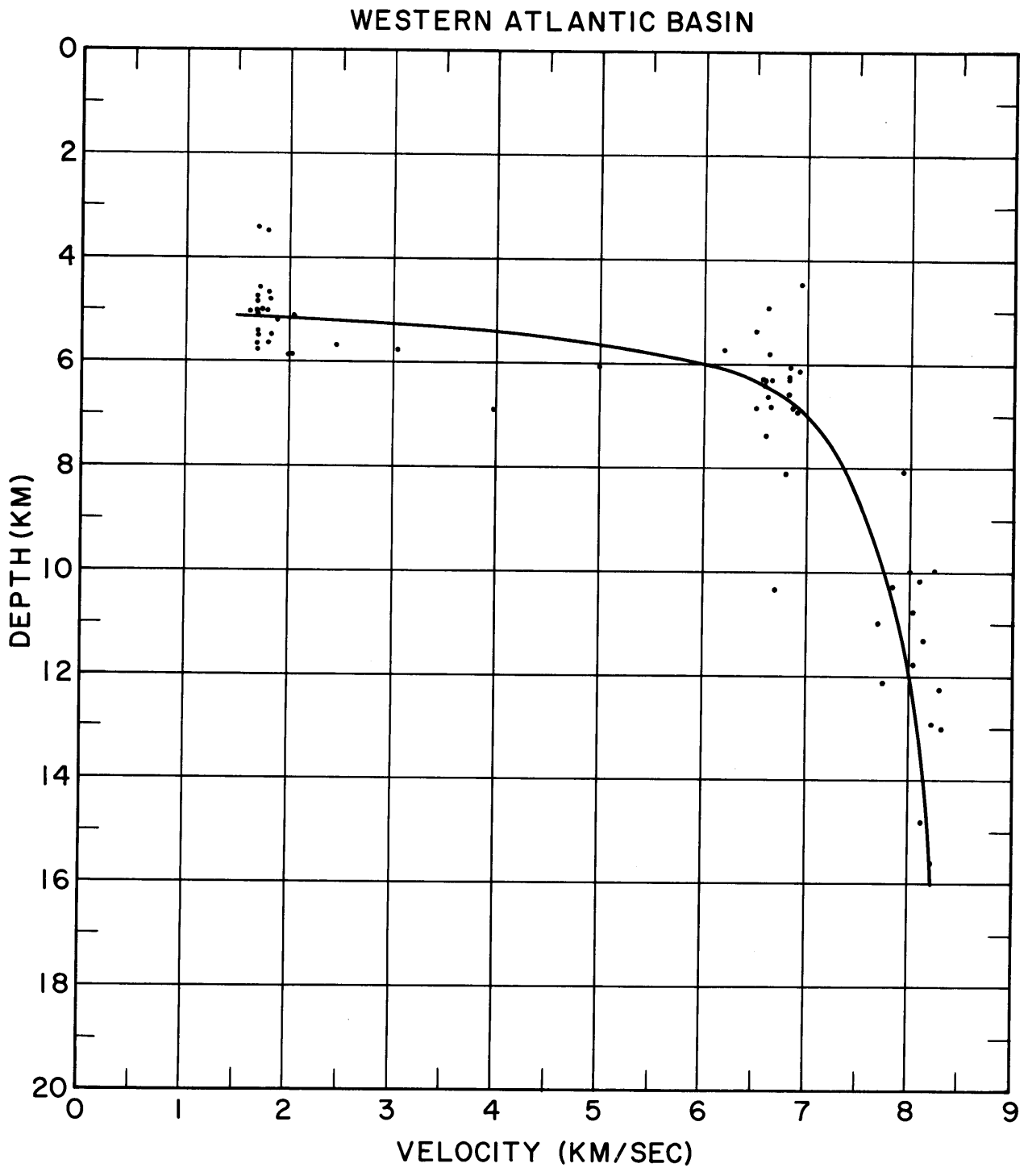


Figure 28. Velocity-Depth Structure - Western Atlantic Basin

CONTINENTAL EUROPE AND ASIA

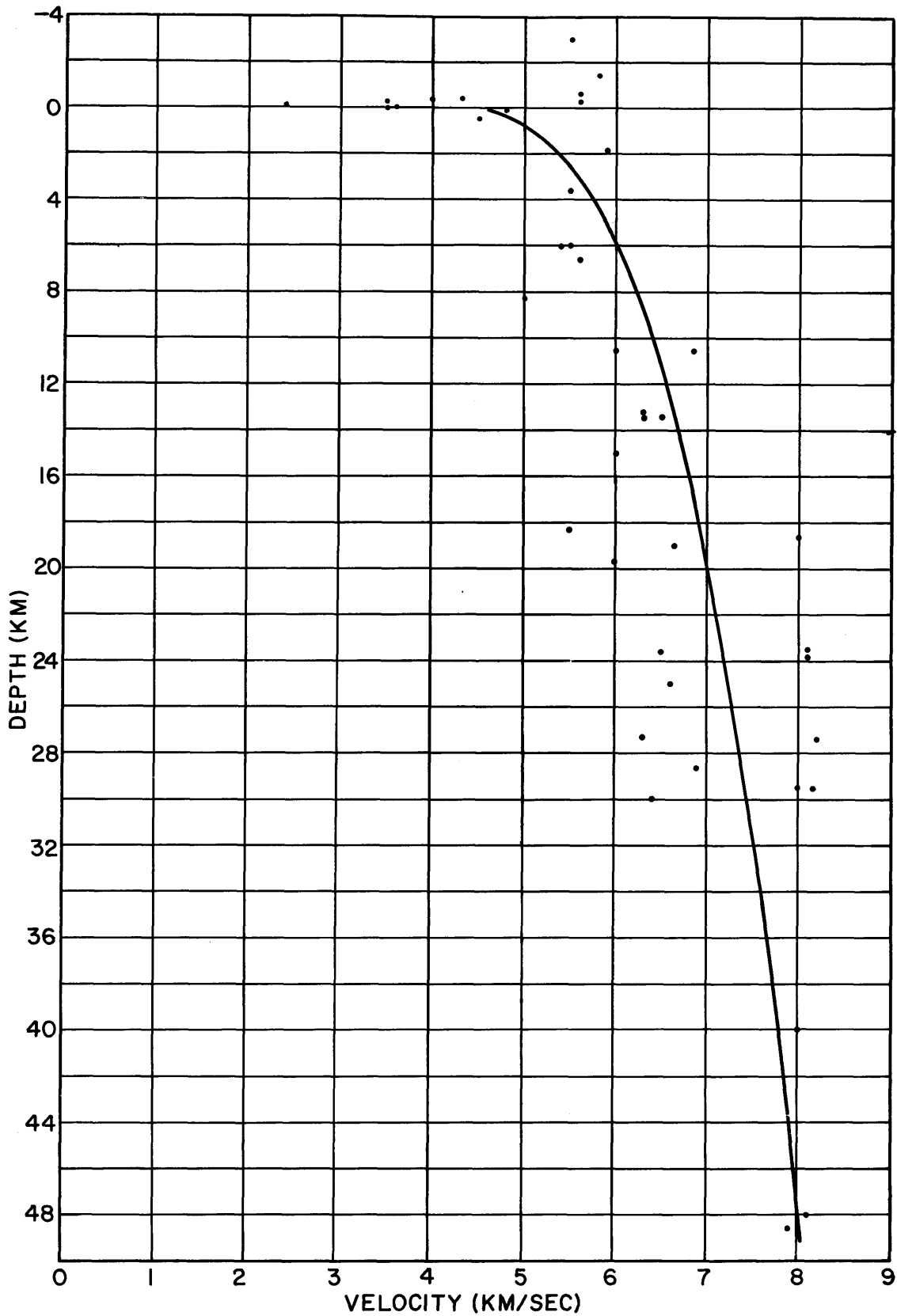


Figure 29. Velocity-Depth Structure - Continental Europe-Asia

COMPARISON OF CRUSTAL STRUCTURE

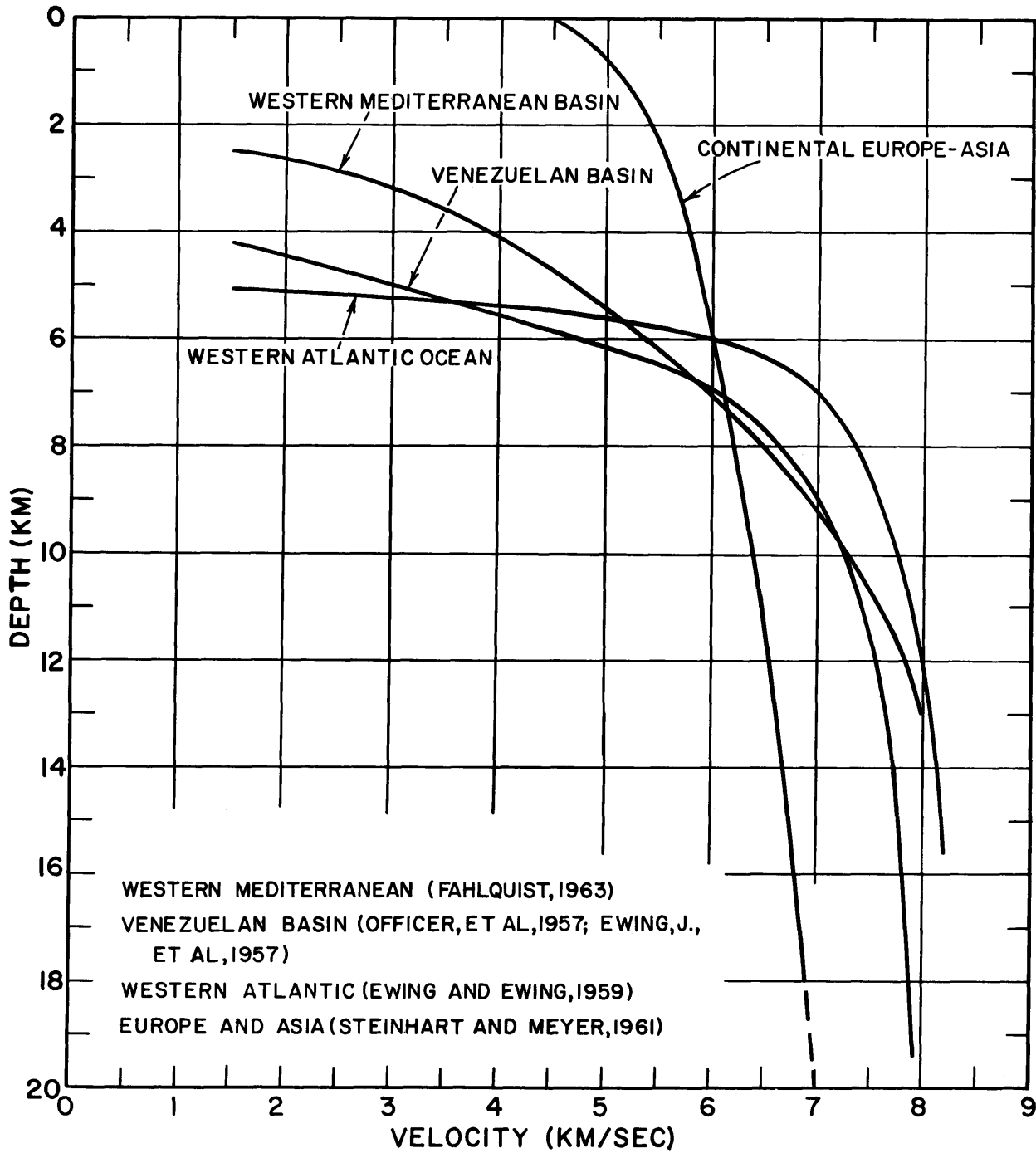


Figure 30. Comparison of Velocity-Depth Structure

in this velocity region.

The Venezuelan Basin curve shows a significantly lower velocity, 7.5 km/sec (12 km. depth), than measured at comparable depths in the deep ocean. Ewing, et al (1957) have suggested that the crust underlying the Venezuelan Basin is presently undergoing alteration from an oceanic to a continental type primarily by upward diffusion of lighter differentiates from the mantle; this process of alteration would lead to velocities less than those normally measured for mantle material.

The curves obtained for the western Mediterranean Basin strengthen the arguments for a close relationship between its structure and origin with that of the ocean basins. At the higher velocities the western Mediterranean curve more closely approaches that for the western Atlantic Basin than for the Venezuelan Basin. It mildly suggests but does not prove different processes of origin for the crust in these two regions of intermediate crustal structure.

Gravity Field

Woollard (1959) develops empirical relationships between crustal thickness and regional Bouguer gravity anomalies, and crustal thickness and surface elevation, and suggests that these relationships can be used to predict crustal thickness with reliability comparable to that

obtained in seismic measurements. Woollard's curves relating depth of the Mohorovicic discontinuity to both the regional Bouguer anomaly and to surface elevation are shown in Figure 31.

It is of interest to compare the crustal thickness obtained by seismic refraction measurement with independent results obtained from the gravity data. Published pendulum gravity measurements for the western Mediterranean region include studies by Pelissier (1939); Cassinis, et al (1934); Cassinis and dePisa (1935) and Vening Meinesz (1932). More recently Worzel (1959) has published several continuous gravity profiles made with the Graf meter in the region of the Strait of Gibraltar and in the Tyrrhenian Sea; these measurements, however, do not include data from the northern part of the western Basin in the region of the seismic data and will be excluded from consideration. Coster (1945) has discussed in detail the gravity field of the Mediterranean and has very conveniently compiled station locations and the measured free air anomaly values in a single table. The quality of the data is difficult to judge. The time base used in these early pendulum measurements were chronometers rated frequently against standard radio time signals. Non-linear drift in the chronometers could have introduced considerable errors; this seems to have been the case with at least two stations measured by Cassinis in the Tyrrhenian Sea which show large

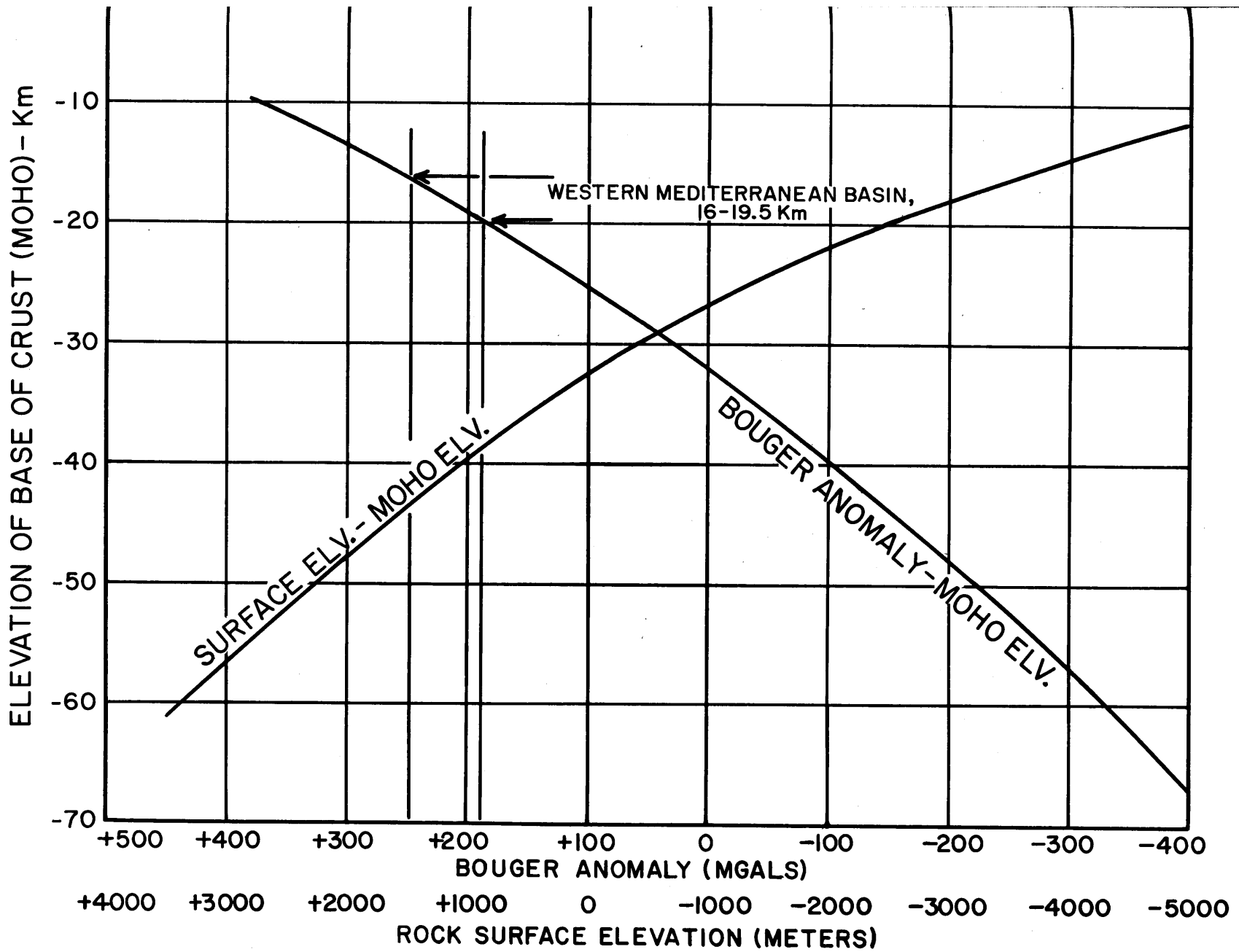


Figure 31. Depth to Mohorovicic Discontinuity as a Function of Bouguer Gravity Anomaly and Surface Elevation (Woolard, 1959)

discrepancies with the measurements of Worzel. Some idea of the consistency of the data can be obtained after computing and replotting the Bouguer anomalies.

To make the Bouguer correction it is necessary to convert the water layer to a layer of equivalent thickness of crustal rock materials. The density contrast between crust and water used in this computation was 1.80 (2.83-1.03) gm/cc. The water depths used in the computation were taken from the values shown by Coster (1945) on his chart. The station depths, particularly those near the margin of the basin, where water depth changes rapidly, may be subject to some error. (An error in depth of 100 meters is equivalent to an error of 7.4 mgals in the computed Bouguer anomaly.) This Bouguer correction is added to the free air anomaly to give the Bouguer anomaly.

$$\text{Bouguer Anomaly (sea)} = \text{Free air} + 2\pi\delta\rho h$$

$$\text{where } \delta = 6.67 \times 10^{-8} \text{ dyne cm}^2/\text{gm}^2$$

(Gravitational constant)

$$\rho = \text{density in gm/cm}^3$$

$$h = \text{water depth in cm}$$

The results of this computation are presented as a contour chart in Figure 32. The removal of the effect of water depth from the measured free air anomaly smooths the measured data markedly. The region

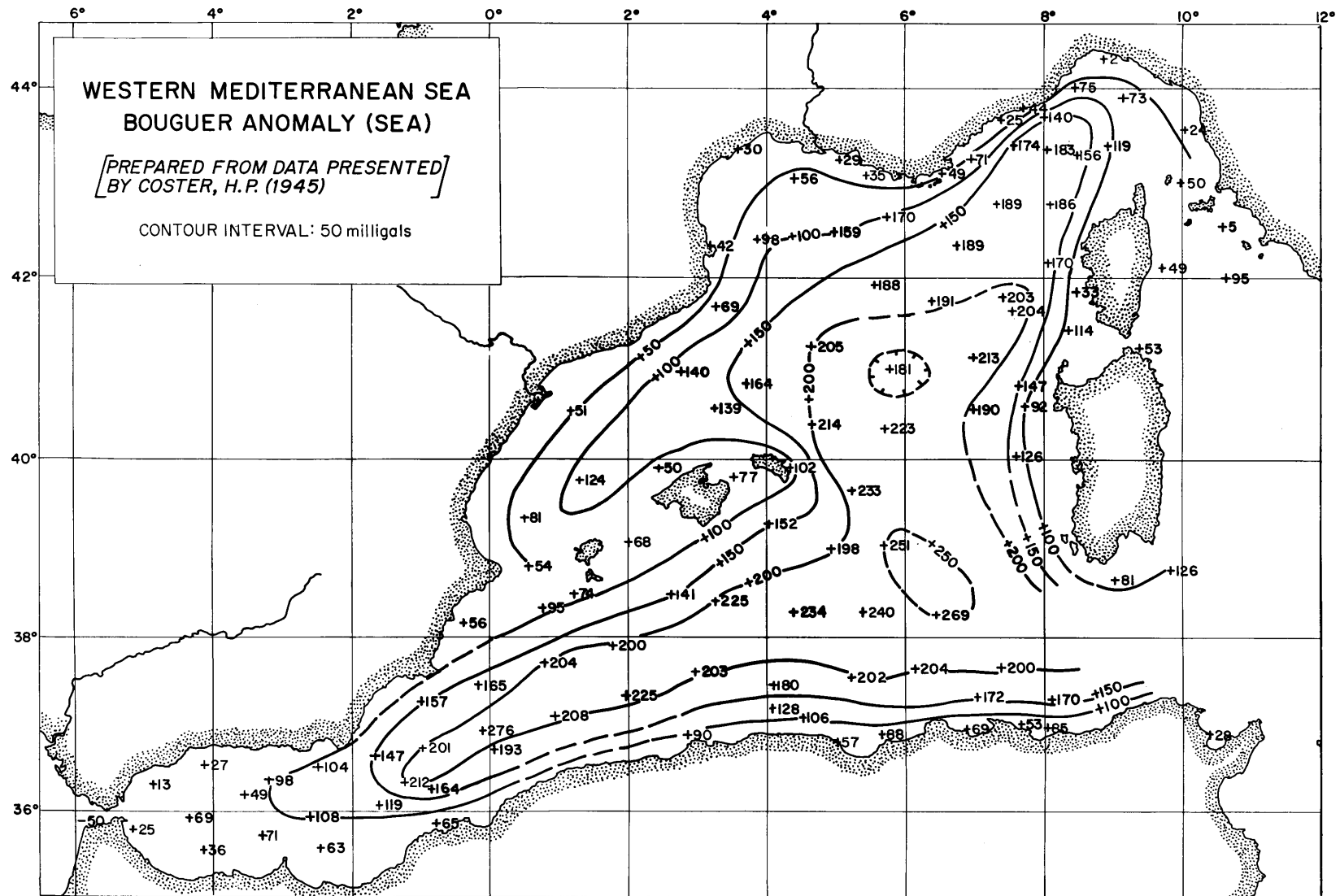


Figure 32. Gravity Field of Western Mediterranean Sea - Bouguer Anomaly

of high Bouguer anomaly ($> +150$ mgals) is nearly coincident with the abyssal plain. The central and south central portions of the Basin show anomalies of > 200 mgals. At the continental margins the anomaly decreases rapidly. Interpreted in terms of crustal thickness or depth to the M discontinuity the region of high anomaly would correspond to a thin crust and shallow mantle depth, the regions of decreasing magnitude to a thickening of the crust and increasing depth to mantle.

To a first approximation, then, the Bouguer anomaly agrees with the results of the seismic measurements, i. e., shallow mantle depths in the deeper portions of the basin and increasing depths to mantle as the margins are approached. The sharp increase in contour density to the south of France lends evidence to the conclusion drawn from the seismic results that the crustal thickening from the basin to the continent takes place in a very short lateral distance.

Referring once more to the curves presented by Woollard (1959) we can now compare the seismically determined mantle depth with that determined from the gravity data. A Bouguer anomaly of $+200$ mgal implies a mantle depth of 19 km.; that of 250 mgal, a depth of 16 km. (Figure 31). The seismic determinations give values of 12 to 14 km. for depth to the top of the mantle. The discrepancy between the sets of measurements is not insignificant, even allowing for a 10% scatter in the Bouguer anomaly-depth curve.

The gravity data do not appear to be grossly inaccurate; the data from four different expeditions when corrected for water depth present a generally consistent and smooth picture. Measurement errors of the order of 50 mgal are needed to restore the gravity data to values that yield the same results as the seismic measurements. Topographic corrections, especially those applied to stations in the center of the basin would alter the results very little. The region peripheral to the basin has been active in geologically recent time; the Alpine orogeny continued into the Miocene and gradual uplift has continued up to the present. This suggests that the region as a whole may not have reached isostatic equilibrium. Uplift of the basin itself is hard to rationalize with the postulated down faulting of the basin in the Oligocene. It seems more likely that the basin has been unable to adjust as rapidly as the continental blocks and that it is still out of isostatic equilibrium.

Hess (1955) computed the total mass in an oceanic and in a continental crustal column (1 cm^2 in area) down to a depth of 40 km. Using the available seismic data and reasonable estimates of the densities he obtained a mass of $11.8 \times 10^3 \text{ kg}$ for the oceanic crust and 11.7 to $11.9 \times 10^3 \text{ kg}$ for the continental crust. He concluded that the continental and oceanic crustal columns are nearly in balance. A comparison of similar computations for Profiles 195 and 5 with the Hess oceanic

section is made in Table 14 (see Appendix II for computations).

Table 14 Total Mass (to 40 km.)

	<u>Mantle Density (gm/cm³)</u>	<u>Total Mass (kg/cm²)</u>	<u>Deviation from Hess (Oceanic)</u>	
Hess (Oceanic)	3.325	11,842		
Profile 195	3.15	11,471	-371	3.1%
Profile 5	3.15	11,549	-293	2.5%
Profile 195	3.325	11,961	+119	1.0%
Profile 5	3.325	12,068	+226	1.9%

The measurements are critically dependent upon the density assigned to the mantle; the velocity of 7.7 km/sec measured on Profiles 195 and 5 leads to a mantle density of 3.15 gm/cm³, a value which is too low for an average mantle density. This density (3.15 gm/cc) in turn contributes strongly to making the western Mediterranean crustal section lighter than the Hess standard crust. The above computations are not sufficiently insensitive to the choice of mantle density to make them a good measure of isostatic equilibrium; the results for the western Mediterranean do not, however, indicate any radical departure from equilibrium.

The explanation does not lie in the interpretation of the seismic data. We have already noted the rather low mantle velocities, 7.7 - 7.8 km/sec, measured on Profile 195 and 5. A change in slope of the high velocity lines to yield an 8.0 km/sec velocity must necessarily

increase the time intercept at zero range on the travel time plot. This would lead to an increase in the thickness of the overlying 6.6 km/sec crustal layer. Although the present velocity lines shown on the travel time graph would seem to fit the travel time data best, a computation has been made for Sections 5.7, 5.8 in which the high velocity lines were altered to yield an approximate reverse velocity of 8.00 km/sec. The resultant layer thickness computations increased the depth to mantle by less than 1.0 km. at both ends of the profile. This increase in depth is insufficient to bring about agreement between the gravity and seismic data. Admittedly the two arrivals at ranges greater than 70 km. (Section 5.8) are weak, but three shots yielding well defined arrivals in the range 45-70 km. give confidence that no large errors are involved in the velocity determinations. The problem cannot be resolved until more extensive knowledge of both the gravity field and the seismically determined crustal structure have been obtained.

Theories of Tectonic Origin

The seismic refraction results indicate that the western Mediterranean Sea is floored by a thin crust. The occurrence of high velocity, high density material at depths of 10 to 12 km. and the presence of material of velocity 6.6 km/sec at shallower depths

on most of the basin profiles imply that the present crust of the Mediterranean has been derived from an older oceanic crust.

The Tethys Seaway, extending from the Himalayas through the Caucasus and Mediterranean region, began to approximate its present shape in the Carboniferous. The extension of the Tethys Seaway from the eastern Mediterranean into the western Mediterranean and the accompanying transgression began in the Permian (Brinkmann, 1960). From the Permian until the Miocene the crust underlying the present Mediterranean and its border regions was exceptionally mobile. Two comprehensive attempts to present a synthesis of the geologic evolution of the western Mediterranean have been made in recent years by Klemme (1958) and by Glangeaud and his students (Glangeaud, 1957; Caire, et al, 1960; Grandjacquet, et al, 1961; and Glangeaud, 1962). The two theories of evolution are summarized briefly below.

Klemme (1958) suggests that the Fennoscandian shield and the Afro-Arabian shield have grown outward to the south and north, respectively, by processes of continental accretion. The result of these processes has been the gradual encroachment of continental crust into the Mediterranean region; the European and African crustal blocks are now in direct contact or close proximity throughout the entire Mediterranean Sea area. On the basis of a series of

isopachous-lithofacies maps of the Circum-Mediterranean region, Klemme has suggested that the principal tectonic elements are: (1) Shield areas - essentially stable units of continental size; (2) Marginal troughs - miogeosynclines with dominant shallow water sediments grading into deep water sediments along the trough axis; (3) Geanticlines - platform areas of relatively thin deposition located outward from the axis of the marginal trough; (4) Internal troughs - narrow troughs, located in the internal parts of the Mediterranean and outward from the geanticline and marginal troughs, which collected thick deposits of sediments ranging from carbonates to clastics (graywacke, flysch, siliceous clays); and (5) Nuclei - uplifted areas of metamorphosed Paleozoic rocks including plutonic rocks and extensive volcanics which were source areas for the bulk of sediments deposited in the internal troughs. He maintains that some sediments were deposited at the margins of the nuclei next to the internal troughs; some of the nuclei later foundered to become sites of thick tertiary sedimentation. Outward migration of the marginal troughs and geanticline axes coupled with folding of sediments in the internal troughs (Rif-Betic Cordillera, Atlas, Pyrenees, Appenines, Alps) have permitted the continents of Europe and Africa to encroach from north and south upon the Tethys Seaway. The axes of the internal troughs (Triassic through the

Eocene) are now represented by the Late Tertiary mountain ranges encircling the western Mediterranean. Klemme suggests that most of the present western Mediterranean represented a nucleus, i. e., a source of sediment, during the Permian-Triassic time; the nucleus, for unspecified reasons, sank in the Late Tertiary.

Glangeaud (1957, 1962) has attempted to synthesize a complete structural evolution of the Mediterranean Sea encompassing both geophysical and geologic data. He suggests that the crust underlying the Paleozoic Tethys was oceanic in character. By the end of the Carboniferous the Hercynian mountain chains had been completely accreted to the cratonic shield areas and a single continuous continental land mass extended from northern Europe to well south of the Sahara. During the Permian and Triassic the Mediterranean region stood as an emerged continental land mass completely joining Europe and Africa. At the beginning of the Triassic, according to Glangeaud, the European and African continent pulled apart, the crust fracturing and/or thinning in a broad zone of rupture. This rupturing is accompanied by the marine transgression into the western Mediterranean in the Middle and Upper Triassic and by volcanism which had commenced in the Permian. He infers that the Mesozoic Tethys (the area of Profiles 194, 198 and 199) as a result would have been floored by a very complex crust, in places stripped of sialic material, in other places thinned or broken into blocks.

After the Triassic extension, the African-European blocks were far apart, and the intervening seaway (300 km. wide) was flooded by a dominantly simatic crust. Now follows the phase called by Glangeaud "tectorogene biliminnaire". Geanticlinal areas at the north and south margins of the rifted zone supplied sediments to the internal trough. Beginning in the Oligocene this internal trough was compressed, thrust up and outward to both the north and south forming the present Betic-Rif system. The Betic-Rif "tectorogene biliminnaire" was continuous to the south of Sardinia. In the Lower Miocene the compressive forces relaxed and the zone collapsed to become an area for the present day accumulation of sediments. Glangeaud suggests that the northern portion of the western Mediterranean, emerged during most of this time, also began to collapse in the early Miocene as the sea reinvaded the area.

The theories of Glangeaud require large lateral movements (rifting) as well as vertical movements; the ideas of Klemme do not seem to require such violent lateral tectonic movements. Both theories consider the northern part of the western Mediterranean to have been composed originally of a section of Mid-Paleozoic sialic rocks that were incorporated into the crust during the Hercynian orogeny.

Kuenen (1959) supports this concept. From studies of Cretaceous and Oligocene flysch deposits in the Maritime Alps (present coast of France and Italy between Menton and Genoa), he concluded that the source area for these deposits must have been to the south in the present Ligurian and western Mediterranean Seas. From studies of the age limits and volumes of these deposits he concludes that the land mass from which these sediments were derived must have been larger than the present Ligurian Sea. He further concludes that over 3000m of subsidence must have taken place here since the Oligocene.

The seismic data obtained in this present study reveal the presence of approximately 5 to 6 km. of rocks with intermediate velocities (3.5 - 5.0 km/sec) overlying the high velocity (6.6 km/sec) crust in the northern part of the western Mediterranean Basin at Profiles 195 and 5. These velocities appear to be too low to represent the Paleozoic basement complex (nucleus) suggested as existing in this region by both Klemme and Glangeaud. In addition, the thickness of these layers, up to 6 km. (over 18,000 ft.), suggests, if anything, that this was a zone of deposition in the geologic past. The thickness of the sediments alone is sufficient to discard this part of the Mediterranean as a nucleus in the sense used by Klemme.

Although the seismic data in the southern half of the basin are scant, an exceedingly thick section of material of velocity 3.5 to 5.25 km/sec is present to the southeast of Sardinia (Profile 194). Although no correlation has been attempted with the profiles further to the north, the results of Profiles 194, 198 and 199 suggest that the entire basin may include a similar section of material of common origin.

The measurement of high velocity (7.2 to 7.7 km/sec) material at shallow depth in the southern part of the basin is consonant with Glangeaud's ideas of rifting but the results do not in any way prove his theories. It seems likely that a complete north-south refraction line accompanied by continuous reflection records would detect the large scale tectonic movements postulated by Glangeaud.

Unresolved Problems

A downward displacement of approximately 3 km., perhaps more, in the northern part of the western Mediterranean Basin has been inferred from the seismic measurements presented in this paper. Furthermore, the morphology of the continental slope of Corsica and North Africa suggest that vertical movements, i. e., collapse, may be the dominant tectonic element in controlling the present structural configuration of the western Mediterranean. The fundamental causes of such vertical movements are little

understood. The near zero free air anomaly indicates approximate isostatic equilibrium today. It is difficult to imagine a state of isostatic equilibrium existing prior to the foundering of the basin floor (when its surface stood at or near sea level) without a corresponding change in density distribution in the underlying deep crust or outer mantle: it seems unreasonable that the thin crust (relative to the continent), even in compression, could have supported this uplift without fracturing. If the uplift was not compensated by density changes in the substrata, then forces other than those of isostasy must have played a dominant role in the tectonics of the area. The occurrence of deep "oceanic type" structure under the western Mediterranean argues against major changes in density occurring in the recent geologic past.

APPENDIX I

Profile Evaluations

A qualitative appraisal of the data shown on the travel time graphs (Figures 9 to 19) is made in the following section. The velocities discussed in this portion of the text refer to apparent velocities as measured directly from the travel-time graph.

Profile 193: ATLANTIS (SW) - VEMA (NE) (Figure 9).

Two velocities, 4.36 and 7.28 km/sec have been measured by ATLANTIS (SW) and are well established by first arrival evidence. Velocities of 3.92 and 6.96 km/sec are similarly well established at VEMA (NE). The reverse points for the higher velocity lines are in excellent agreement, but reverse points for the low velocity lines differ by 0.75 seconds. The profile has therefore been computed as two independent unreversed stations.

The two shooting ship tracks do not show comparable topography. The northeast end of the ATLANTIS shooting track crosses two hills having 180 meters (100 fathoms) of relief. The topography suggests complexity in the geologic structure of the shallower layers sufficient to account for the extreme disagreement in reverse points for the low velocity lines.

All arrivals have been topographically corrected to the base line shown on the bathymetric profile (Figure 9). The corrections

have been made for differences in water path only; i. e., bottom topography has been assumed to exist in all the deeper layers.

Profile 194: ATLANTIS (Figure 10). Profile 194 is an end to end profile received by ATLANTIS. Water depth along the profile is uniform at 2840 meters (1553 fathoms).

The 2.66 km/sec velocity (NW) is well established on the basis of good first arrivals in the range interval 4 to 6.5 seconds. The identification of the corresponding velocity to the southeast of the receiving position is based on two excellent first arrivals and several second arrivals.

The 3.89 km/sec velocity (SE) is determined by measured first arrivals recorded on 10 shots extending over 8 seconds of range. The 3.44 km/sec velocity is adequately determined.

The existence of the 5.29 - 5.23 km/sec velocity is established by first arrival evidence on the northwest segment of the profile. This layer is masked to the southeast where only fair second arrival evidence is present.

The evidence for the existence of a velocity slightly greater than 7.00 km/sec is good. However, the shot lines, both to the northwest and southeast, are too short to establish this velocity with the same confidence as the lower velocities.

Profile 195: ATLANTIS (S) - VEMA (N) - (Figure 11). The water depth along the section increases from 2430 meters (1329 fathoms) at VEMA (N) to 2630 meters at ATLANTIS (S); the bottom slopes 0.32° toward the south.

A layer of velocity 2.03 km/sec based on second arrival evidence is established at the ATLANTIS (S) end only. A velocity of 2.01 km/sec has been assumed for the VEMA (N) end of the profile. The 2.88 km/sec velocity is moderately well established by second arrivals recorded by VEMA (N); evidence for the corresponding velocity at the ATLANTIS (S) end of the profile is poor. Five arrivals recorded over the range 4.5 - 6.5 seconds and a single weak arrival at a range of approximately 9 seconds have been used to establish the 2.93 km/sec velocity line.

The 4.18 - 4.19 km/sec horizon is well established by excellent first arrival evidence at both the north and south ends of the profile.

The 4.91 km/sec and 4.93 km/sec velocities measured respectively by VEMA (N) and ATLANTIS (S) are well established. First arrivals were recorded by VEMA over the range 12 to 18 seconds and by ATLANTIS over the range 11 to 16 seconds. Second arrivals associated with the 4.93 km/sec velocity line were recorded by ATLANTIS at shorter ranges (7 to 11 seconds). In this range interval the first

arrivals identified with the 4.20 km/sec velocity line are characteristically weak and poorly defined. The second arrivals associated with the 4.93 km/sec velocity are clearly identified by a very strong initial pulse followed by a second strong pulse delayed in time by the appropriate bubble pulse interval. A line drawn through these arrivals (dashed on the travel time graph) yields a velocity of 4.86 km/sec as compared with the 4.93 km/sec line previously mentioned. The 4.93 km/sec velocity line with an intercept of 4.70 seconds has been used in the final computations.

The 6.63 km/sec velocity is clearly defined by both first and second arrivals at ATLANTIS (S). First arrivals establishing the 7.76 km/sec velocity appear at a range of 24 seconds. The last four shots show strong arrivals on this high velocity line. The 6.66 km/sec horizon is poorly established at VEMA (N). The line, dashed on the travel time graph, has been drawn using the reverse point obtained by ATLANTIS and assumes that refractions from this layer are masked and never seen as a first arrival. Several second arrivals received at ranges greater than twenty seconds can be associated with this velocity. The 7.70 km/sec velocity recorded by VEMA (N) is well defined.

Profile 196: ATLANTIS (S) - VEMA (N) - (Figure 12). The northern section of the profile (196. 1, 196. 2), 36 kilometers in length, is reversed; the southern portion of the profile (196. 3), unreversed, is approximately 24 kilometers in length and was recorded by ATLANTIS as VEMA opened range toward the south. Water depth varies from 1,280 meters (700 fathoms) at the north to 1360 meters (749 fathoms) at the south.

The lowest velocity measured is 2.08 - 2.10 km/sec on the northern reversed section of the profile; the corresponding velocity measured by ATLANTIS on 196. 3 is 2.14 km/sec. The velocity line is moderately well determined over short ranges (up to 8 seconds) on the VEMA records (196. 1) and the ATLANTIS unreversed section (196. 3), although, with the exception of a single first arrival recorded by VEMA, this velocity determination is based entirely on second and later arrivals. No refraction arrivals were obtained at ranges of less than 8 seconds on the southern section of the reversed profile (196. 2). It is possible that arrivals from the low velocity horizon are masked in this region by multiple refraction arrivals from a high velocity layer.

Good second arrival evidence for the layer having apparent velocities ranging from 3.00 to 3.12 km/sec is obtained on all three sections of the profile.

The determination of the 3.81 - 3.89 km/sec velocities is based on three first arrivals recorded by VEMA and a series of second arrivals showing considerable scatter recorded by ATLANTIS. Evidence for this velocity on the unreversed portion (196.3) of the profile is poor.

The dominant features of the travel time graphs are the 5.84, 5.80 and 5.48 km/sec velocities measured respectively on sections 196.1, 196.2 and 196.3. These velocities are established by first arrivals over the entire profile at all ranges greater than 5 seconds. The reverse points for 196.1, 196.2 are in excellent agreement, but the zero intercepts for the 5.46 - 5.80 km/sec lines measured by ATLANTIS (end to end) disagree by 0.35 seconds. Sections of the highest velocity line are offset by 0.15 to 0.20 seconds. This feature has been noted by the inclusion of dashed lines on the travel time graph indicating the approximate delays in the arrival times over portions of the profile.

Profile 197: ATLANTIS (S) - VEMA (N) - (Figure 13). The bottom topography along this profile shallows from 950 meters (520 fathoms) at the north to 770 meters (420 fathoms) at the south. Reverse points for the high velocity lines differ by 0.31 seconds and those of the lower velocity lines show an even greater discrepancy.

Two velocities, 1.80 km/sec and 3.49 km/sec, have been measured at VEMA (N) on the basis of second or later arrival evidence only. A velocity of 3.70 km/sec, again based on second arrival evidence, has been measured by ATLANTIS (S).

The 4.71 km/sec velocity obtained at the north end of the profile is well established. The corresponding velocity measured by ATLANTIS (S) is 4.76 km/sec. The arrivals establishing this velocity show considerable scatter on the travel time plot.

The highest velocities measured are 6.85 km/sec at ATLANTIS (S) and 6.58 km/sec at VEMA (N). The VEMA data are excellent; the ATLANTIS determination is only fair.

Profile 198: ATLANTIS (SW) - VEMA (NE) (Figure 14).

Profile 198 is a reversed profile located in a uniform water depth of 2750 meters (1504 fathoms).

The lowest velocity measured is 3.46 km/sec. This measurement is based on two good first arrivals and several second arrivals recorded by ATLANTIS (SW) and extending over 14 seconds of range. The corresponding velocity line at VEMA (NE) is poorly determined by second or third arrival evidence; consequently the line has been dashed on the travel time graph.

Three velocities have been measured by VEMA (NW). These velocities 4.24 km/sec, 5.54 km/sec, and 6.67 km/sec, are all

based on excellent first arrival evidence. The corresponding velocities measured by ATLANTIS (SW) are 4.28 km/sec, 5.66 km/sec, and 6.98 km/sec. The 6.98 km/sec velocity is clearly defined by first arrival evidence. The 4.28 km/sec velocity line includes two first arrivals and several possible second or later arrivals. Excellent sub-bottom reflections were obtained from the top surface of the 4.24 - 4.28 km/sec layer at short ranges at both the VEMA and ATLANTIS ends of the profile. These reflection arrivals provide strong additional evidence for the existence of the 4.28 km/sec velocity horizon measured by ATLANTIS on only fair refraction data. The 5.66 km/sec velocity (SW) is established primarily by the VEMA reverse point (5.44 km/sec) and a few first arrivals at ranges of 9 to 12 seconds from ATLANTIS. The region where first arrivals might be expected from this horizon (7.5 to 12 seconds) is complicated by evidence of structure in the underlying layer. This structure may also be present in the 5.66 km/sec velocity layer and for these reasons it has not been possible to make an unambiguous interpretation of the travel time graph in this region.

Offsets of 0.23 to 0.25 seconds appear on both ATLANTIS and VEMA high velocity lines, 6.67 and 6.98 km/sec. The offset segments do not reverse. The navigation plotted for the two shooting tracks shows that although parallel, the tracks have four to five miles

separation. Both ATLANTIS and VEMA drifted about four miles to the west during their respective recording periods. This inability to duplicate exactly the same shooting track along the profile may account for the fact that the offsets in the high velocity lines do not reverse.

Profile 199: ATLANTIS (E) (Figure 15). This is an unreversed profile recorded by ATLANTIS. The bottom shoals gradually from 2084 meters (1140 fathoms) at the east end of the profile to 1884 meters (1030 fathoms) at a range of 33 kilometers toward the west. It then shallows abruptly to 1152 meters (630 fathoms) and then gradually deepens again to 1829 meters (1000 fathoms) at the west end of the profile.

The refraction arrivals have been corrected for topography to the base line shown on the bathymetric profile (Figure 15); the surface topography was assumed to be reflected in all layers. The corrections affect only the last few arrivals from the deepest refraction interface; the scatter in these arrivals is appreciably reduced by the correction.

Three velocities, 2.92 km/sec, 5.10 km/sec, and 7.70 km/sec are all well determined.

Profile 2: WINNARETTA SINGER - CHAIN (Figure 16).

Section 2.1: WINNARETTA SINGER - (unreversed). The 3.60 km/sec velocity, the lowest velocity measured on the section is well determined by first arrival evidence. At a range of 8 seconds, arrivals from this layer become exceedingly weak; strong second arrivals, noted in this same region, are associated with the 4.21 km/sec velocity line. The second arrivals and several first arrivals define the 4.21 km/sec velocity; excellent first arrival evidence for this velocity is found on the adjoining section, 2.2. The 5.66 km/sec velocity is established by good first arrival evidence over the last 6 kilometers of the profile. The 6.77 km/sec layer is identified by only second arrival evidence, but strong evidence for the existence of this layer is found on the long reverse, Sections 2.7, 2.8.

Sections 2.2, 2.3: WINNARETTA SINGER (NW) - CHAIN (SE). Three velocities, 3.39 km/sec, 4.18 km/sec, and 5.67 km/sec have been determined on the basis of first arrival evidence. The corresponding reverse velocities measured by CHAIN (SE), 3.32 km/sec, 4.00 km/sec, and 5.67 km/sec, although determined on the basis of somewhat less dense shot spacing, are also well established. The 6.69 km/sec velocity measured on Section 2.2 is based only on second arrivals; supporting evidence for the present interpretation is found on Sections 2.7, 2.8. The reverse

points for Sections 2. 2, 2. 3 are in disagreement by approximately 0. 3 seconds; the reverse points for Section 2. 3 are consistently higher than those on Section 2. 2. The evidence strongly indicates that this delay in the travel time on Section 2. 3 is localized in the region of the receiving position for this profile. The sections to the east are markedly different in character from Section 2. 3. The topographic rise of approximately 365 meters (200 fathoms) already noted begins just to the east of the receiving position for Section 2. 3.

Sections 2. 4, 2. 5: CHAIN (NW) - WINNARETTA SINGER (SE). At the conclusion of Section 2. 3, the shooting program was interrupted for several hours in order to resupply the WINNARETTA SINGER with explosives and to repair electronic equipment. The drift during this period of time accounts for the marked difference in receiving positions for Section 2. 3 and 2. 4.

Three velocities, 3. 28 km/sec, 4. 61 km/sec, and 5. 86 km/sec were measured by CHAIN (NW). The high velocity line, 5. 86 km/sec, is based on first arrivals recorded over almost the entire length of the profile. Arrivals on this line show consistent delays of slightly more than 0. 20 seconds for all shots recorded at ranges greater than 9 seconds. The 4. 61 km/sec velocity is poorly determined on this end of the profile; evidence for this velocity is limited to second arrivals. However, a velocity of 4. 58 km/sec

is well determined by WINNARETTA SINGER (Section 2.5) and supports the above interpretation of Section 2.4.

Three velocities, 3.17 km/sec, 4.58 km/sec, and 6.13 km/sec have been measured by WINNARETTA SINGER on Section 2.5. The high velocity line, 6.13 km/sec, shows a delay of 0.19 seconds for those shots fired at ranges of less than 11.5 seconds from WINNARETTA SINGER. The offset point in the two segments of the high velocity line on Sections 2.4, 2.5, reverse each other; the travel time delays in both sections are due to the same structure. The 4.58 km/sec velocity determination is excellent.

The topography noted at the western end of Sections 2.4, 2.5 may be related to the structure indicated by the well-defined offsets in the high velocity lines measured at both ends of the profile. Similar structure may be present in the lower velocity layers but the present seismic evidence is inconclusive. The CHAIN receiving position is poorly located for detailing this structure in the upper layers. The scatter in the data points defining the 3.28 km/sec velocity measured by CHAIN may be an indication of complexity in the shallow layers.

Section 2.6: WINNARETTA SINGER. Section 2.6 is the easternmost section of Profile 2. The 3.42 km/sec and 6.41 km/sec velocities are well determined, although the high velocity line shows

considerable scatter in the data points. A poorly determined 4.67 km/sec velocity is also shown in the travel time graph. Evidence for this velocity is based on a few second arrivals and the adequate determination of a layer of comparable velocity on Section 2.5. The zero intercepts for the 6.13 km/sec and the 6.41 km/sec lines on Sections 2.4 and 2.5 are in disagreement by more than 0.30 seconds; this is a further indication of structural complexities unresolved by the seismic data.

Sections 2.7, 2.8: WINNARETTA SINGER (NW) - WINNARETTA SINGER (SE). The receiving positions for Sections 2.7, 2.8 coincide approximately with the end point of Section 2.1 and the receiving positions for Sections 2.5, 2.6. The profile is approximately 90 kilometers long.

Three lower velocities measured on Section 2.7, 3.43 km/sec, 4.40 km/sec, and 5.61 km/sec, agree well with the velocities obtained on Sections 2.1 and 2.2.

On Section 2.8 (SE), a 5.14 km/sec velocity is well determined. The 6.74 km/sec velocity is established on the basis of two strong first arrivals and a good second arrival. No indications of a higher velocity were noted. The corresponding velocity of 7.10 km/sec on Section 2.7 is based on two possible first arrivals, two excellent second arrivals, and two poor second arrivals recorded on the last

two shots.

The evidence for the 8.05 km/sec velocity shown on Section 2.7 is excellent; however, no evidence for this velocity was obtained on Section 2.8.

Profile 3: WINNARETTA SINGER - CHAIN (Figure 17).

Section 3.1: WINNARETTA SINGER (unreversed). The sea floor slopes 3.79° to the southwest along this section. The two velocities, 4.13 km/sec and 6.41 km/sec, are well established by first arrival evidence. These velocities are unreversed and are considerably higher than the reversed velocities measured on the adjoining Sections 3.2, 3.3.

Sections 3.2, 3.3: WINNARETTA SINGER (NW) - CHAIN (SW). This reversed profile is made over bottom topography sloping 4.03° upward toward the southeast. The two velocities measured on Section 3.2 are 4.03 and 7.02 km/sec. The 4.03 km/sec line is based on excellent first and second arrival evidence. The 7.02 km/sec line is also well determined. The corresponding velocity lines measured on Section 3.3 are 3.00 and 4.29 km/sec. After completing the topographic corrections the reverse points are in excellent agreement for both lines. The large disparity in magnitudes of the pairs of apparent velocities 3.00 and 4.03 km/sec and 4.29 and 7.02 km/sec, indicate that the refracting horizons approximately

parallel the bottom topography. The bottom slope accounts for the large disparity in the measured apparent up-dip and down-dip velocities.

Sections 3.4, 3.5: CHAIN (NW) - WINNARETTA SINGER (SE). This profile was made over a bottom sloping approximately 2° to the southeast. Velocities of 2.10 km/sec, 3.00 km/sec and 4.71 km/sec were measured by CHAIN (NW). The 2.10 km/sec velocity is established by excellent first arrival evidence and a few second arrivals. This is the only section of Profile 3 on which this low velocity was detected. The receiving position for Section 3.4 is located at less than 1200 meters (656 fathoms) water depth, the shallowest depth occurring at any receiving position on Profile 3. The shallow water depth here is more favorable for the measurement of low velocities associated with the upper sediment layers than elsewhere along the section.

Two velocities, 3.31 km/sec and 6.31 km/sec, were measured by WINNARETTA SINGER (SE), the latter velocity established by excellent first arrival evidence.

A velocity of 2.24 km/sec (dashed line) was assumed for the overlying sediment layer to reverse the 2.10 km/sec velocity measured on Section 3.4.

Profile 3.6: WINNARETTA SINGER (unreversed). The bottom shallows to the southeast along this profile and has a slope of 2.43° . A velocity of 2.58 km/sec was measured on the basis of only second arrival evidence. The 3.78 km/sec and 6.77 km/sec velocity lines are well determined.

Sections 3.7, 3.8: WINNARETTA SINGER (NW) - WINNARETTA SINGER (SE). The shots at ranges greater than 16 seconds on Section 3.7 and all shots on 3.8 were 300# depth charges. The velocities measured on Sections 3.7 and 3.8 are 5.86 km/sec and 5.76 km/sec respectively. No higher velocity was measured on this profile. The last shot on Section 3.8, at a range of 35.3 seconds, shows a strong arrival 0.30 seconds earlier than expected for the 5.86 km/sec line. This is the only evidence of an arrival possibly associated with a higher velocity obtained in this section. Again the topographic corrections for this profile appreciably reduced scatter in the data points. However, the reverse points disagree by 0.40 seconds.

Profile 4: WINNARETTA SINGER - CHAIN (Figure 18).

Section 4.1: WINNARETTA SINGER (unreversed). The lowest velocity measured on Section 4.1, 2.38 km/sec, is established by fair second arrival evidence only. The 3.16 km/sec

velocity is moderately well determined by both first and second arrivals. To the southeast on Section 4. 2 a comparable velocity, 3. 36 km/sec, was measured on the basis of much stronger evidence. The zero range intercepts for the adjoining profiles, Sections 4. 1 and 4. 2, agree very well. Beyond a range of 6. 5 seconds, a few first arrivals lie on a line having a velocity of 4. 19 km/sec; these arrivals cease abruptly at a range of eight seconds. The measurement of the 4. 19 km/sec velocity line is only poor, but evidence for a comparable velocity is considerably stronger on Sections 4. 2, 4. 3. Two good sub-bottom reflections, possibly from this refracting interface, provide additional supporting evidence for the existence of this layer. The evidence for the 6. 50 km/sec layer consists of three good arrivals at the extreme end of the profile. Evidence for a layer of this velocity would be extremely weak on the basis of data presented in this short profile, but its existence is confirmed on the long reverse profile, Sections 4. 7, 4. 8.

Sections 4. 2, 4. 3: WINNARETTA SINGER (NW) - CHAIN (SE). The reversed Profile 4. 2, 4. 3 abuts and lies southeast of 4. 1; it extends to a range of approximately 18 seconds.

The lowest velocity measured on Section 4. 2 is 2. 49 km/sec and is established by second arrival evidence on only a few shots. The corresponding velocity on Section 4. 3, 2. 42 km/sec, is also

established by second arrival evidence only. The next higher velocities measured on Sections 4. 2 and 4. 3 are 4. 22 km/sec and 4. 13 km/sec respectively. The 4. 13 km/sec velocity line is established by good first arrival evidence. Data establishing the 4. 22 km/sec line is poor. No arrivals are found for this velocity line in the range 12 to 14 seconds where it should be seen as a first arrival. The reason for this is not known.

Evidence for the 6.01 and 6. 10 km/sec velocities is good when supplemented by the evidence from the longer reversed profile, Sections 4. 7, 4. 8.

Sections 4. 4, 4. 5: CHAIN (NW) - WINNARETTA SINGER (SE). The velocities obtained on Sections 4. 4, 4. 5 are similar to those velocities already described for Section 4. 3. The lowest velocities measured, 2. 44 km/sec and 2. 33 km/sec, on Sections 4. 4, 4. 5, are based entirely on second arrivals. Along the entire profile the surface of this layer nearly coincides with the sea floor.

The next higher velocities, 3. 43 km/sec and 3. 46 km/sec, are based on good first and second arrival evidence. On Section 4. 5 first arrivals on this velocity line extend over the range 4 to 7. 5 seconds. The evidence on Section 4. 4 is not as well defined as on Section 4. 5. The 3. 43 km/sec horizon is underlain by 4. 06 km/sec material. The velocity contrast is low between these two horizons and it is difficult to separate these two velocities definitively; a single line would give

a reasonable fit to all the points. On Section 4.5 the 3.46 km/sec horizon is underlain with material having a velocity of 4.48 km/sec. Here the evidence clearly supports the interpretation of two distinct layers in this velocity range. The interpretation of Section 4.4 is therefore supported by the evidence found on Section 4.5.

Fairly good second arrival evidence and a few first arrivals at the extreme end of the profile define a velocity of 5.73 km/sec on Section 4.5. The corresponding velocity measured on Section 4.4 is 6.07 km/sec but is based on only a few second arrivals. Evidence on Section 4.7 supports this interpretation.

Section 4.6: WINNARETTA SINGER (unreversed). Section 4.6 is the only profile along this section showing good first arrival evidence for a velocity in the range 2.3 to 2.4 km/sec. A velocity of 2.35 km/sec is measured on Section 4.6. The underlying 3.23 km/sec layer was measured by second arrival evidence only. The evidence for the 4.54 km/sec layer is excellent. Three possible arrivals from the 6.43 km/sec layer are present; this velocity line has been dashed to indicate its speculative nature.

Sections 4.7, 4.8: WINNARETTA SINGER (NW) - WINNARETTA SINGER (SE). A mantle velocity of 7.99 km/sec is measured on Section 4.8. The determination is excellent. The comparable line on Section 4.7 is poorly determined and has been dashed on the

travel time graph. Two shots, both 300# depth charges, fired at ranges of 24 and 32 seconds, give no indication of arrivals from the mantle. However, a shot fired at 41 seconds shows energy arriving well before it would be expected from the overlying layer, but the signal level is weak and the initial onset of the wave train cannot be picked.

The 2.38, 3.23, and 4.25 km/sec velocities, although based on relatively few shots, are in excellent agreement with the results obtained on Sections 4.1 and 4.2. The 6.07 km/sec velocity is well determined on Section 4.7.

Profile 5: WINNARETTA SINGER - CHAIN (Figure 19).

Section 5.1: WINNARETTA SINGER (unreversed). Two velocities, 3.66 km/sec and 4.74 km/sec, are established by excellent first arrival evidence. The two lower velocities, 2.15 km/sec and 2.79 km/sec are established by second or later arrival evidence only. Two strong second arrivals have been placed on a line having a velocity of 6.10 km/sec; the velocity line is dashed to indicate some degree of doubt in the identification of these arrivals. A comparable velocity is well established on Sections 5.7, 5.8.

Sections 5.2, 5.3: WINNARETTA SINGER (NW) - CHAIN (SE). Velocities of 3.63 km/sec and 4.70 km/sec are established by first arrival evidence at WINNARETTA SINGER (NW). The comparable

velocities measured at CHAIN (SE) are 3.48 km/sec and 4.71 km/sec. The 3.48 km/sec velocity line, although almost masked by the 4.71 km/sec line, includes two good first arrivals in addition to the second arrival evidence.

In the range 7 to 9.5 seconds the arrivals associated with the 4.70 km/sec line (Section 5.2) appear consistently early by as much as 0.35 seconds. This sag in the travel time curve has been interpreted as the result of local structural changes in the neighborhood of the shot points. The corresponding velocity line (4.71 km/sec) on Section 5.3 is extremely well determined and shows no pronounced scatter nor early arrivals. The inference is clear, however, that energy originating from shots in this region of Section 5.2 has either traveled through higher velocity material along a portion of its path or that the path length itself is shorter. A similar effect is probably present in the 3.63 km/sec line. There is, in addition, evidence of a slight topographic rise in the middle of Section 5.2 as shown by the CHAIN echo-sounding profile. The echo-sounding profile for 5.3 shows no similar topographic feature. This undulation in the topography may very well be a surface expression of the structural complexity beneath the bottom as inferred from the seismic data.

The 2.58 km/sec (NW) and 2.52 km/sec (SE) velocity lines

are entirely based on second or later arrivals. The evidence for this horizon is excellent on the adjoining profile, Section 5. 4, and the determination is therefore considered good. No evidence for a lower velocity has been found by WINNARETTA SINGER (NW); CHAIN (SE) obtained a few late arrivals in the range 6 to 7. 5 seconds which establish a velocity of 2. 01 km/sec. A velocity line of 2. 09 km/sec, reversing the 2. 01 km/sec measurement, has been dashed on the travel time graph of Section 5. 2.

The 6. 36 km/sec (SE) and 6. 79 km/sec (NW) velocity lines are based on a few arrivals obtained from shots fired at the extreme ends of the profile. The establishment of these velocities on the strength of the evidence acquired on the short profiles alone is questionable. However, the existence of this horizon is extremely well determined on the long reverse profile, Sections 5. 7, 5. 8.

Sections 5. 4, 5. 5: CHAIN (NW) - WINNARETTA SINGER (SE). The lowest velocity measured by WINNARETTA SINGER (SE) is 2. 04 km/sec. Existence of this line is based entirely on late arrival evidence at short ranges. The corresponding velocity at the northwest end of the profile, 2. 00 km/sec, has been assumed. A few weak arrivals can be found to support evidence for such a velocity.

The evidence for the 2. 47 km/sec (NW) and 2. 56 km/sec (SE)

velocities is also based entirely on second or later energy arrivals at ranges of less than 10 seconds.

The 3.86 km/sec velocity (NW) and 3.81 km/sec velocity (SE) are well established by both first and second arrivals. The 4.74 km/sec velocity (SE) is also well established; the corresponding velocity measured by CHAIN (NW) is 4.79 km/sec. The arrivals are almost masked at this end (NW) of the profile and only a single first arrival can be identified with this velocity line; however, second arrival evidence for this velocity is excellent.

At a range of 12 to 14 seconds the 4.74 - 4.79 km/sec velocity lines break to lines having velocities of 6.63 km/sec. First arrival evidence for this velocity, although present over limited range, is good. Strong second or third arrivals, all recorded at ranges greater than 15 seconds, have been tentatively assigned to lines (dashed) having velocities 7.78 km/sec (NW) and 7.64 km/sec (SE). Strong supporting evidence for this interpretation is found on the long reverse profile, Sections 5.7, 5.8.

Section 5.6: WINNARETTA SINGER (unreversed). Direct evidence for the existence of the low velocity, 2.03 km/sec, is poor and consequently the line is dashed on the travel time graph. Good second arrival evidence has been used to establish the 2.53 km/sec velocity. The 3.71 km/sec and 4.70 km/sec velocities are established

by first arrival evidence. Two second arrivals for shots recorded at ranges greater than 11 seconds are tentatively identified with a line (dashed) of velocity 6.56 km/sec.

Sections 5.7, 5.8: WINNARETTA SINGER (NW) - WINNARETTA SINGER (SE). The 6.48 km/sec (NW) and 6.60 km/sec (SE) velocities are established by both first and second arrival evidence; the measurement is considered excellent. The 7.82 km/sec (NW) and 7.63 km/sec (SE) velocities are well established by first arrival evidence. The measurement at the southeast end of the profile extends out to a range of 90 km.

APPENDIX II

Total Mass Computations to 40 km. (1 cm² area)

1. Oceanic Column (Hess, 1955)

Thickness km.		Density gm/cc		Mass kg
5.3	x	1.03	=	546
0.7	x	2.30	=	161
4.0	x	2.90	=	1,160
30.0	x	3.325	=	<u>9,975</u>
				11,842 kg

2. Profile 195

Mantle density (a) 3.15 gm/cc

(b) 3.325 gm/cc

(a)			(b)		
Thickness km.	Density gm/cc	Mass kg	Thickness km.	Density gm/cc	Mass kg
2.50	x	1.03 = 257.5			257.5
0.50	x	1.95 = 97.5			97.5
0.80	x	2.20 = 176.0			176.0
2.10	x	2.40 = 504.0			504.0

Profile 195 (continued)

(a)			(b)				
Thickness km.		Density gm/cc	Mass kg	Thickness km.	Density gm/cc	Mass kg	
3.50	x	2.50 =	875.0			875.0	
2.60	x	2.85 =	741.0			741.0	
28.00	x	3.15 =	<u>8,820.0</u>	28.00	x	3.325 =	<u>9,310.0</u>
			11,471 kg				11,961 kg

Profile 5

Mantle density (a) 3.15 gm/cc

(b) 3.325 gm/cc

(a)			(b)				
Thickness km.		Density gm/cc	Mass kg	Thickness km.	Density gm/cc	Mass kg	
2.60	x	1.03 =	267.8			267.8	
0.35	x	1.95 =	68.2			68.2	
0.65	x	2.10 =	136.5			136.5	
1.55	x	2.30 =	356.5			356.5	
2.90	x	2.50 =	725.0			725.0	
2.30	x	2.85 =	655.5			655.5	
29.65	x	3.15 =	<u>9,339.7</u>	29.65	x	3.325 =	<u>9,858.6</u>
			11,549 kg				12,068 kg

ACKNOWLEDGEMENTS

The seismic refraction and reflection measurements discussed in this thesis have been made possible through the cooperation of scientists and technical personnel of three research institutions, the Woods Hole Oceanographic Institution, Lamont Geological Observatory, and the Musee Oceanographique de Monaco. The studies were conducted from the research vessels ATLANTIS and CHAIN (Woods Hole Oceanographic Institution), VEMA (Lamont Geological Observatory), and WINNARETTA SINGER (Musee Oceanographique de Monaco). Much of the success of the experimental phase of the research was due to the fine cooperation of Captains W. S. Bray (ATLANTIS), H. C. Kohler (VEMA), W. S. Olivey (CHAIN), M. Wanecque (WINNARETTA SINGER), and E. H. Hiller (CHAIN), and the officers and crew of each research vessel.

Numerous individuals in the scientific complement assigned to each ship contributed to the success of the research program and made this investigation possible. The chief scientists aboard the research vessels were R. S. Edwards

(ATLANTIS), C. L. Drake (VEMA), J. B. Hersey (CHAIN, 1959), D. A. Fahlquist (WINNARETTA SINGER), and J. B. Hersey and E. E. Hays (CHAIN, 1961). The refraction studies were under the direction of D. A. Fahlquist and J. Antoine (ATLANTIS), C. L. Drake (VEMA), J. B. Hersey and H. R. Johnson (CHAIN, 1959), and D. A. Fahlquist (WINNARETTA SINGER).

The continuous seismic reflection studies were conducted by J. B. Hersey, E. E. Hays, and D. D. Caulfield. The assistance of these and the many other individuals who contributed to the experimental phases of this study is gratefully acknowledged.

The 1959 refraction studies could not have been made without the kind cooperation of the Musee Oceanographique de Monaco and its Director, Captain J. Y. Cousteau, who arranged for the use of the WINNARETTA SINGER by Woods Hole Oceanographic Institution scientists. The author would like to acknowledge with gratitude not only the facilities and personnel made available for the study by Captain Cousteau, but also the personal interest and encouragement he has shown in the work.

The refraction data obtained from VEMA were given to the author through the courtesy of C. L. Drake.

I wish to thank T. F. Gaskell of the British Petroleum Company and L. Glangeaud of the Faculte des Sciences de

l'Universite, Paris, for several valuable and stimulating discussions concerning the Mediterranean region. P. N. S. O'Brien of the British Petroleum Company and H. Closs of the Geological Survey of West Germany have kindly discussed with me some of the tentative results of their most recent seismic crustal investigations in the Maritime and Swiss Alps. J. Bourcart of the Faculte des Sciences de l'Universite, Paris, made several suggestions as to location of profiles during the 1959 studies. The bathymetric data obtained by Woods Hole Oceanographic Institution during numerous cruises to the Mediterranean Sea have been analyzed by R. M. Pratt; these data were made available to the author.

Several people have critically reviewed various portions of the manuscript. I wish to thank E. T. Bunce, J. W. Graham, C. O. Bowin, and J. B. Hersey for helpful suggestions and criticisms.

The travel time graphs and many of the figures were drafted under the direction of C. Innis. The computations were programmed for the Recomp II computer by C. Gifford and the final draft of the manuscript was typed by J. Nolan.

The author extends his deep appreciation to J. B. Hersey, not only for supervising this thesis and making the experimental

work possible, but for his continuing interest and encouragement during the writing of this paper.

The experimental and analysis phases of the work have been supported by the U. S. Navy under Contracts Nonr-1367(00) with the Office of Naval Research and Contract NObsr-72521 with the Bureau of Ships.

BIBLIOGRAPHY

- Bäth, M., Crustal structure of Iceland, *J. Geoph. Research*, 65, 1793-1807, 1960.
- Beaufils, Y., J. Coulomb, R. Geneslay, G. Jobert, Y. Labrouste, E. Peterschmitt, and J. P. Rothé, Enregistrement des ondes seismiques provoquées par de grosses explosions, Champagne 1952, Publ. Bureau Central seismologique international, Serie A, *Travaux Scientifiques* 19, Toulouse, 327-329, 1956.
- Birch, F., The velocity of compressional waves in rocks to 10 kilopars: Part I; *J. Geoph. Research*, 65, 1083-1112, 1960.
- Bourcart, J., Recherches de géologie sous-marine profonde, *Soc. Geol. France*, B. s. 6, t. 4, (1954); 557-564, 1955.
- Essai de carte sous-marine de l'ouest de la Corse, *Rev. Geog. Phys. et Geol. Dyn*, s. 2, 1, 31-36, 1957.
- Problèmes de géologie sous-marine, Masson et Cie Paris, 125 pp., 1958.
- Carte éditée par le Musée Océanographique de Monaco No. 3, 1^{re} édition, (Chart includes all of western Mediterranean exclusive of Tyrrhenian Sea); 1959a.
- Morphologie du précontinent des Pyrénées a la Sardaigne, in La topographie et la géologie des profondeurs océaniques, Centre National de la Recherche Scientifique, Paris, 33-52, 1959b.
- Note explicative de la carte topographique du fond de la Méditerranée Occidentale, *Bull. Inst. Oceanogr. Monaco*, No. 1163, 3-20, 1960.
- Bourcart, J., A. de la Bernardie, and C. Lalou, La rech Lacaze-Duthiers, cañon sous-marine du plateau continental du Roussillon, *Acad. Sci., Paris, C. R. t. 226*, 1632-1633, 1948.

- Bourcart, J., G. Houot, and C. Lalou, Sur la topographie sous-marine au large de Toulon, Acad. Sci., Paris, C. R. t. 230, 561-563, 1950.
- Bourcart, J., G. Houot, and C. Lalou, Recherches sur la topographie sous-marine entre la presqu'île de Grens et Saint Tropez, Acad. Sci., Paris, C. R. t. 234, 1077-1079, 1952.
- Brinkmann, R., Geologic evolution of Europe, translated from the German by J. E. Sanders, Hafner Publishing Company, New York, 161 pp., 1960.
- Bunce, E., and D. Fahlquist, Geophysical investigation of the Puerto Rico trench and outer ridge, J. Geoph. Research, 67, 3955-3972, 1962.
- Caire, A., L. Glangeaud, and C. Grandjacquet, Les grand traits structuraux et l'évolution du territoire Calabro-Sicilien (Italie Méridionale), Bull. Soc. Géol. France, 7^e serie, t.II, 915-938, 1960.
- Caloi, P., La struttura della crosta terrestre, con particolare riguardo alle zolle continentali, quale risulta dallo studio dei terremoti e delle grande esplosioni (Eurasia), presented at XI General Assembly of the I. U. G. G., Toronto, 1957.
- La crosta terrestre, dagli Appennini all' Atlantico, ricostruita sulla base dei rilievi sismici, Annali di Geofisica 11, 249-264, 1958.
- Cassinis, G., M. de Pisa, and P. Dore, I risultati della crociera gravimetrica del regio sommergibile "Vettor Pisani" e la gravità in Italia, Publ. dell' Instituto di Topogr. e Geod., No. 1, 1934.
- Cassinis, G., and M. de Pisa, La crociera gravimetrica dell regio sommergibile "Vettor Pisani" anno 1931, R. Comm. Geod. Ital., Publ. N. S. 13, 1935.
- Cizaneourt, Henri de, Interprétation géologique des anomalies de la pesanteur en Méditerranée, Acad. Sci. Paris, C. R. t. 226, 2164-2166, 1948.

- Cizancourt, Henri de, Essai d'interprétation de certaines anomalies de la pesanteur en Méditerranée occidentale et en Afrique du Nord, *Ann. Géophys.*, t. 9, 126-152, 1953.
- Coron, S., Contribution a l'etude du champ de la pesanteur en France, *Sci. de la terre*, t. 2, No. 4, 150 pp., 1954.
- Coster, H. P., The gravity field of the western and central Mediterranean (Doctoral Dissertation). Bij J. B. Walters' Uitgevers=Maatschappij n. v. Groningen-Batavia, 1945.
- de Sitter, L. U., Structural geology, McGraw Hill Book Co., New York, 552 pp., 1956.
- Debrazzi, E., and A. G. Segre, Carta Batimetrica del Mediterraneo Centrale; Carta No. 1250, Mare Ligure e Tirreno Settentrionale, Pubblicata dall' Istituto Idrografico della Marina-Genova, 1960.
- Drake, C. L., R. W. Girdler, and M. Landisman, Geophysical measurements in the Red Sea, Abstract, International Oceanographic Congress, edited by M. Sears, 1959.
- Drake, C. L., C. Gaibar-Puertas, J. E. Nafe, and M. Langseth, Prospección sísmica submarina en el Golfo de Cádiz, *Revista de Ciencia Aplicada*, Nos. 69, 70, 71, 1959.
- Ewing, J., J. Antoine, and M. Ewing, Geophysical measurements in the western Caribbean Sea and in the Gulf of Mexico, *J. Geoph. Research*, 65, 4087-4126, 1960.
- Ewing, J., and M. Ewing, Seismic-refraction measurements in the Atlantic Ocean Basins, in the Mediterranean Sea, on the Mid-Atlantic Ridge, and in the Norwegian Sea, *Bull. Geol. Soc. Am.*, 70, 291-318, 1959.
- Ewing, J. I., C. B. Officer, H. R. Johnson, and R. S. Edwards, Geophysical investigations in the eastern Caribbean: Trinidad shelf, Tobago trough, Barbados ridge, Atlantic Ocean, *Bull. Geol. Soc. Am.*, 68, 897-912, 1957.

- Ewing, M., G. P. Woollard, and A. C. Vine, Geophysical investigations in the emerged and submerged Atlantic coastal plain, Part III: Barnegat Bay, New Jersey Section, Bull. Geol. Soc. Am., 50, 257-296, 1939.
- Förtsch, O., Analyse der seismischen registrierungen der grossprengung bei Haslach in Schwarzwald am 28 April, 1948, Geol. Jahrb. 66, 65-80, 1951.
- Gaskell, T. F., M. N. Hill, and J. C. Swallow, Seismic measurements made by HMS CHALLENGER in the Atlantic, Pacific and Indian Oceans and in the Mediterranean Sea, 1950-53, Phil. Trans. Roy. Soc. London, Series A, No. 988, vol. 251, 23-83, 1958.
- Geneslay, R., Y. Labrouste, and J. P. Rothé, Réflexions à grande profondeur dans les grosses explosions (Champagne, October 1952), Publ. Bureau Central séismologique international, Série A, Travaux Scientifiques 19, Toulouse, 331-334, 1956.
- Gignoux, M., Stratigraphic geology, English translation from the fourth French edition, 1950, by G. G. Woodford, W. H. Freeman and Company, San Francisco, 682 pp., 1955.
- Glangeaud, L., Essai de classification géodynamique des chaines et des phénomènes orogéniques, Revue de Géographie Physique et de Géologie Dynamique (2) Vol. 1, Fasc. 4, 200-220, 1957.
- Glangeaud, L., Paléogéographie dynamique de la Méditerranée et de ses bords. Le rôle des phases Ponto-Plio-Quaternaires, in Océanographie géologique et géophysique de la Méditerranée occidentale, Centre National de la Recherche Scientifique, Paris, 125-170, 1962.
- Goguel, J., Carte géologique de la France, Echelle 1 à 1,000,000, 4^{ème} Edition, 1955.
- Grandjacquet, C., L. Glangeaud, R. Dubois, and A. Caire, Hypotheses sur la structure profonde de la Calabre (Itali), Revue de Geographie Physique et de Geologie Dynamique (2), Vol. IV, Fasc. 3, 131-147, 1961.
- Greenspan, M., and Tschiegg, C., Sing-around ultrasonic velocimeter for liquids, Rev. Sci. Instr. 28, 897-901, 1957.

- Gutenberg, B., and C. F. Richter, Seismicity of the earth, 2nd edition, Princeton University Press, 310 pp., 1954.
- Hays, E. E., Comparison of directly measured sound velocities with values calculated from hydrographic data, *J. Acoust. Soc. Am.*, 33, 85-88, 1961.
- Hersey, J. B., Findings made during the June 1961 cruise of CHAIN to the Puerto Rico Trench and Caryn Sea Mount, *J. Geoph. Research*, 67, 1109-1116, 1962.
- Hersey, J. B., Continuous reflection profiling, in The Sea, John Wiley and Sons, New York (in press).
- Hess, H., The oceanic crust, *Jour. Mar. Res.*, 14, 423-439, 1955.
- Hofman, B. J., The gravity field of the west Mediterranean area, *Geologie en Mijnbouw*, Nw. serie, 14e, 297-305, 1952.
- Hoskins, H., and S. T. Knott, Geophysical investigation of Cape Cod Bay, Massachusetts, using the Continuous Seismic Profiler, *J. Geol.*, 69, 330-340, 1961.
- Klemme, H. D., Regional geology of circum-Mediterranean region, *Bull. A. A. P. G.*, 42, 447-512, 1958.
- Knopoff, L., and F. Press, A Proposal for the study of the crust and upper mantle structure of the western Mediterranean by surface wave dispersion, *Rapports et Proces - Verbaux des reunions de la CIESMM*, Vol. 16^e, 711-715, 17^e Assemblee pleneire, Monaco, 1960.
- Kuenen, Ph. H., L'age d'un bassin Méditerranéen, in La topographie et la géologie des profondeurs océaniques, Centre National de la Recherche Scientifique, Paris, 157-163, 1959.
- Leenhardt, O., Dépouillement d'un profil sismique par la methode de réfraction tiré au large de la côte varoise, *C. R. Soc. Geol. France*, No. 4, 125-126, 1962.
- Lejay, P., and S. Coron, Mesures de pesanteur au Maroc, *Acad. Sci., Paris, C. R. t.* 231, 501-504, 1950.

- Lejay, P., and S. Coron, Etude gravimetrique de la Corse, Acad. Sci., Paris, C. R. t. 237, 447-450, 1953.
- Muraour, P., J. Merle, and J. Ducrot, Observations sur le plateau continental à la suite d'une étude seismique par réfraction dans le golfe du Lion, Acad. Sci., Paris, C. R. t. 254, 2801-2803, 1962.
- Nafe, J. E., and C. L. Drake, Physical properties of crustal materials as related to compressional wave velocities; paper presented at Annual Meeting of Society of Exploration Geophysics, Dallas, Texas, (unpublished), 1957.
- Nafe, J. E. and C. L. Drake, The structure of the outer ridge north of Puerto Rico, Resume 49, paper presented at meeting of Association of Seismology and Physics of the Earth's Interior, IUGG, Helsinki, Finland, 1960.
- Officer, C. B., Introduction to the theory of sound transmission with application to the ocean, McGraw-Hill Book Company, Inc., New York, 284 pp., 1958.
- Officer, C. B., J. I. Ewing, J. F. Hennion, D. G. Harkrider, and D. E. Miller, Geophysical investigations in the eastern Caribbean: Summary of 1955 and 1956 cruises, Physics and Chemistry of the Earth, Vol. 3, Pergamon Press, London, 1959.
- Officer, C. B., J. I. Ewing, R. S. Edwards, and H. R. Johnson, Geophysical investigations in the eastern Caribbean: Venezuelan basin, Antilles Island arc, and Puerto Rico trench, Bull. Geol. Soc. Am., 68, 359-378, 1957.
- Officer, C. B., Jr., and P. C. Wuenschel, Reduction of deep-sea refraction data: Palisades, N. Y., Lamont Geological Observatory Tech. Rept. 1, 1951.
- Officer, C. B., M. Ewing, and P. C. Wuenschel, Seismic refraction measurements in the Atlantic Ocean, Part IV: Bermuda Rise and Nares Basin, Bull. Geol. Soc. Am., 63, 777-808, 1952.

- Pelissier, M. L., Détermination de l'intensité de la pesanteur en mer. Rapport sur les croisières gravimétriques en Méditerranée occidentale des sous-marins français "Fresnel" (1933-34) et "Espoir" (1936), présenté à la septième Assemblée générale de l'Union géodésique et géophysique internationale tenue à Washington en Septembre 1939.
- Petterson, H., Oceanographic work in Mediterranean, Geog. Jour., 107, 163-166, 1946.
- Rothé, J. P., L'enregistrement dans les stations françaises des ondes sismiques de l'explosion d'Heligoland, Acad. Sci., Paris, C. R. t. 224, 1572-1574, 1947.
- Quelques expériences sur la structure de la croûte terrestre en Europe occidentale, in Contributions in Geophysics, Gutenberg volume, Pergamon Press, New York, 135-151, 1958.
- Rothe, J. P., and E. Peterschmitt, Etude séismique des explosions d'Haslach, Ann. Inst. de Phys. Globe Met., 3^e partie, Géophysique, t. V, Strasbourg, 13-38, 1950.
- Steinhart, J. S., and R. P. Meyer, Explosion studies of continental structure, Carnegie Institution of Washington Publication 622, 1961.
- Sutton, G. H., and C. R. Bentley, Topographic correction curves: Palisades, N. Y., Lamont Geological Observatory Tech. Rept. 3, 1953.
- Tardi, P., Summary of seismic experiments in the Alps sponsored by Comité National Français de Géodésie et Géophysique, Acad. Sci., Paris, C. R. t. 243, 1089-1090, 1956.
- Expériences séismiques dans les Alpes occidentales en 1956; résultats obtenus par le (Groupe d'Etudes des Explosions Alpines), Acad. Sci., Paris, C. R. t. 244, 1114-1117, 1957.
- van Bemmelen, R. W., Gravity field and orogenesis in the West-Mediterranean region, Geologie en Mijnbouw, Nw. serie, 306-315, 1952.

- Vening Meinesz, F.A., Gravity expeditions at sea 1923-1930, Vol. 1, Publication of Netherlands Geodetic Commission, 1932.
- Weibull, W., The thickness of ocean sediments measured by a reflection method, Med. Oceanogr. Inst., Goteborg 12, ser. B, Bd. 5, No. 4, 1 - 17, 1947.
- Sound Explorations, Rep. Swedish Deep-Sea Expedition, 1947-1948, Vol. IV, Bottom Investigations, No. 1, 1955.
- Willmore, P. L., Seismic experiments on the north German explosions, 1946 to 1947, Phil. Trans. Roy. Soc. London, 242A, 123-151, 1949.
- Woollard, G. P., Crustal structure from gravity and seismic measurements, J. Geoph. Research, 64, 1521-1544, 1959.
- Worzel, J. L., Continuous gravity measurements in a surface ship with the Graf sea gravimeter, J. Geoph. Research, 64, 1299-1316, 1959.

BIOGRAPHY

The author, Davis Armstrong Fahlquist, was born in Providence, Rhode Island on July 16, 1926. He attended grammar schools in Massachusetts and Rhode Island. In 1938 his family established permanent residence in Barrington, Rhode Island, where he attended high school. Immediately upon graduation in June, 1944, he entered the United States Navy where he served on active duty in New Guinea and the Philippines for two years. In June, 1946, he was honorably discharged from active duty, continuing as a member of the inactive reserve until 1950. At the time of discharge he held the rating of Electrician's Mate 3/c. In September, 1946, he entered Brown University and in June, 1950, he graduated with a Bachelor of Science degree in Physics.

For two and one-half years he was employed as a product development engineer by Owens Corning Fiberglas Corporation.

In September, 1953, he entered graduate school as a candidate for the degree of Ph. D. in Geophysics. His interest in marine geophysics stems from participation in geophysical studies of the West Indies island arc under the direction of C. B. Officer and John I. Ewing in the summer of 1957. Since that time he has participated in several geophysical studies of the earth's crust both of the continental

shelf and in deep water areas.

In May, 1952, he married Miss Shirley E. Sanborn of Somerset, Massachusetts; the couple now have three children. He is a member of Sigma Xi, the American Geophysical Union, and the Society of Exploration Geophysics. During the course of his research at the Massachusetts Institute of Technology and the Woods Hole Oceanographic Institution he has given several papers at scientific meetings and has contributed to the following publications in geophysical literature.

Marshall, D. J., D. A. Fahllquist, A. S. Neves, and T. R. Madden, Background effects in the induced polarization method of geophysical exploration, A. E. C. Progress Report 1956-1957, Contract AT(05-1)-718, Dept. of Geology and Geophysics, M. I. T.

Fahllquist, D. A., Preliminary results of seismic investigation in the western Mediterranean Sea, Abstract 107, Assoc. de Seism. et Phys. d l'interieur de la terre, I. U. G. G. (Helsinki), 1960.

Bunce, E. T., and D. A. Fahllquist, New seismic observations across the Puerto Rico trench, Abstract 106, Assoc. de Seism. et Phys. d l'interieur de la terre, I. U. G. G. (Helsinki), 1960.

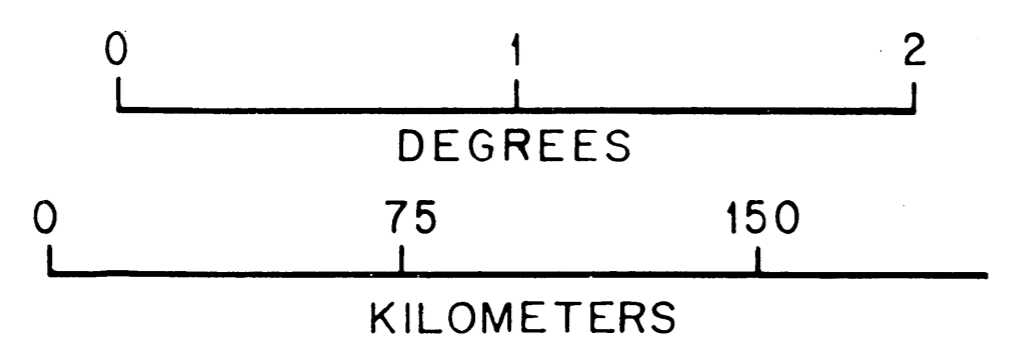
Steinhart, S. T., R. P. Meyer, B. F. Howell, Jr., D. A. Fahllquist, W. E. Bonini, and T. Asada, Maine seismic experiment: General crustal results, Abstract, A. G. U., 43rd Ann. Meet., 1962.

- Meyer, R. P., J. S. Steinhart, B. F. Howell, Jr., W. E. Bonini, D. A. Fahlquist, and L. T. Aldrich, Cooperative Maine experiment in crustal seismology: Method and application of fixed linear recording arrays to crustal measurements, Abstract, A. G. U., 43rd Ann. Meet., 1962.
- Bunce, E. T., and D. A. Fahlquist, Recent geophysical investigation of the Puerto Rico trench and outer ridge: Results and interpretation, Abstract, A. G. U., 43rd Ann. Meet., 1962.
- Bunce, E. T., and D. A. Fahlquist, Geophysical investigation of the Puerto Rico trench and outer ridge, J. Geophys. Research, 67, 3955-3972, 1962.
- Fahlquist, D. A., Seismic refraction measurements in the western Mediterranean Sea, Résumé, Commission Internationale pour l'Exploration Scientifique de la Mer Méditerranée, 18^e Assemblée plénière, Monaco, 1962.

7° 6° 5° 4° 3° 2° 1° 0° 1° 2° 3° 4° 5° 6° 7° 8° 9° 10°

WESTERN MEDITERRANEAN SEA

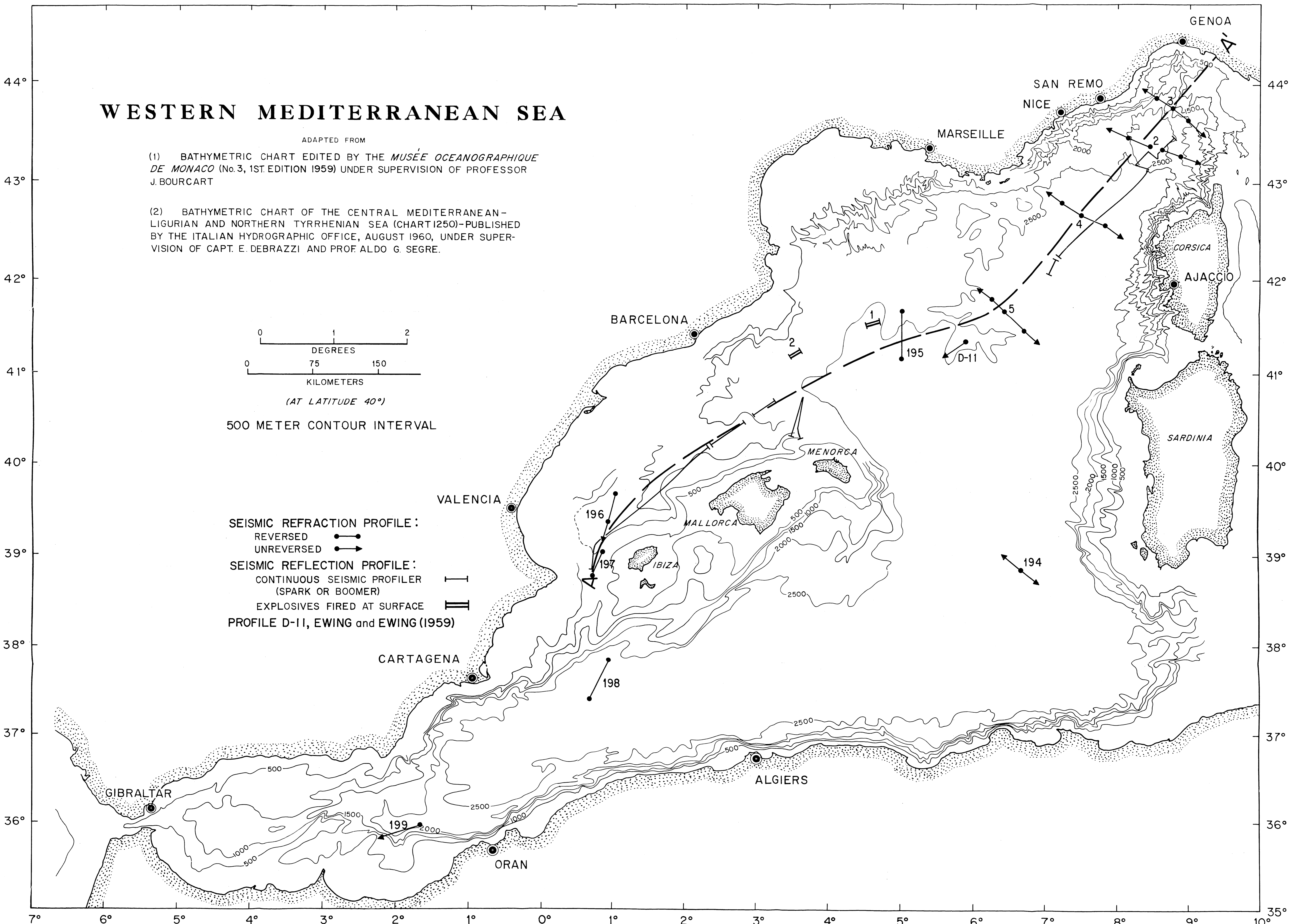
ADAPTED FROM
 (1) BATHYMETRIC CHART EDITED BY THE *MUSÉE OcéANOGRAPHIQUE DE MONACO* (No. 3, 1ST. EDITION 1959) UNDER SUPERVISION OF PROFESSOR J. BOURCART
 (2) BATHYMETRIC CHART OF THE CENTRAL MEDITERRANEAN-LIGURIAN AND NORTHERN TYRRHENIAN SEA (CHART 1250)-PUBLISHED BY THE ITALIAN HYDROGRAPHIC OFFICE, AUGUST 1960, UNDER SUPERVISION OF CAPT. E. DEBRAZZI AND PROF. ALDO G. SEGRE.



(AT LATITUDE 40°)

500 METER CONTOUR INTERVAL

SEISMIC REFRACTION PROFILE:
 REVERSED —●—
 UNREVERSED —▶—
 SEISMIC REFLECTION PROFILE:
 CONTINUOUS SEISMIC PROFILER (SPARK OR BOOMER) —|—
 EXPLOSIVES FIRED AT SURFACE —||—
 PROFILE D-11, EWING and EWING (1959)



STRUCTURE SECTION ACROSS THE WESTERN MEDITERRANEAN

